Andrew G. Myers

Kevin Zong

Saturday Group Meeting - Seminar

September 27th, 2025

Andrew G. Myers

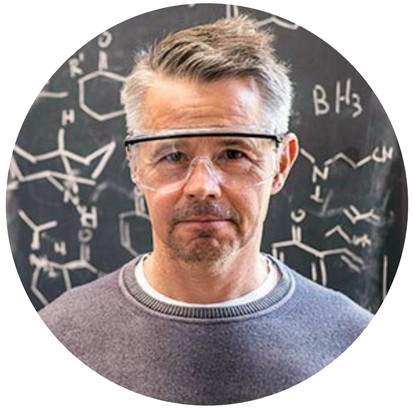

Andrew G. Myers

B.Sc.

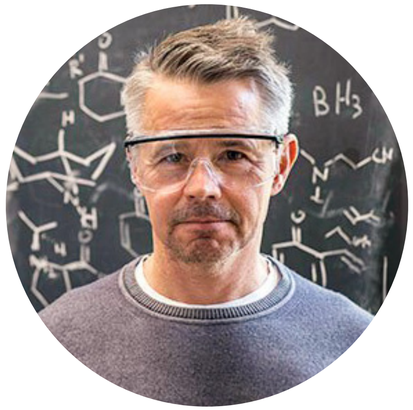

William R. Roush

1977 — 1981

Total Synthesis of the Right-Hand Half of Antibiotic X-14547A

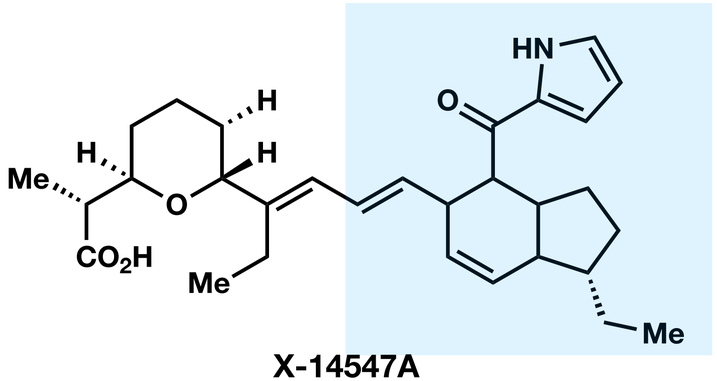

X-14547A

antibiotic activity against gram-positive bacteria

J. Org. Chem. **1981**, 46, 1509-1511

Andrew G. Myers

PhD and Post Doc

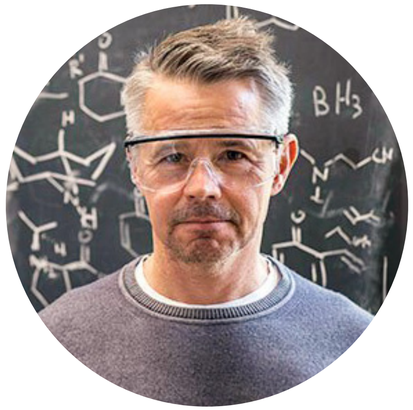

E. J. Corey

1981 — 1986

Total Synthesis and Structural Revision of (±) -Antheridium-Inducing Factor (A_{An}, 2)

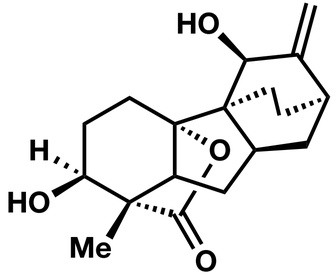

misassigned

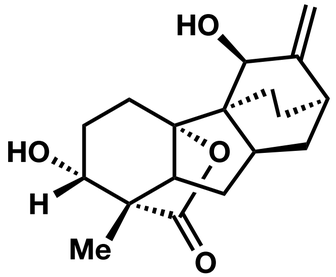

revision

J. Am. Chem. Soc. **1985**, 107, 5574-5576

Andrew G. Myers

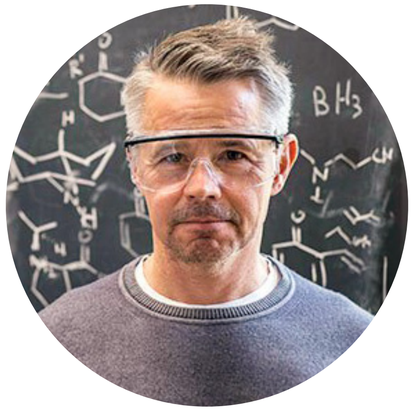

1986

Assistant, Associate, and
then Full Professor (1994)

1998

Andrew G. Myers

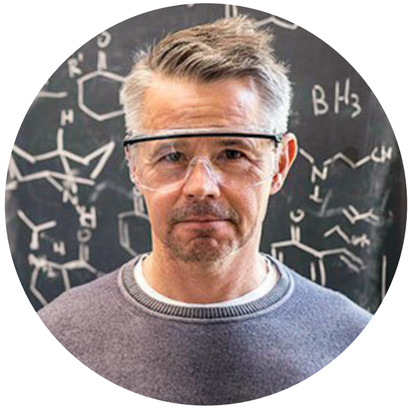

Assistant, Associate, and
then Full Professor (1994)

Department Chair 2007-2010

1986

1998

Present

Andrew G. Myers

Assistant, Associate, and then Full Professor (1994)

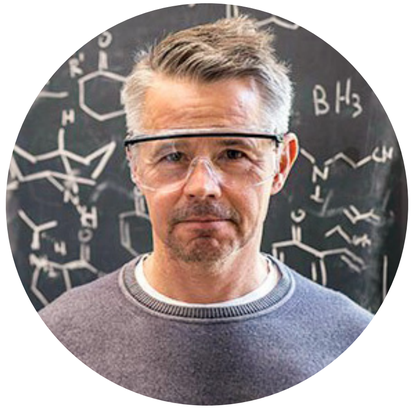

Department Chair 2007-2010

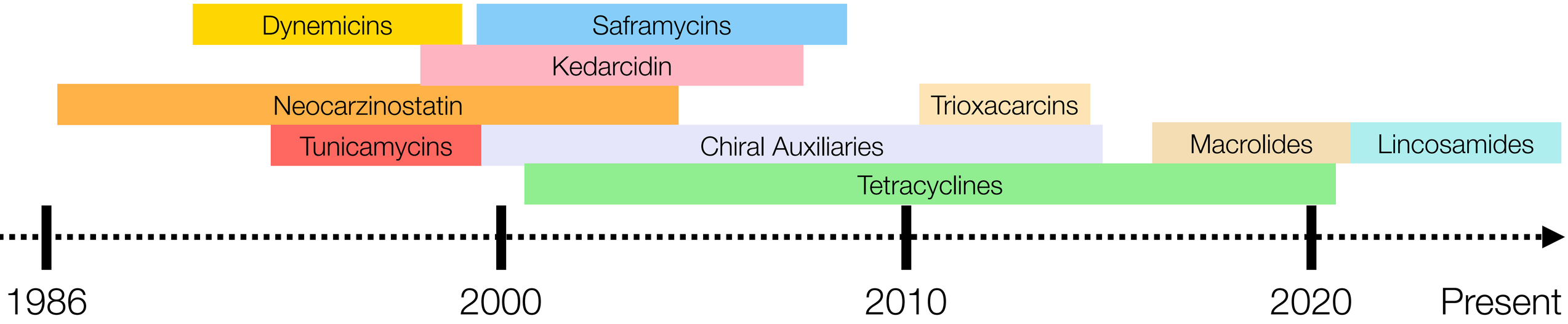

Not Covered Today

avrainvillamide and stephacidin

cytochalasin

cortistatin

salinosporamide A

tunicamycins

most method development and reagent development

Method Development

Chiral Auxiliary

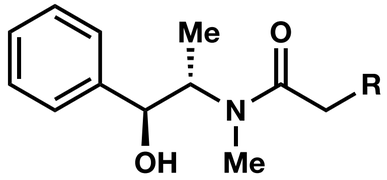

Silicon-Directed Aldol

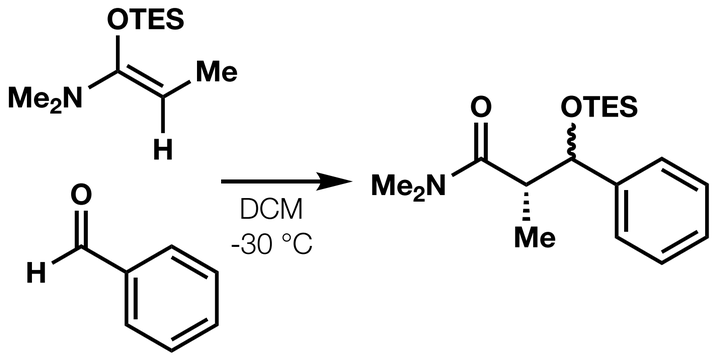

Decarboxylative Palladiation

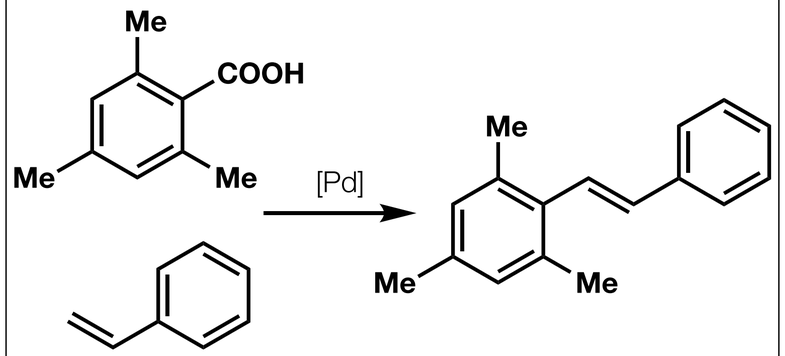

Hydrazine/Hydrazone

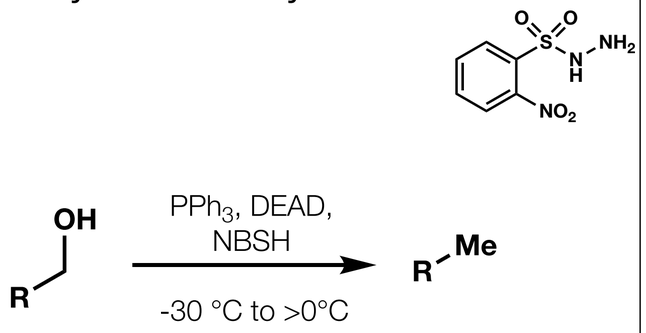

Allene and Ene-Diyne Synthesis

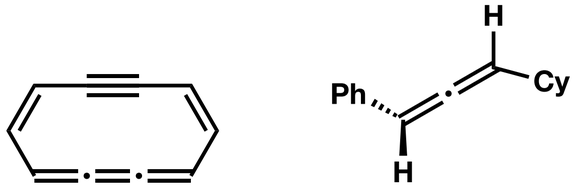

Pseudoephedrine Auxiliary

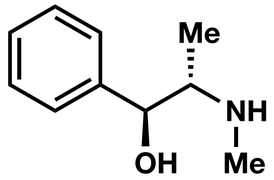

pseudoepedrine

The racemic mixture is also known as Sudafed, which is commonly used as an oral decongestant

Used to be widely available and cheap, but since it can be used to make meth, it is now quite hard to purchase

First reported as an effective auxiliary in 1994 by Myers

JACS. **1994**; 116(20): 9361–9362.

Pseudoephedrine Auxiliary

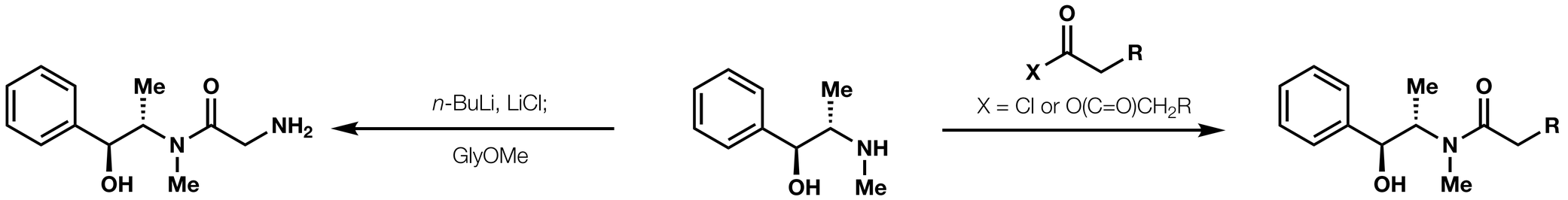

dehydrated starting material shown, but hydrate can also be used directly with LiHMDS

Tet. Lett. **1995**; 36(26): 4555–4558.
JACS. **1995**; 117(32): 8488–8489.
Tet. Lett. **1995**; 36(52): 9429–9432.
JOC. **1999**; 64(9): 3322–3327.

Pseudoephedrine Auxiliary

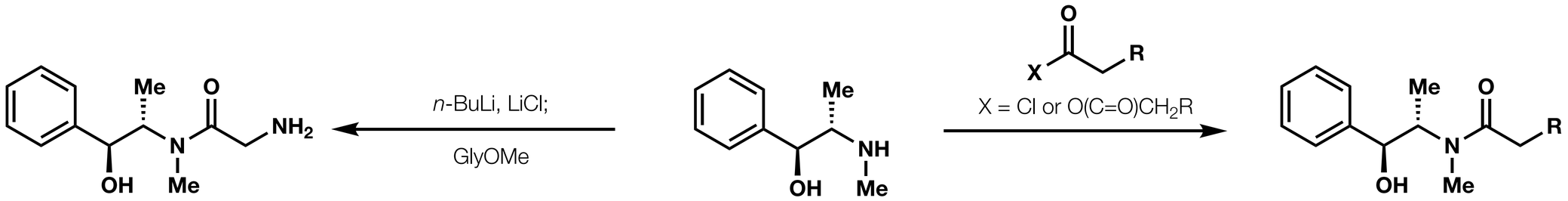

dehydrated starting material shown, but hydrate can also be used directly with LiHMDS

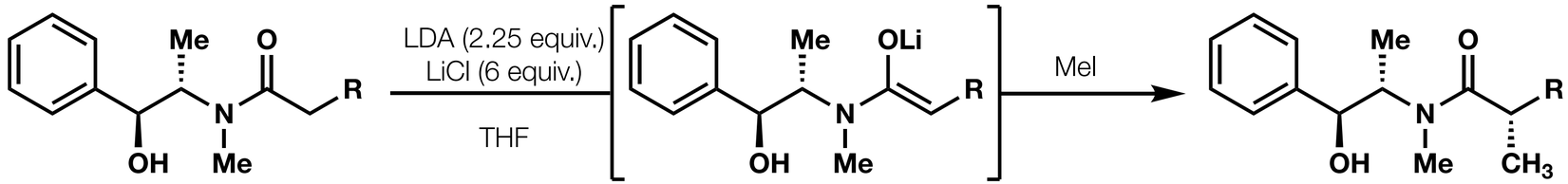

94% yield
94% d.e.

*Reactions in the presence of less than 4 equiv of LiCl are slower and do not proceed to completion; the diastereoselectivity of the alkylation reactions do not appear to be greatly affected by the concentration of LiCl

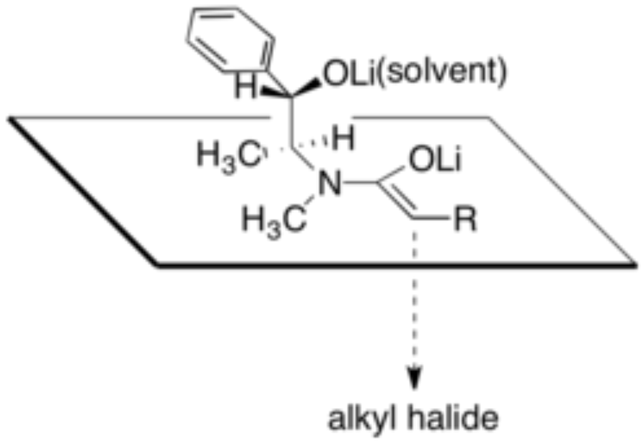

Tet. Lett. **1995**; 36(26): 4555–4558.
JACS. **1995**; 117(32): 8488–8489.
Tet. Lett. **1995**; 36(52): 9429–9432.
JOC. **1999**; 64(9): 3322–3327.

Quaternary Centers

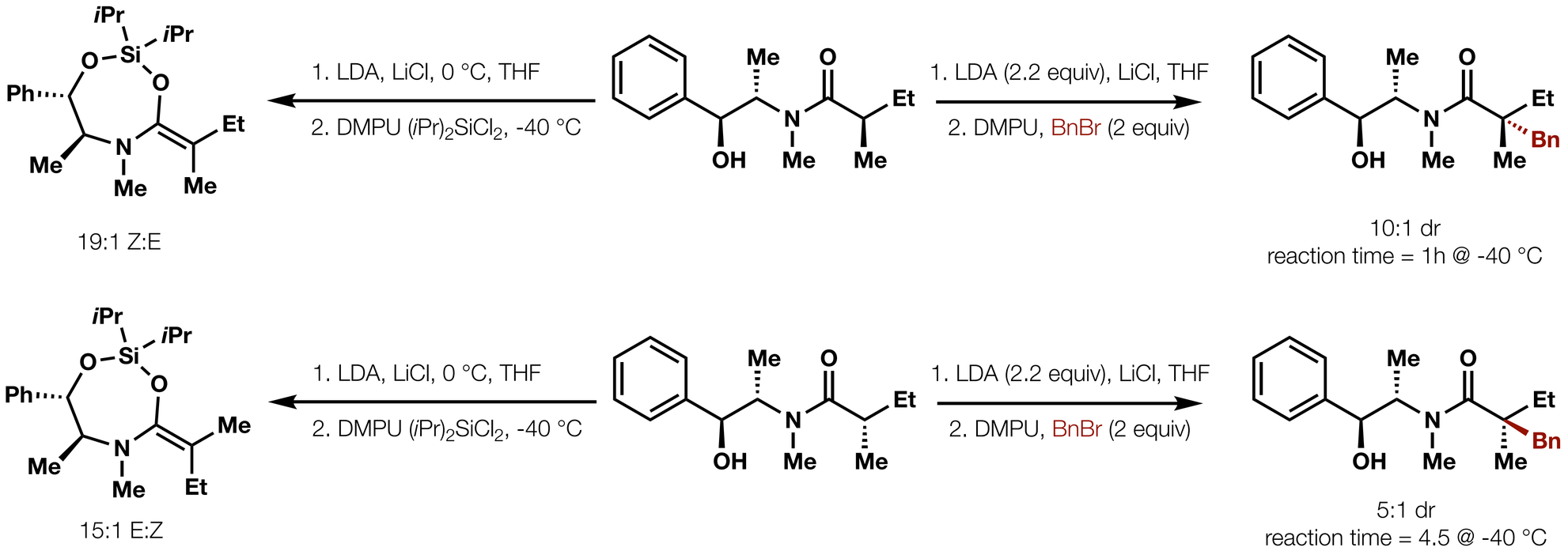

The E and Z enolates are both alkylated from the enolate π-face opposite the alkoxide side chain

Interesting Observation: The Z enolate reacts about 4x faster than the E enolate and is more diastereoselective at lower conversion, which led the authors to use excess enolate for higher diastereoselectivity

JACS. **2008**, 130, 13231–13233

Quaternary Centers

Interesting Observation: The Z enolate reacts about 4x faster than the E enolate and is more diastereoselective at lower conversion, which led the authors to use excess enolate for higher diastereoselectivity

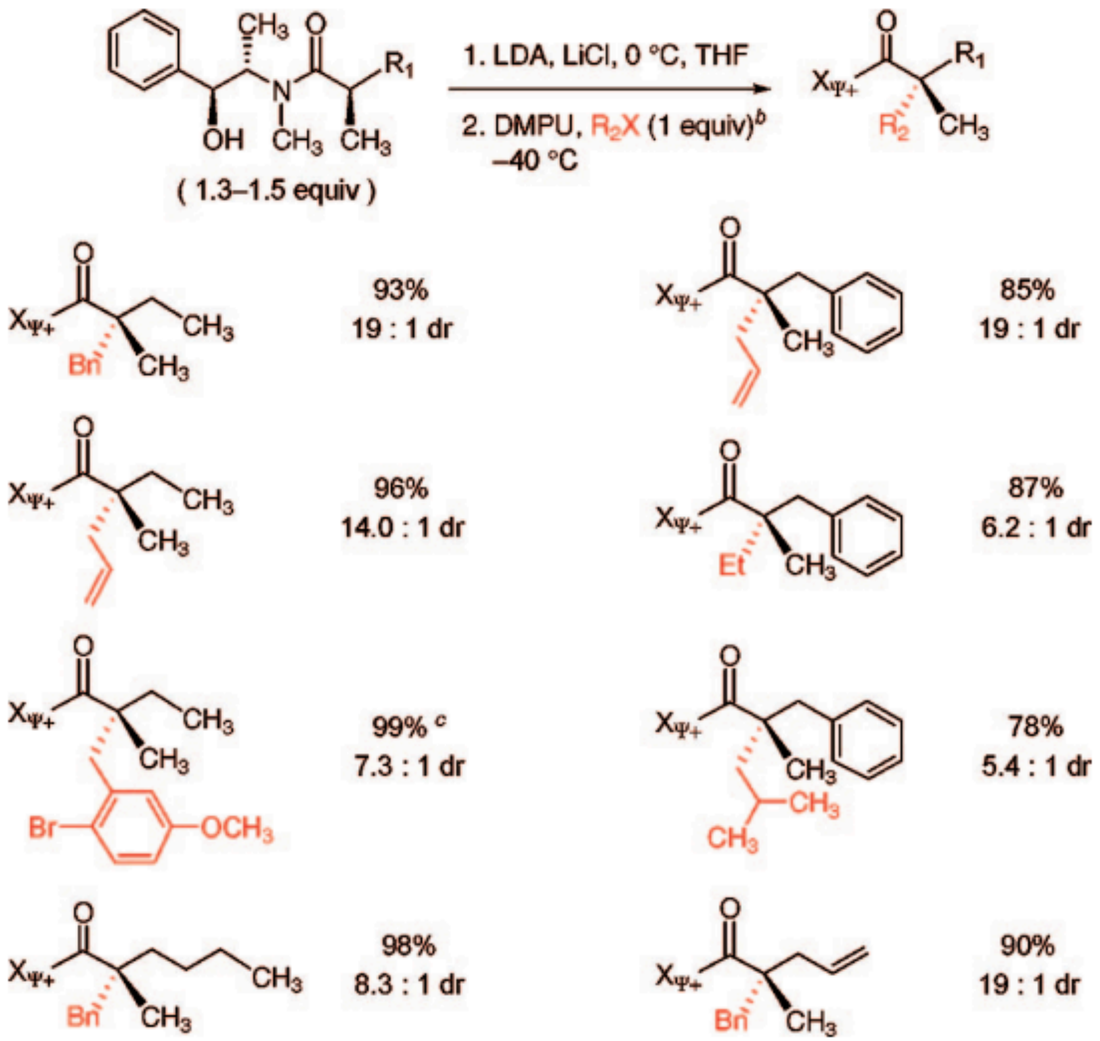

JACS. **2008**, 130, 13231–13233

Quaternary Centers

Another Interesting Observation: Both diastereomers of **alpha-phenyl amides** converge to the same product, suggesting that the E- and Z-alpha-phenyl-alpha-ethyl enolate intermediates might interconvert under the reaction conditions. This is supported by silanol trapping

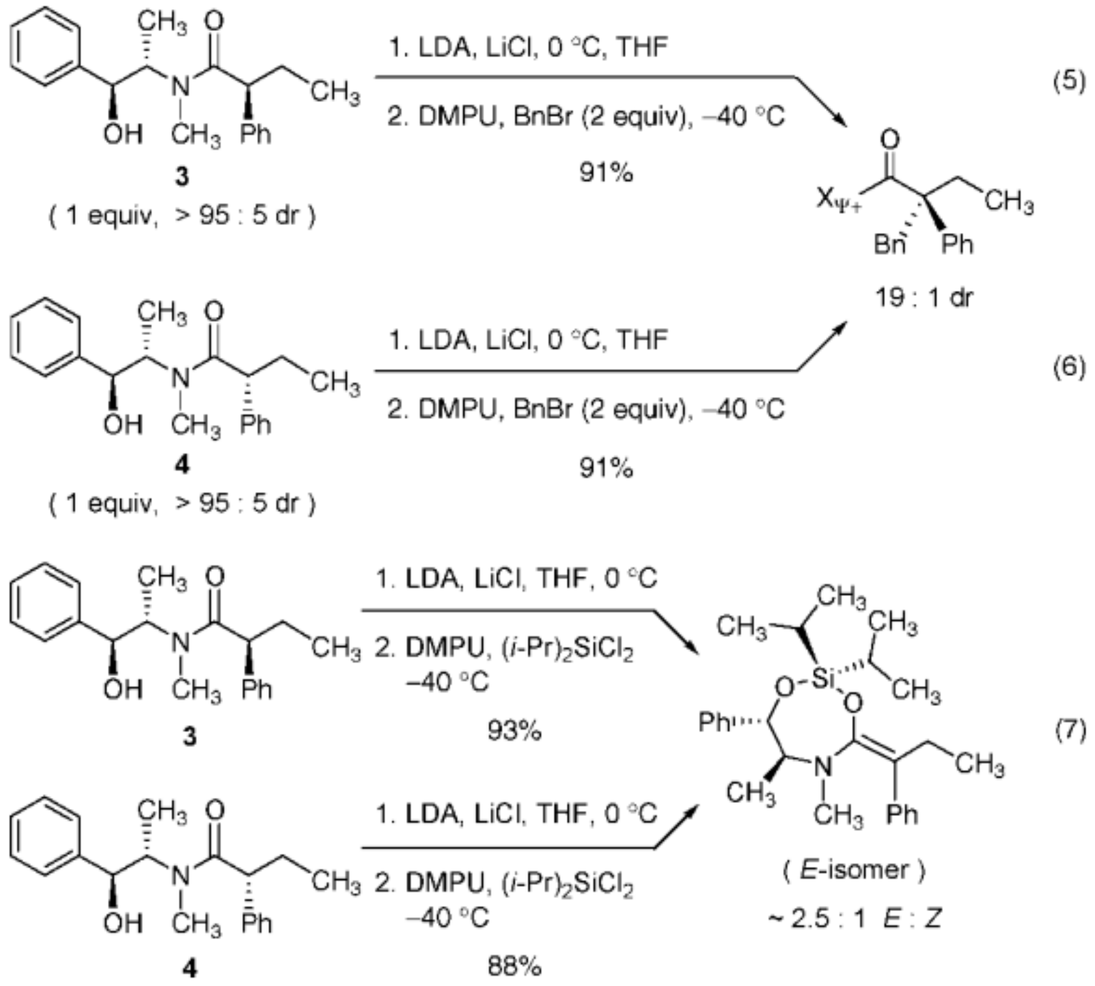

JACS. **2008**, 130, 13231–13233

Iteration

Iterative addition to set multiple stereo centers

Strategy could be used to iteratively alkylate, reduce, alkylate, repeat

Enables asymmetric synthesis of 1,3-dialkyl substituted carbon chains of any stereochemical configuration

Facilitated by the development of LAB (LiH2NBH3), a reductant that can selectively reduce tertiary amides to primary alcohols

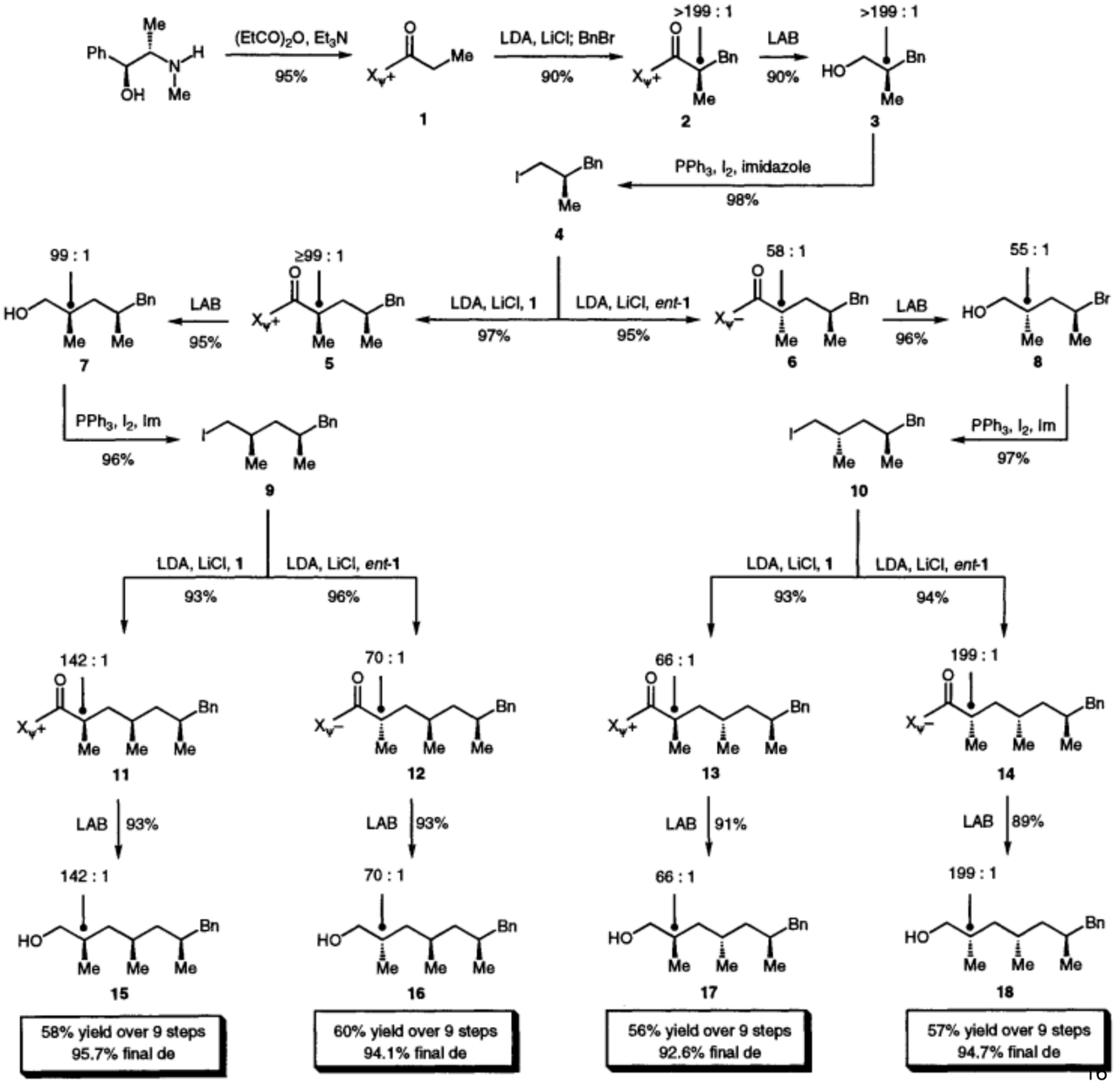

Tetrahedron Letters. **1996**; 37(21): 3623–3626.
Synlett. **1997**; 457–459.

Pseudoephedrine Auxiliary

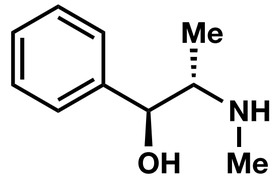

Restricted

Pseudoephedrine Auxiliary

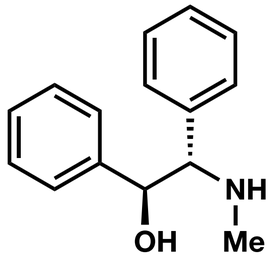

Pseudoephenamine

First Generation Synthesis

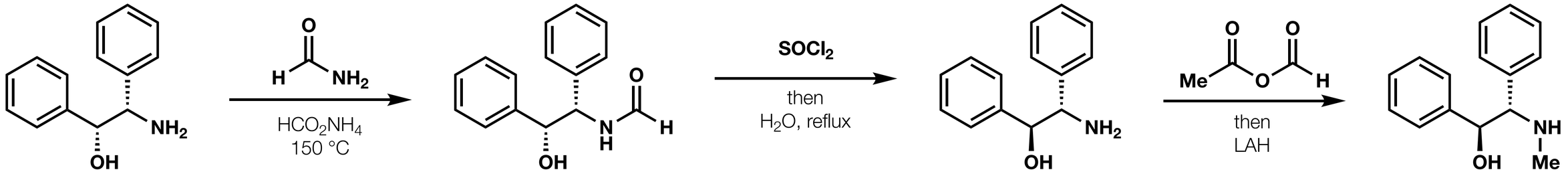

(1R, 2S)-1,2-diphenyl-2-aminoethanol
~$1-2 per gram

Pseudoephedrine Auxiliary

Second Generation Synthesis: Chiral Resolution Starting with Benzil

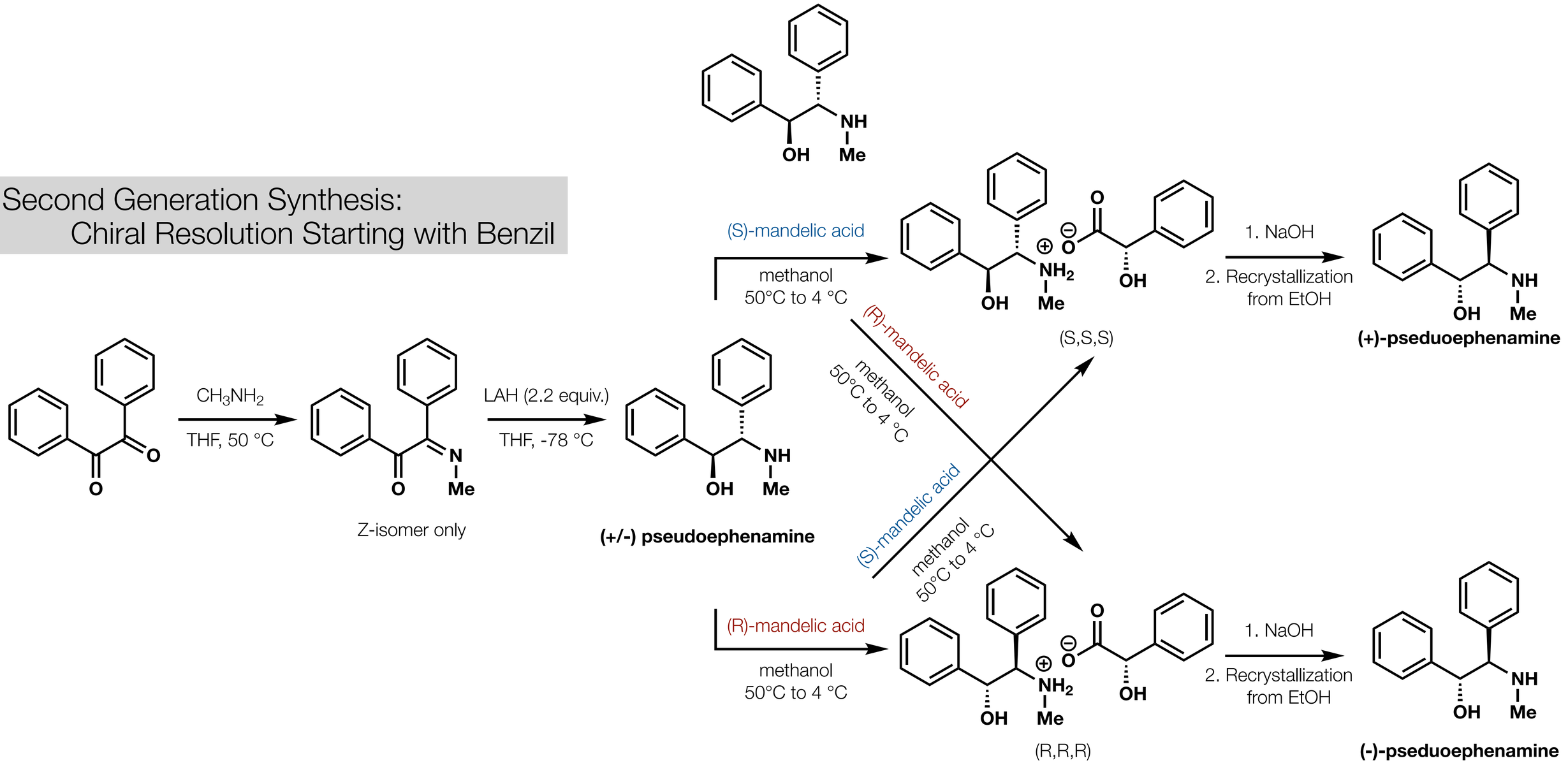

Ene-diynes

neocarzinostatin chromophore

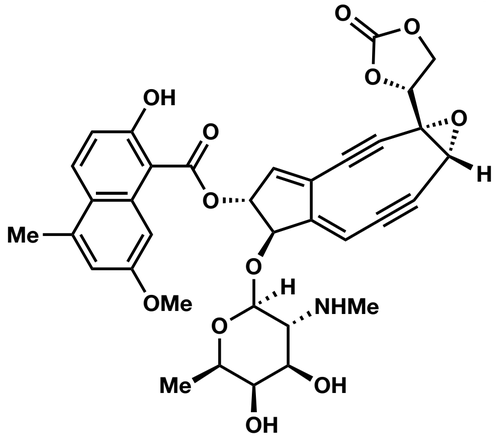

dynemicin A

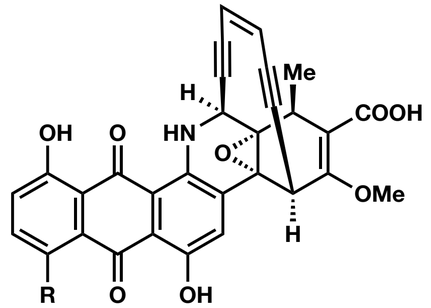

kedarcidin chromophore

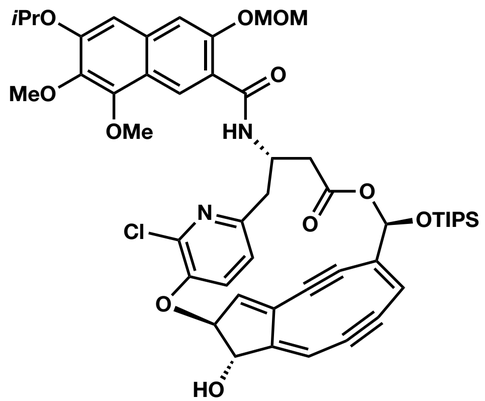

N1999A2

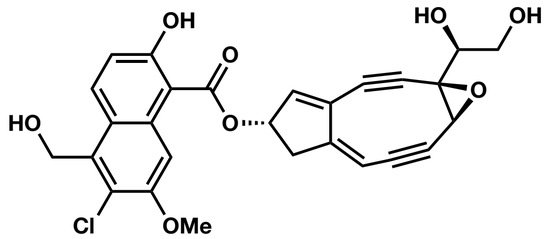

Ene-diynes

Synthetically Challenging

Chemically **unstable** compounds - often cannot be stored neat in the absence of radical inhibitors

Analog development demands flexible, **convergent** synthetic approaches

General Reactivity

Nucleophilic attack triggers conformation change to initiate a **Bergman Cyclization**, forming diradicals that abstract hydrogens from DNA, resulting in **β-scission** of the DNA backbone

neocarzinostatin chromophore

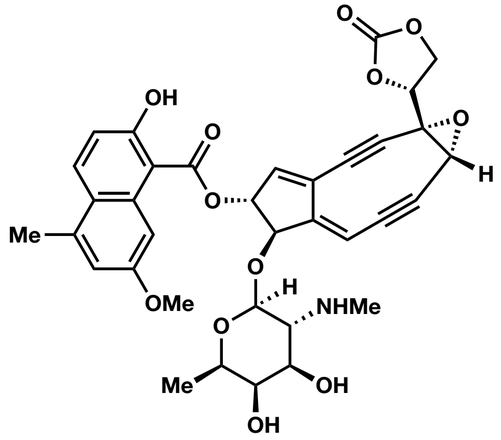

dynemicin A

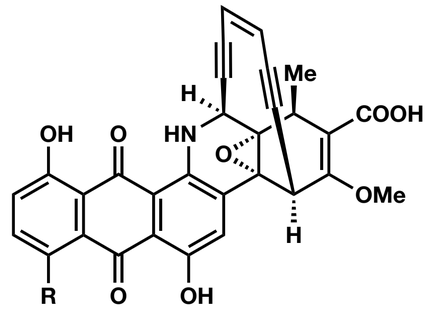

kedarcidin chromophore

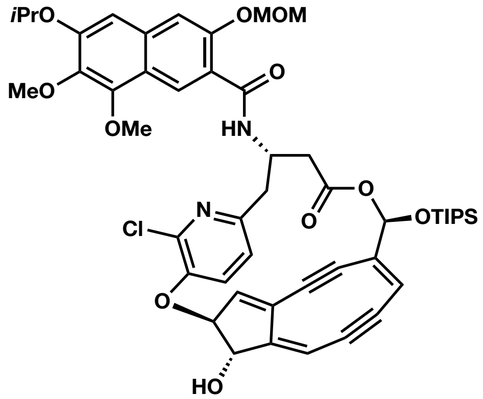

N1999A2

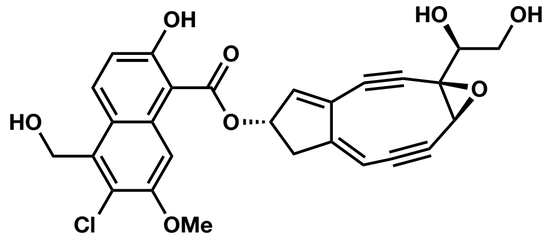

Neocarzinostatin

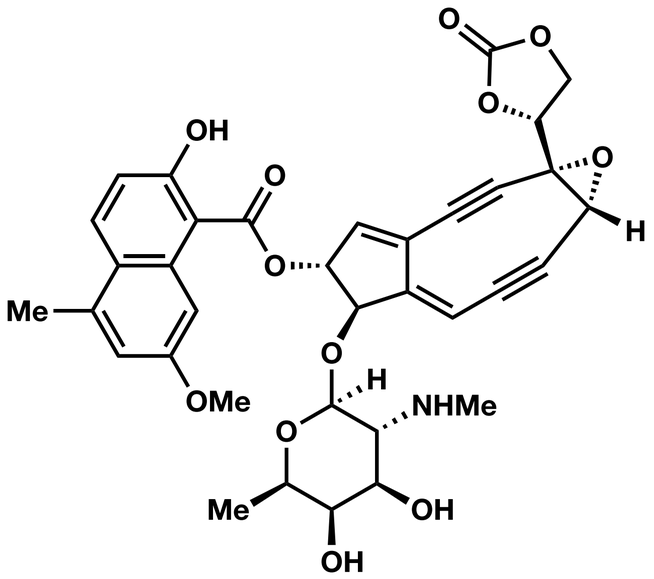

(+)-NCS chromophore

- Isolated from *Streptomyces carzinostaticus*

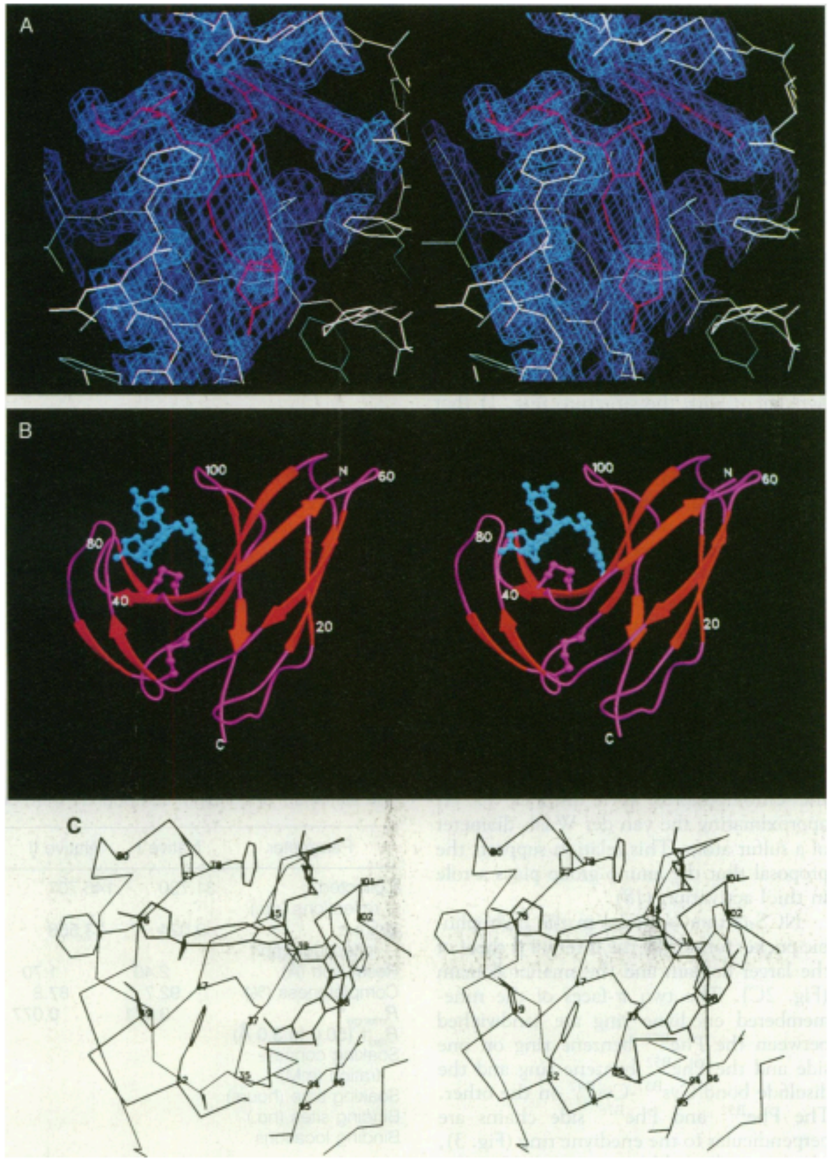

Fig. 2. (**A**) Stereoview of the electron density map (blue) of the region surrounding NCS-chrom (red) and neighboring protein (white). The map was calculated with $2|F_o| - |F_c|$ coefficients for data between 5 to 1.8 Å resolution and contoured at 1.0σ. (**B**) Stereoview of the polypeptide fold of holo-NCS. NCS-chrom and cysteine residues are represented by ball-and-stick models. (**C**) Stereoview of the protein environment of NCS-chrom. Residues within 4 Å of the NCS-chrom are labeled. Both (B) and (C) were drawn with the program SETOR (*33*).

Science **1993**, 262, 2035–2040.

Neocarzinostatin

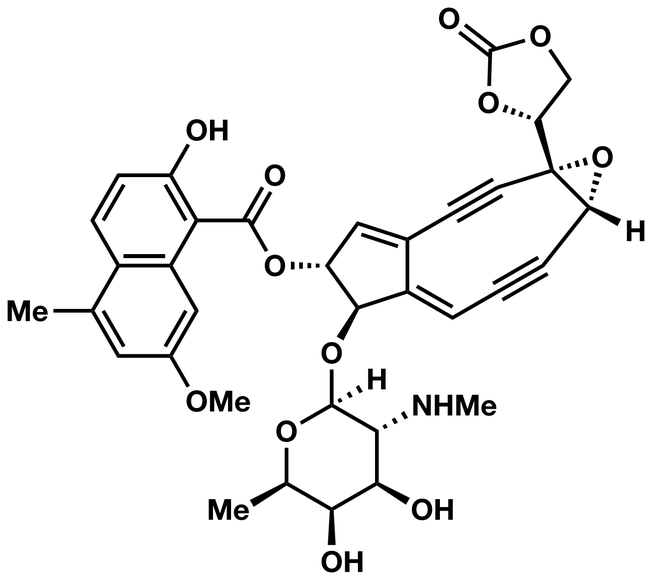

(+)-NCS chromophore

- Isolated from *Streptomyces carzinostaticus*
- Composed of a 113-amino acid protein component (apoNCS) and a chromophore component (NCS-chrom)

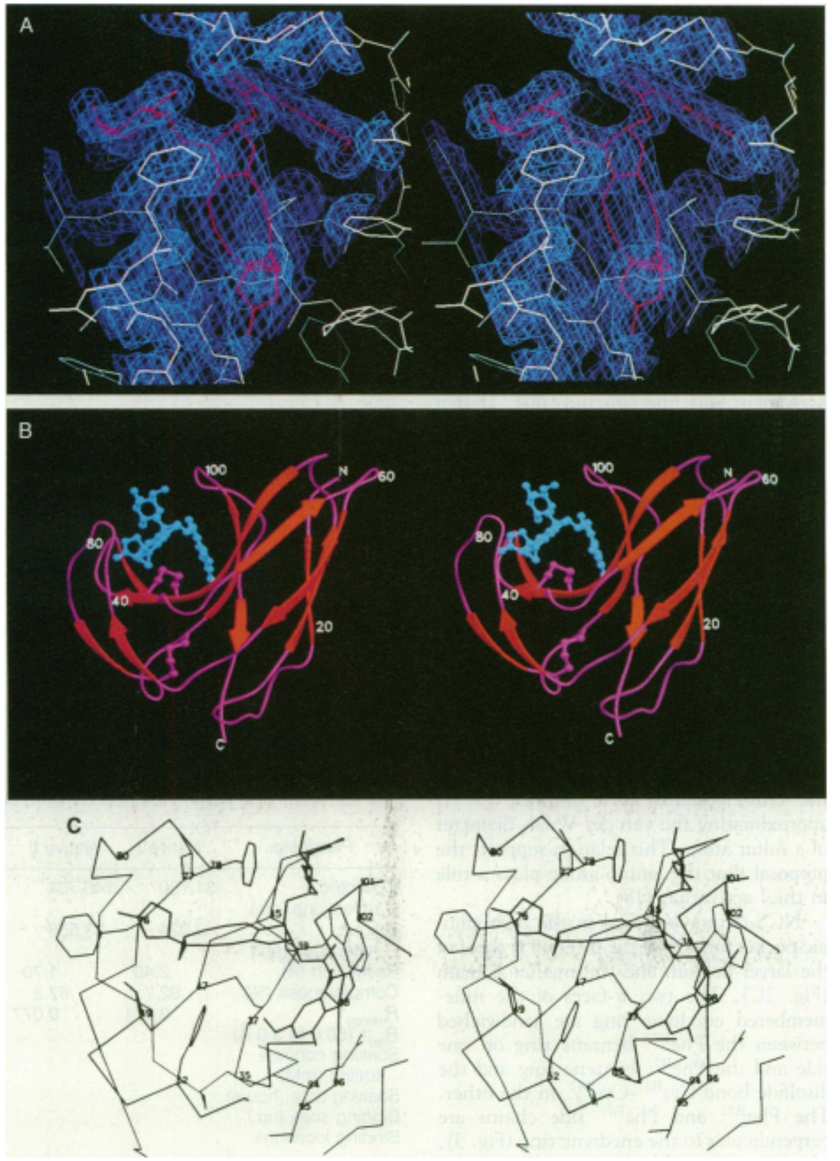

Fig. 2. (**A**) Stereoview of the electron density map (blue) of the region surrounding NCS-chrom (red) and neighboring protein (white). The map was calculated with $2|F_o| - |F_c|$ coefficients for data between 5 to 1.8 Å resolution and contoured at 1.0σ. (**B**) Stereoview of the polypeptide fold of holo-NCS. NCS-chrom and cysteine residues are represented by ball-and-stick models. (**C**) Stereoview of the protein environment of NCS-chrom. Residues within 4 Å of the NCS-chrom are labeled. Both (B) and (C) were drawn with the program SETOR (*33*).

Science **1993**, 262, 2035–2040.

Neocarzinostatin

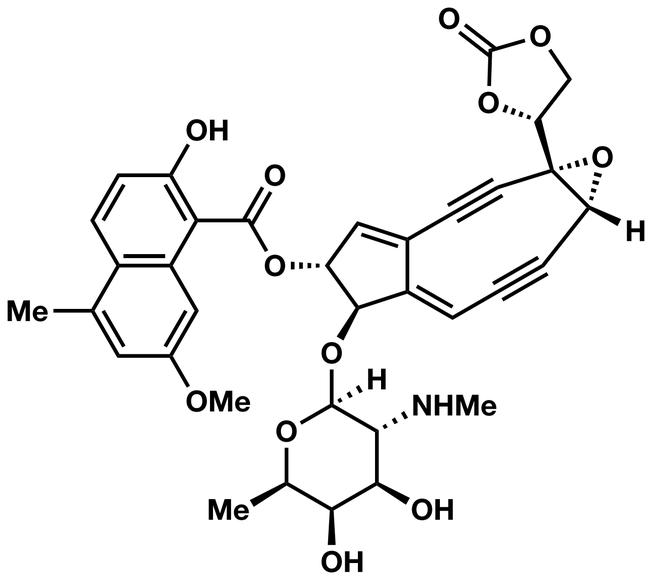

(+)-NCS chromophore

- Isolated from *Streptomyces carzinostaticus*
- Composed of a 113-amino acid protein component (apoNCS) and a chromophore component (NCS-chrom)
- Potent DNA cleaving agent, mechanism of action was heavily studied by Kappen, Goldberg, Saito, **Myers**, and others.

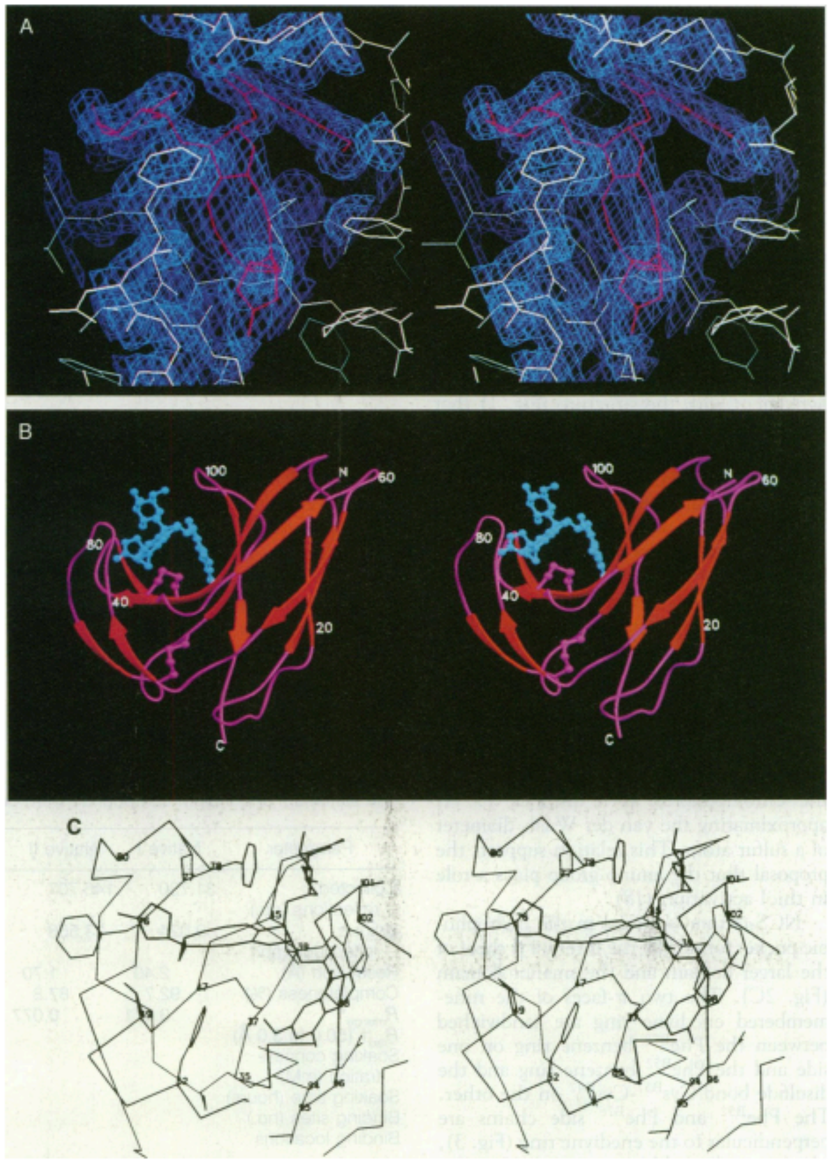

Fig. 2. (**A**) Stereoview of the electron density map (blue) of the region surrounding NCS-chrom (red) and neighboring protein (white). The map was calculated with $2|F_o| - |F_c|$ coefficients for data between 5 to 1.8 Å resolution and contoured at 1.0σ. (**B**) Stereoview of the polypeptide fold of holo-NCS. NCS-chrom and cysteine residues are represented by ball-and-stick models. (**C**) Stereoview of the protein environment of NCS-chrom. Residues within 4 Å of the NCS-chrom are labeled. Both (B) and (C) were drawn with the program SETOR (*33*).

Science **1993**, 262, 2035–2040.

Neocarzinostatin

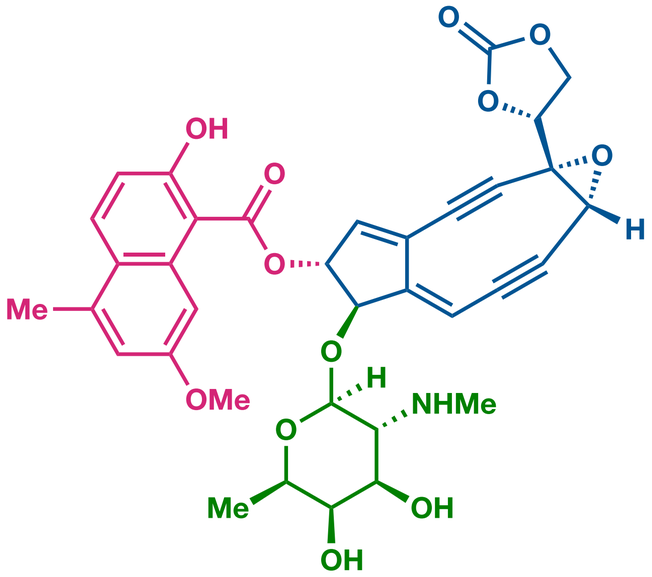

(+)-NCS chromophore

- Isolated from *Streptomyces carzinostaticus*
- Composed of a 113-amino acid protein component (apoNCS) and a chromophore component (NCS-chrom)
- Potent DNA cleaving agent, mechanism of action was heavily studied by Kappen, Goldberg, Saito, **Myers**, and others.
- Chromophore features a key epoxy-enediyne core, a napthoic acid, and an aminosugar

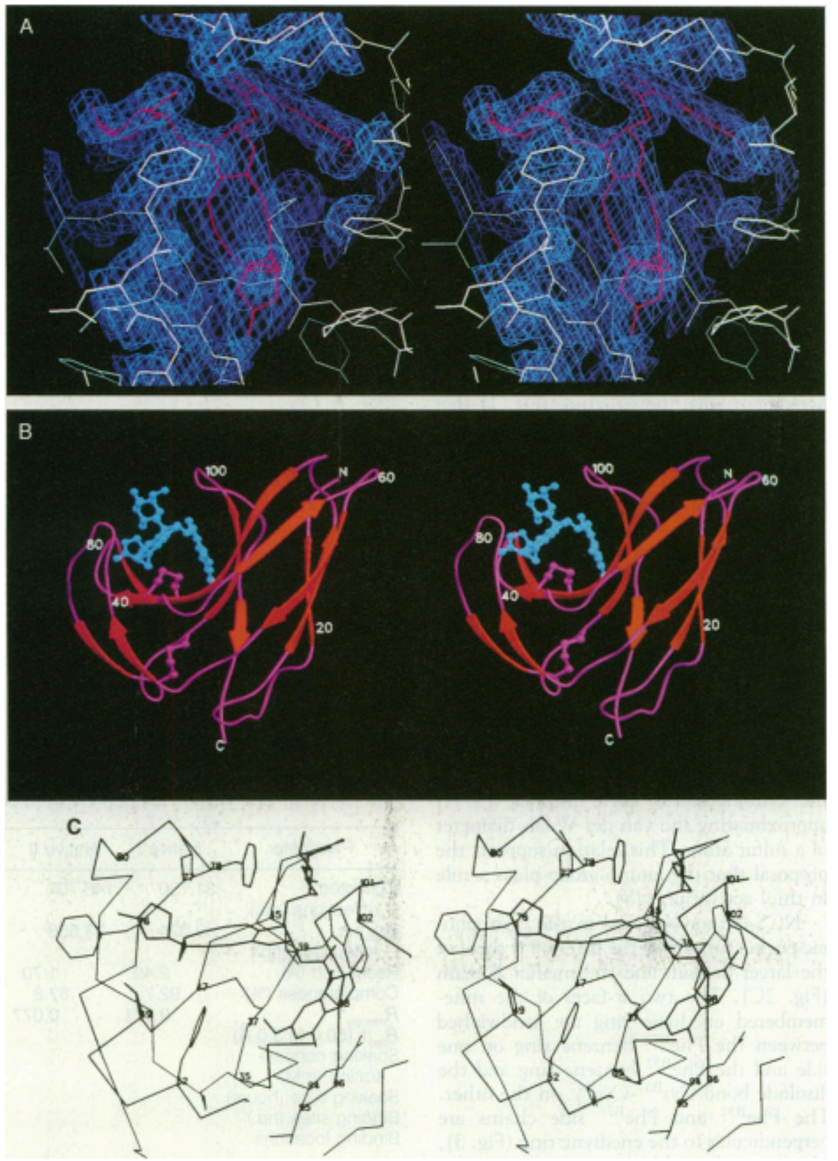

Fig. 2. (**A**) Stereoview of the electron density map (blue) of the region surrounding NCS-chrom (red) and neighboring protein (white). The map was calculated with $2|F_o| - |F_c|$ coefficients for data between 5 to 1.8 Å resolution and contoured at 1.0σ. (**B**) Stereoview of the polypeptide fold of holo-NCS. NCS-chrom and cysteine residues are represented by ball-and-stick models. (**C**) Stereoview of the protein environment of NCS-chrom. Residues within 4 Å of the NCS-chrom are labeled. Both (B) and (C) were drawn with the program SETOR (*33*).

Science **1993**, 262, 2035–2040.

Neocarzinostatin

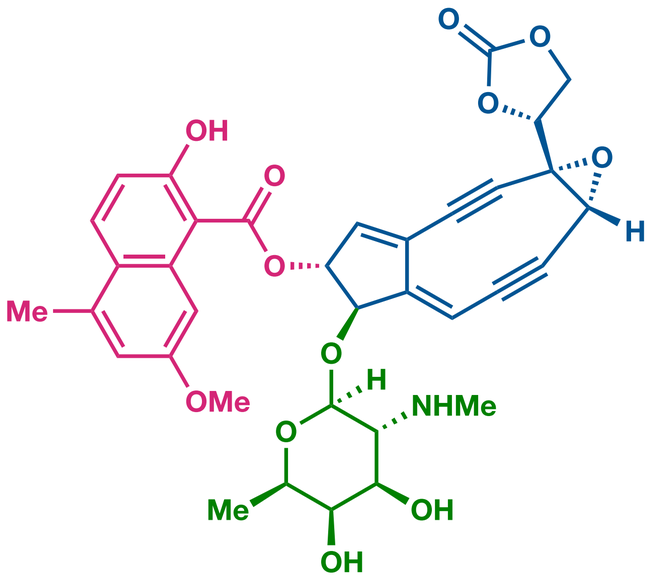

(+)-NCS chromophore

- Isolated from *Streptomyces carzinostaticus*
- Composed of a 113-amino acid protein component (apoNCS) and a chromophore component (NCS-chrom)
- Potent DNA cleaving agent, mechanism of action was heavily studied by Kappen, Goldberg, Saito, **Myers**, and others.
- Chromophore features a key epoxy-enediyne core, a napthoic acid, and an aminosugar
- Crystal structure of Holo NCS elucidated by Rees in 1993 by Rees (X-Ray, 1.8 A resolution)

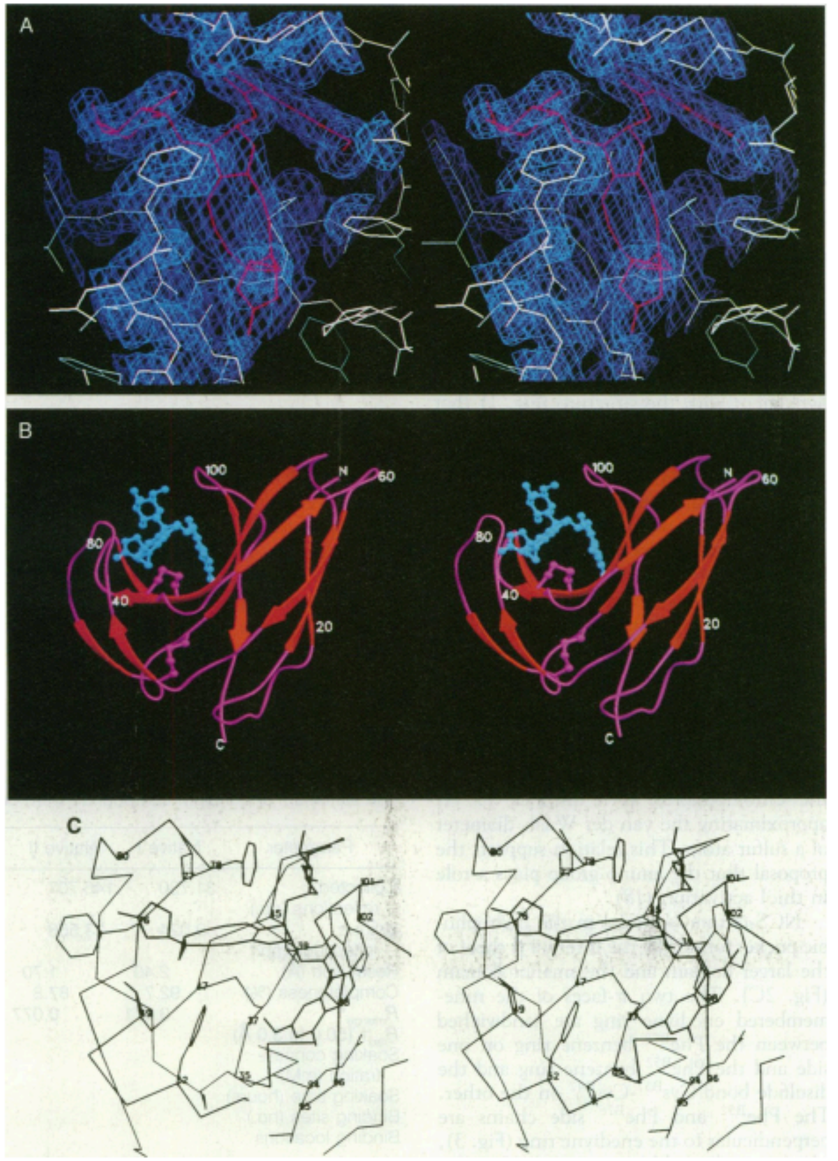

Fig. 2. (**A**) Stereoview of the electron density map (blue) of the region surrounding NCS-chrom (red) and neighboring protein (white). The map was calculated with $2|F_o| - |F_c|$ coefficients for data between 5 to 1.8 Å resolution and contoured at 1.0σ. (**B**) Stereoview of the polypeptide fold of holo-NCS. NCS-chrom and cysteine residues are represented by ball-and-stick models. (**C**) Stereoview of the protein environment of NCS-chrom. Residues within 4 Å of the NCS-chrom are labeled. Both (B) and (C) were drawn with the program SETOR (*33*).

Science **1993**, 262, 2035–2040.

NCS - Mechanism of Action

What was known prior to Myers' Independent Career

Mostly work by Kappen and Goldberg (1979-1980)

- Clear dependency on thiols for activation
- Reacting the chromophore with methyl thioglycolate leads to a compound that appears to be the adduct with two extra hydrogens
- Hypothesized that a radical intermediate abstracts the 5' hydrogen on the sugar backbone, leading to DNA cleavage
- DNA cleavage is not aerobically dependent
- Napthoate functionality was hypothesized to intercalate into the DNA minor groove

NCS - Mechanism of Action

What was known prior to Myers' Independent Career

Mostly work by Kappen and Goldberg (1979-1980)

- Clear dependency on thiols for activation
- Reacting the chromophore with methyl thioglycolate leads to a compound that appears to be the adduct with two extra hydrogens
- Hypothesized that a radical intermediate abstracts the 5' hydrogen on the sugar backbone, leading to DNA cleavage
- DNA cleavage is not aerobically dependent
- Napthoate functionality was hypothesized to intercalate into the DNA minor groove

Myers' First Paper (1987)

PROPOSED STRUCTURE OF THE NEOCARZINOSTATIN CHROMOPHORE-METHYL THIOGLYCOLATE ADDUCT; A MECHANISM FOR THE NUCLEOPHILIC ACTIVATION OF NEOCARZINOSTATIN

Andrew G. Myers
Contribution No. 7628 from the Arnold and Mabel Beckman Laboratory of Chemical Synthesis
California Institute of Technology, Pasadena, California 91125

Tetrahedron Letters. **1987**; 28(39): 4493–4496.

NCS - Mechanism of Action

Myers' First Paper (1987)

PROPOSED STRUCTURE OF THE NEOCARZINOSTATIN CHROMOPHORE-METHYL THIOGLYCOLATE ADDUCT; A MECHANISM FOR THE NUCLEOPHILIC ACTIVATION OF NEOCARZINOSTATIN

Andrew G. Myers
Contribution No. 7628 from the Arnold and Mabel Beckman Laboratory of Chemical Synthesis
California Institute of Technology, Pasadena, California 91125

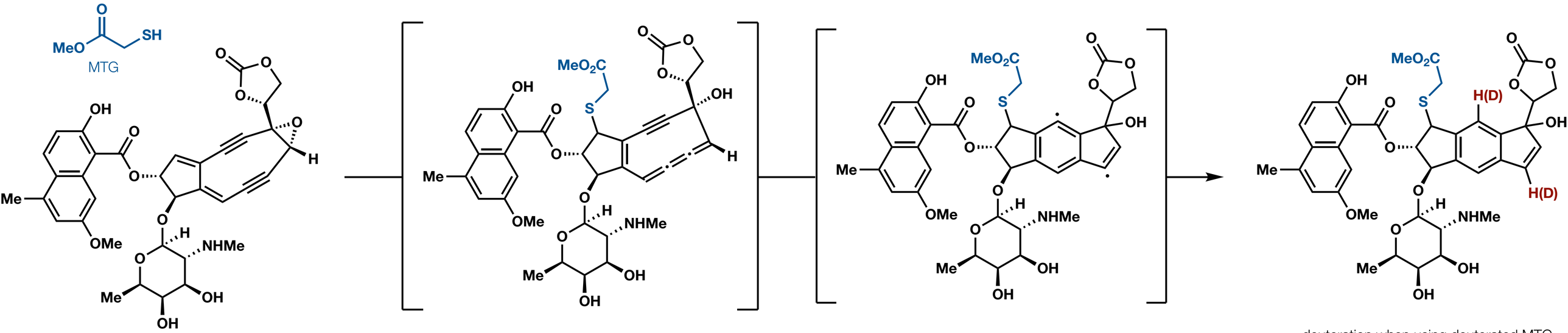

deuteration when using deuterated MTG

Tetrahedron Letters. **1987**; 28(39): 4493–4496.

NCS - Mechanism of Action

Myers' First Paper (1987)

PROPOSED STRUCTURE OF THE NEOCARZINOSTATIN CHROMOPHORE-METHYL THIOGLYCOLATE ADDUCT; A MECHANISM FOR THE NUCLEOPHILIC ACTIVATION OF NEOCARZINOSTATIN

Andrew G. Myers
Contribution No. 7628 from the Arnold and Mabel Beckman Laboratory of Chemical Synthesis
California Institute of Technology, Pasadena, California 91125

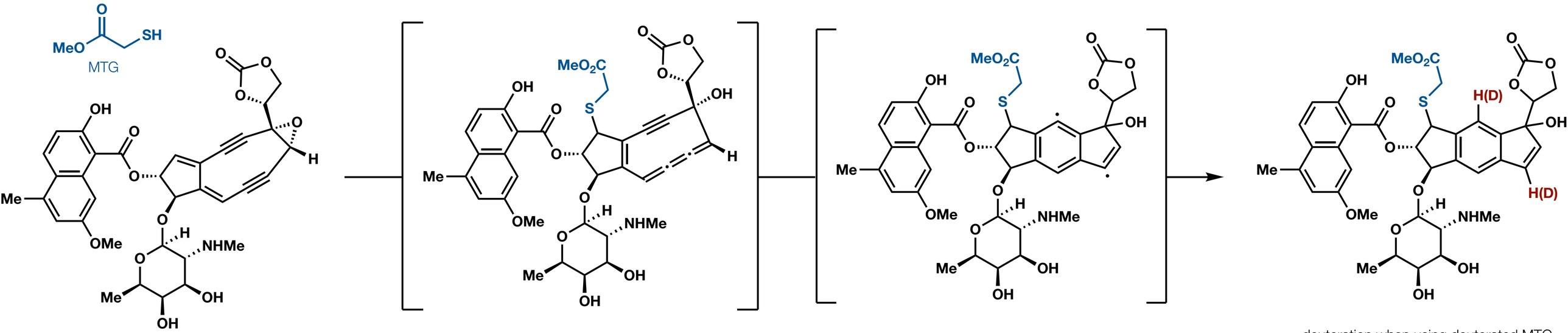

deuteration when using deuterated MTG

Subsequent studies also confirmed the epoxide stereochemistry

Tetrahedron Letters. **1987**; 28(39): 4493–4496.

NCS - Role of Aminoglycoside

NCS

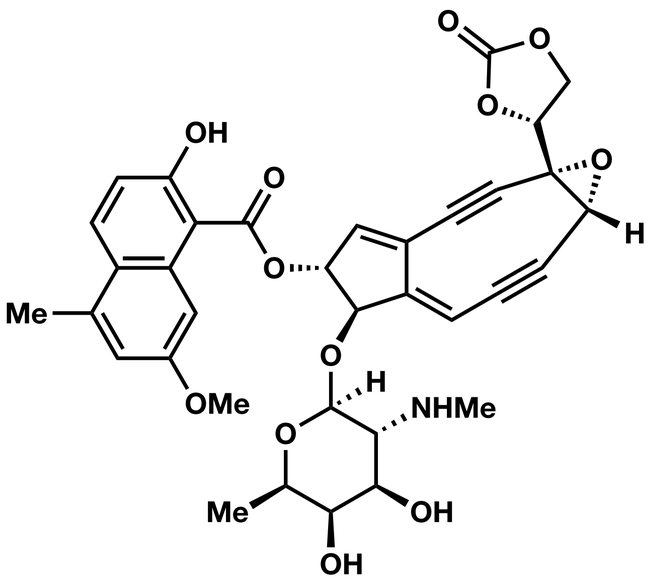

Model system for studying the NCS Core

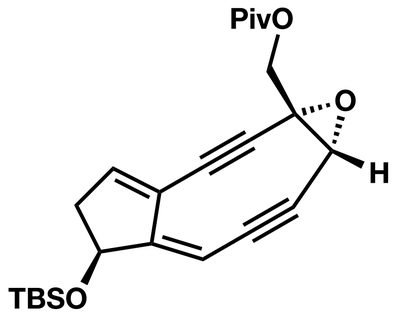

Journal of the American Chemical Society. **1992**; 114(3): 1086–1087.

NCS - Role of Aminoglycoside

NCS

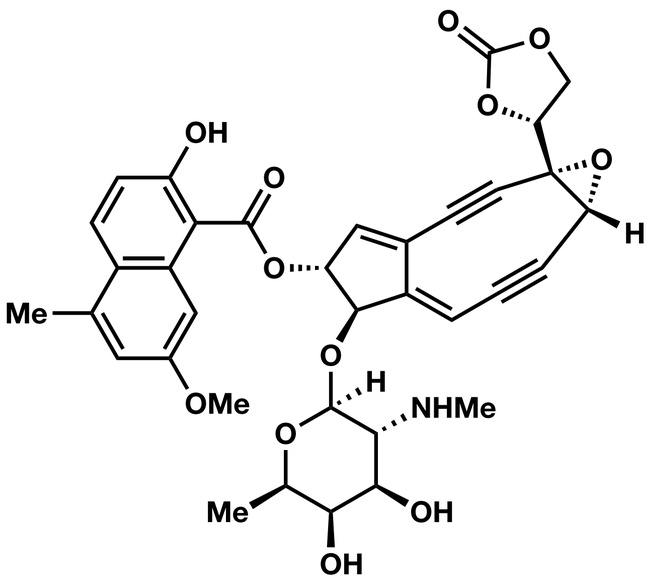

Model system for studying the NCS Core

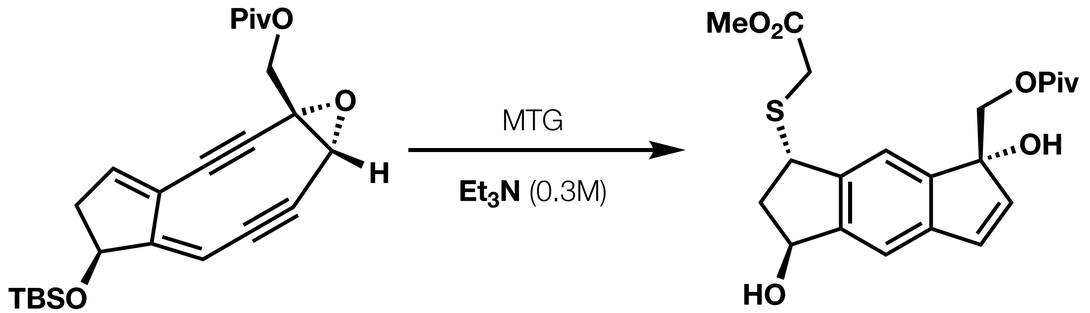

- Reacts readily with MTG at -70°C

- Highly unstable neat
- But completely inert to MTG (up to 60 °C) in the absence of external base

Journal of the American Chemical Society. **1992**; 114(3): 1086–1087.

NCS - Role of Aminoglycoside

NCS

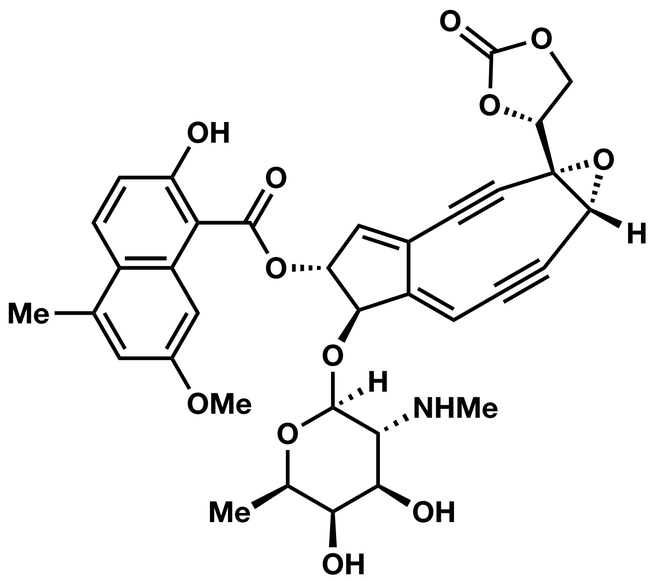

- Reacts readily with MTG at -70°C

Model system for studying the NCS Core

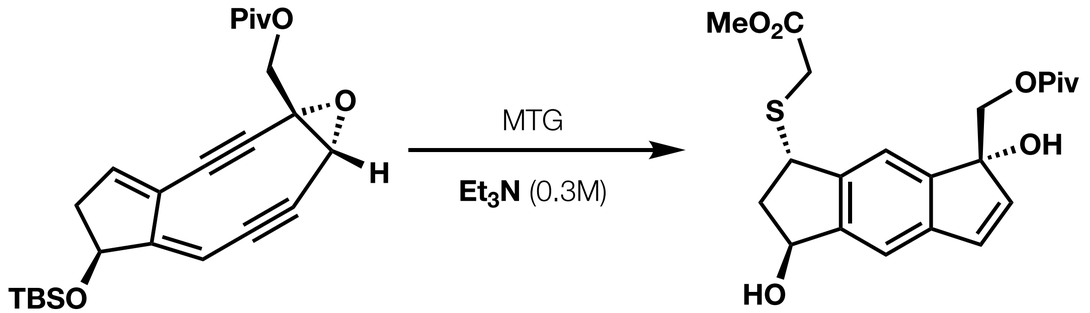

- Highly unstable neat
- But completely inert to MTG (up to 60 °C) in the absence of external base

Strong evidence that the amino sugar serves as an internal base to facilitate thiol addition

Analogous roles of aminoglycosides observed in other natural products (i.e. calichemicin)

Journal of the American Chemical Society. **1992**; 114(3): 1086–1087.

Synthesis of NCS

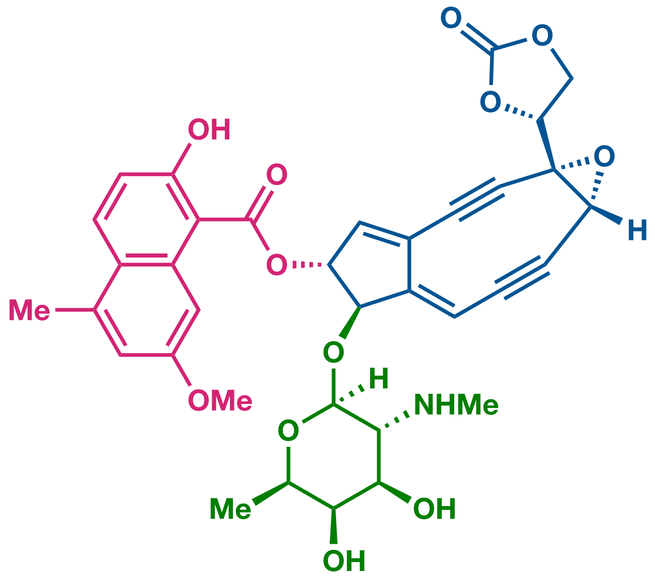

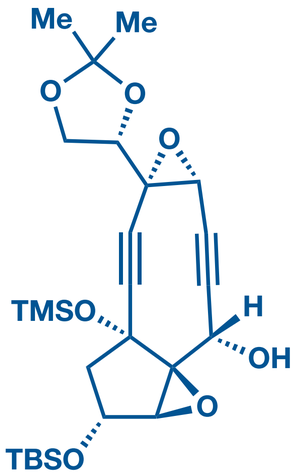

JACS **1991**; 113(2): 694–695.

JACS **1996**: 118(41): 10006–10007.

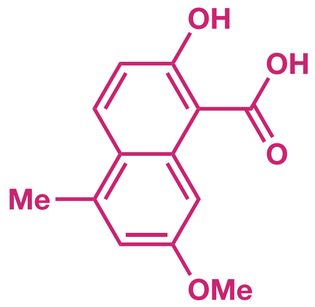

Tetrahedron Letters. **1996**; 37(5): 587–590.

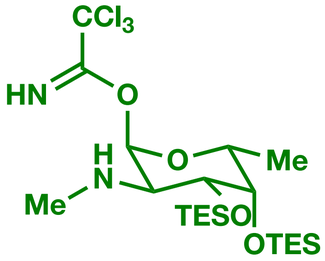

JACS **1998**; 120(21): 5319–5320.

NCS - Fragment Syntheses

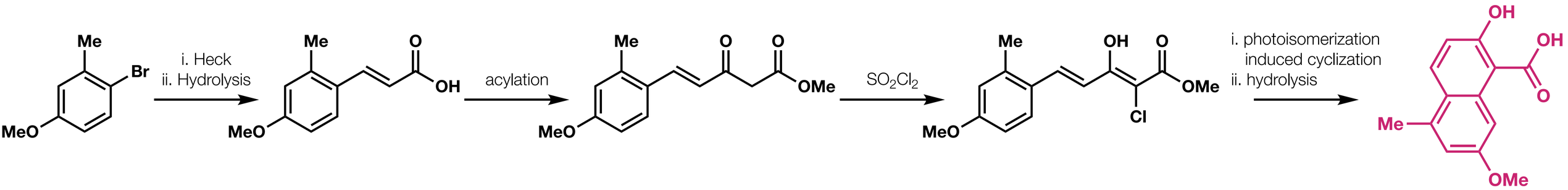

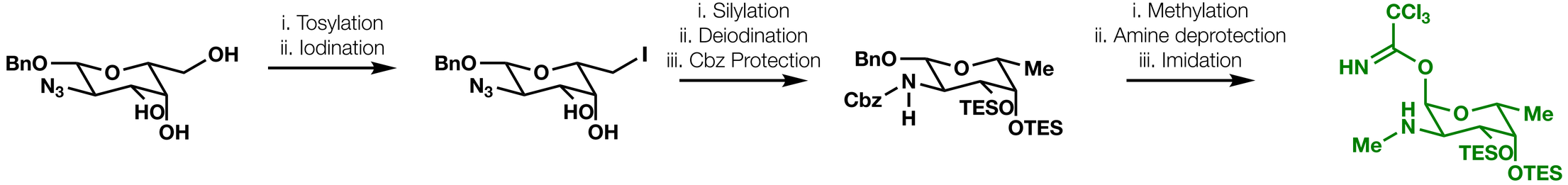

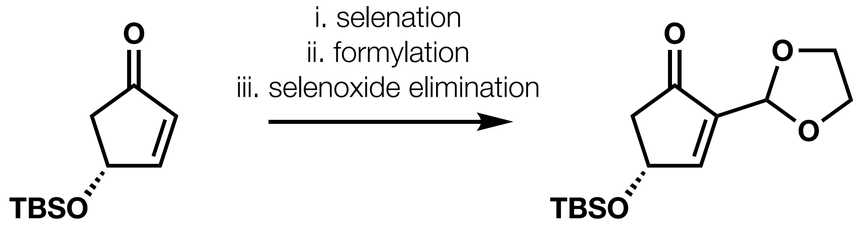

A

Tetrahedron Letters. **1996**; 37(18): 3083–3086.

Tetrahedron Letters. **1996**; 37(5): 587–590.

JACS **1998**; 120(21): 5319–5320.

Synthesis of NCS-chrom Aglycon

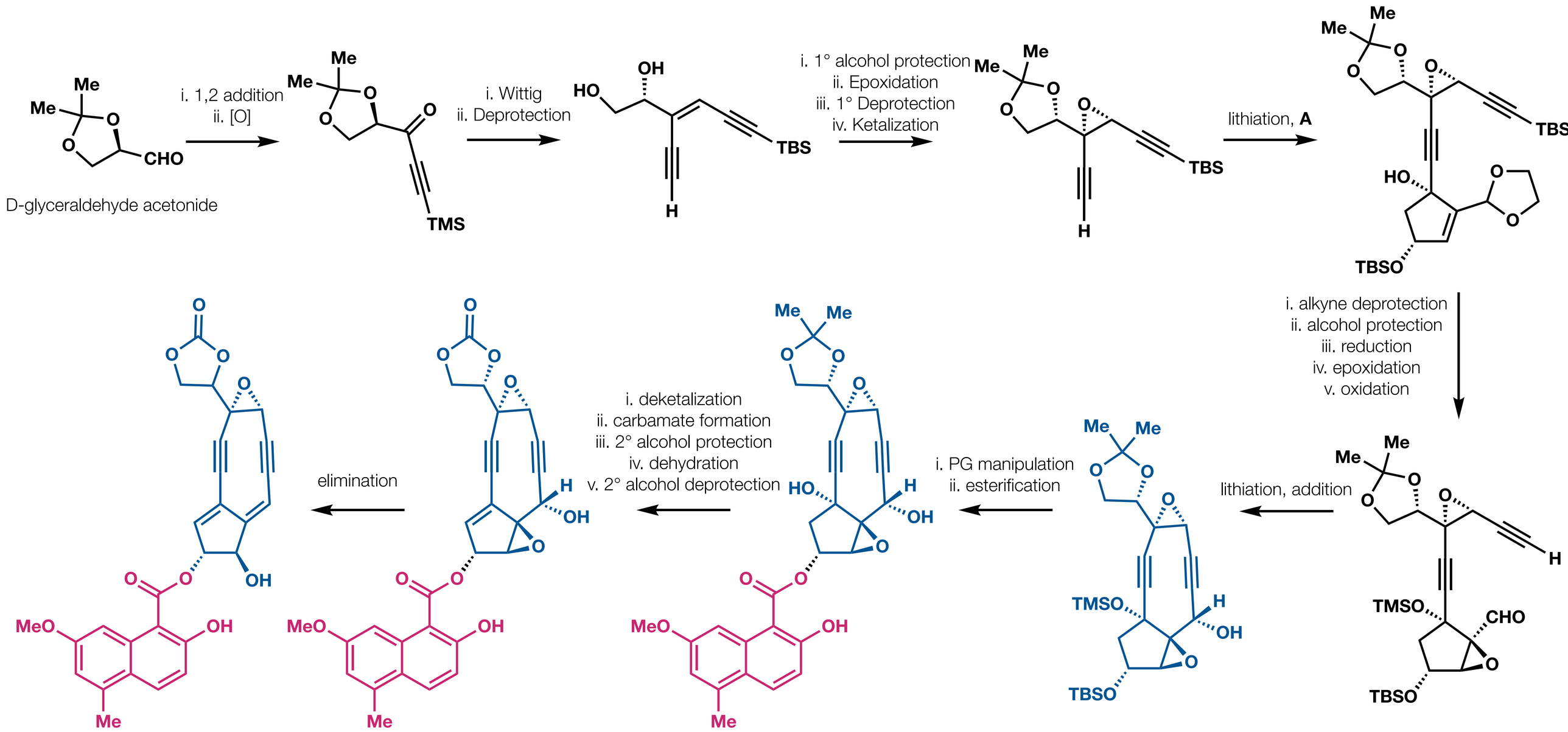

JACS **1996**: 118(41): 10006–10007.

NCS-chrom Aglycon

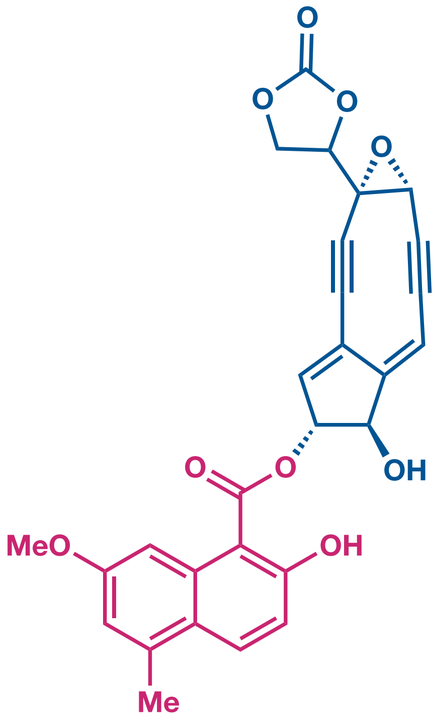

NCS-chrom aglycon

- First synthesis
- Highly Unstable
- Fresh batches were prepared and purified before biological studies

NCS-chrom Aglycon

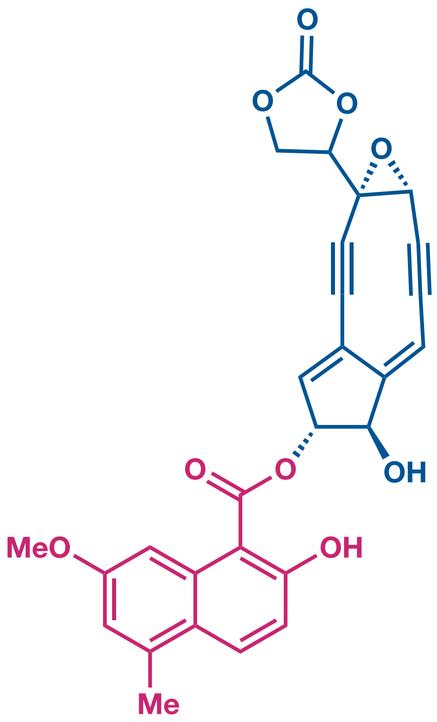

NCS-chrom aglycon

- First synthesis
- Highly Unstable
- Fresh batches were prepared and purified before biological studies

Comparison of aglycon to NCS-chrom in DNA Cleavage Assays

Key takeaways:

Aglycon does not react with thiol nucleophiles in the absence of base and DNA (consistent with model substrate studies)

When incubated with DNA and apo-NCS, 10x the concentration of the aglycon was needed to promote cleavage

MTG induced cleavage reactions with NCS-chrom are less efficient in the absence of apo-NCS

Supporting evidence that apo-NCS still binds to the aglycon

Sequence specificity of cleavage is the same (mainly AT pairs)

Kinetic studies reveal the the RDS is likely thiol addition, which occurs as a ternary complex of NCS, thiol nucleophile, and DNA

Role of sugar is hypothesized to

- Stabilize NCS-chrom (as a steric group to slow down the approach of free radicals)
- Not be responsible for DNA cleavage
- Serve as an internal base to catalyze thiol attack

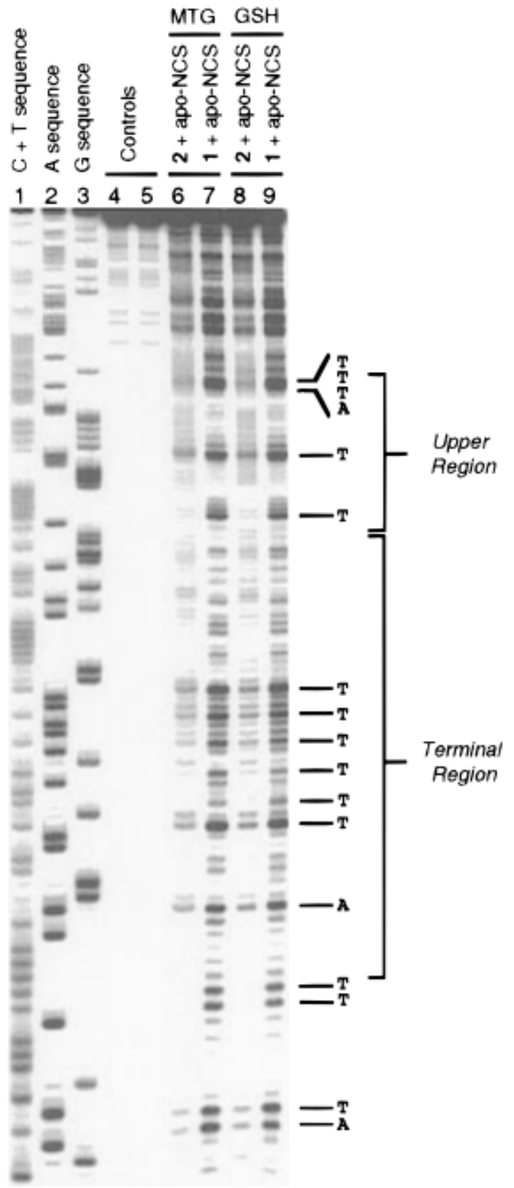

JACS **1997**; 119(13): 2965–2972.

Total Synthesis of NCS-chrom

Completion of NCS total synthesis: glycosylation

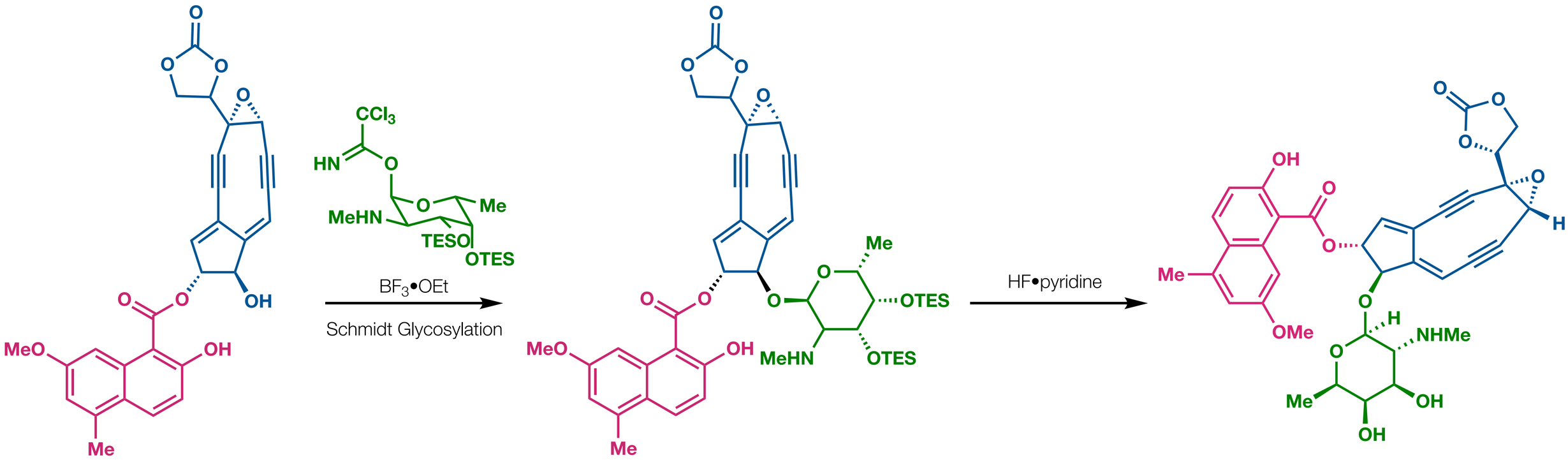

NCS-chrom aglycon

NCS-chrom

Comparison to Fucose Analog

Fucose analog

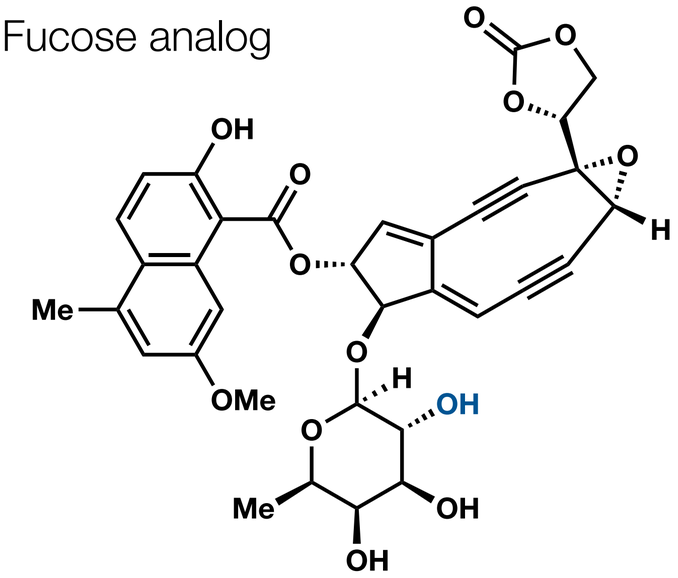

NCS-chrom

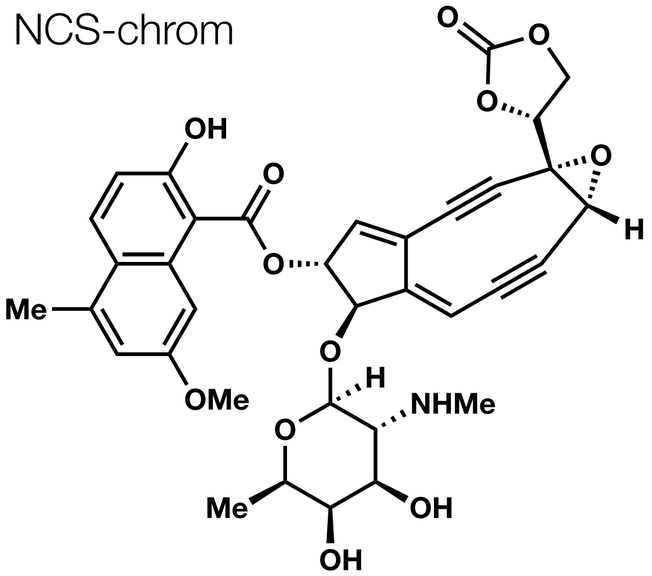

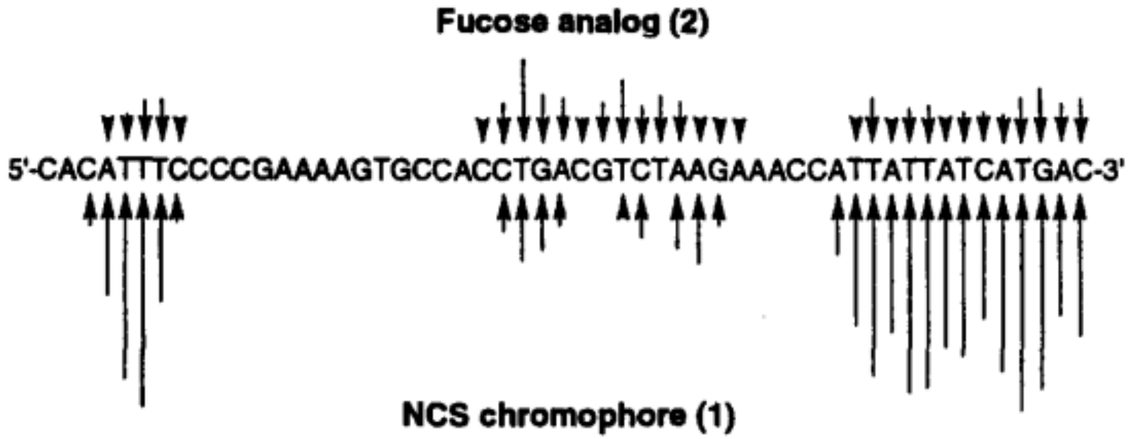

Figure 1. Histogram of DNA cleavage, upper: **2** (0.05 mM), calf thymus DNA (1 mM), 3′-^{32}P labeled DNA (see text, 50 kcpm), NaCl (20 mM), Tris–HCl (50 mM, final pH 7.5), MTG (3 mM), at 2°C; lower: **1** at 2.5-fold lower concentration (0.02 mM). DNA cleavage is normalized to the concentration of cleaving agent. After 30 min, each reaction was quenched; DNA cleavage products were assayed by denaturing 8% polyacrylamide gel electrophoresis using storage phosphor autoradiography for quantitative analysis

Tetrahedron Letters. **1999**; 40(28): 5129–5133.

Comparison to Fucose Analog

Fucose analog

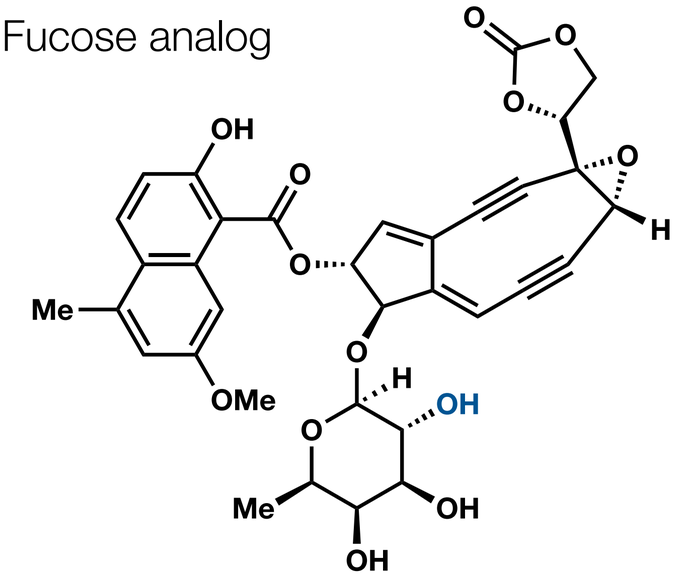

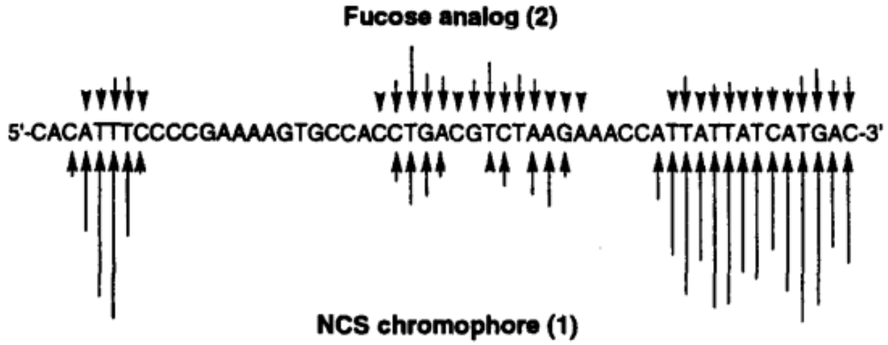

Figure 1. Histogram of DNA cleavage, upper: **2** (0.05 mM), calf thymus DNA (1 mM), 3′-^{32}P labeled DNA (see text, 50 kcpm), NaCl (20 mM), Tris–HCl (50 mM, final pH 7.5), MTG (3 mM), at 2°C; lower: **1** at 2.5-fold lower concentration (0.02 mM). DNA cleavage is normalized to the concentration of cleaving agent. After 30 min, each reaction was quenched; DNA cleavage products were assayed by denaturing 8% polyacrylamide gel electrophoresis using storage phosphor autoradiography for quantitative analysis

NCS-chrom

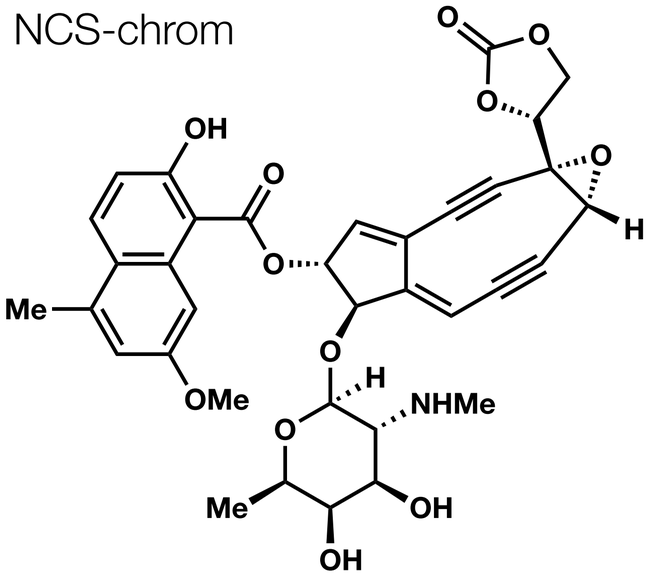

Key Takeaways

Kinetic profiles for DNA cleavage showed that the fructose analog is 3.3 (with MTG) or 4.6 (with GSH) fold slower with excess thiol

The two compounds have similar patterns of DNA cleavage

Pre-incubating the fucose analog with apo-NCS protects it from thiol activation, likely a consequence of tight binding

Tetrahedron Letters. **1999**; 40(28): 5129–5133.

Kedarcidin

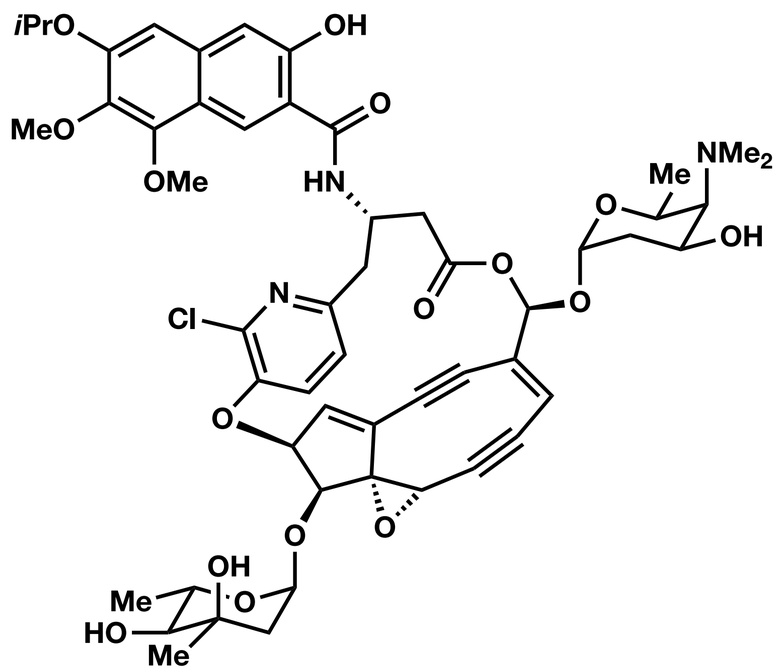

Kedarcidin Chromophore

First discovered by BMS in 1992 through fermentation of an Actinomycete strain

Like NCS, is composed of a enediyne chromophore and an apoprotein for stabilization

Kedarcidin

Structural Revisions Throughout the Years

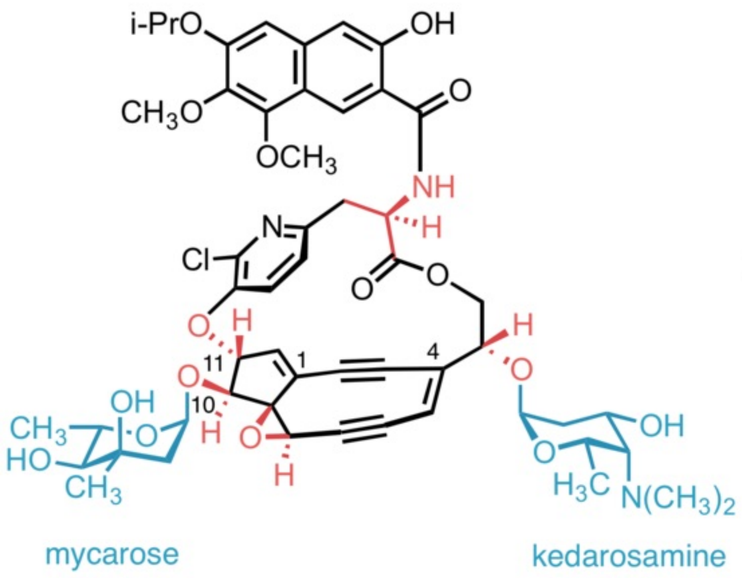

Originally proposed structure, 1993
Leet, J. E. *et al.*

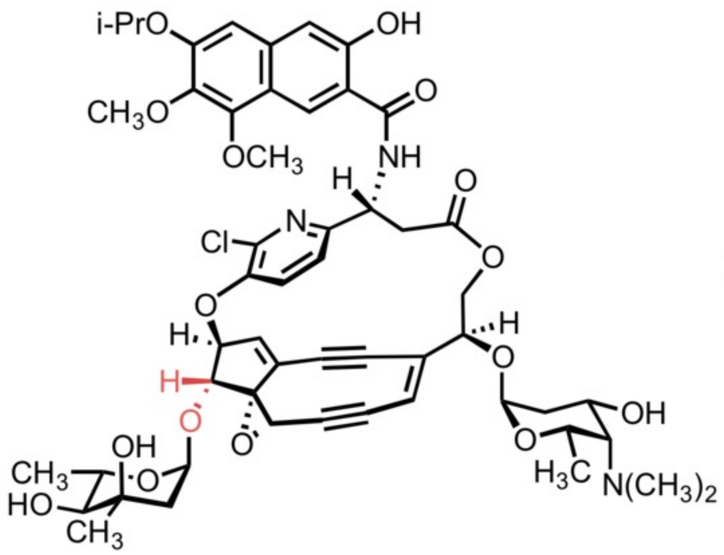

Revised structure, 1997
Hirama, M. *et al.*

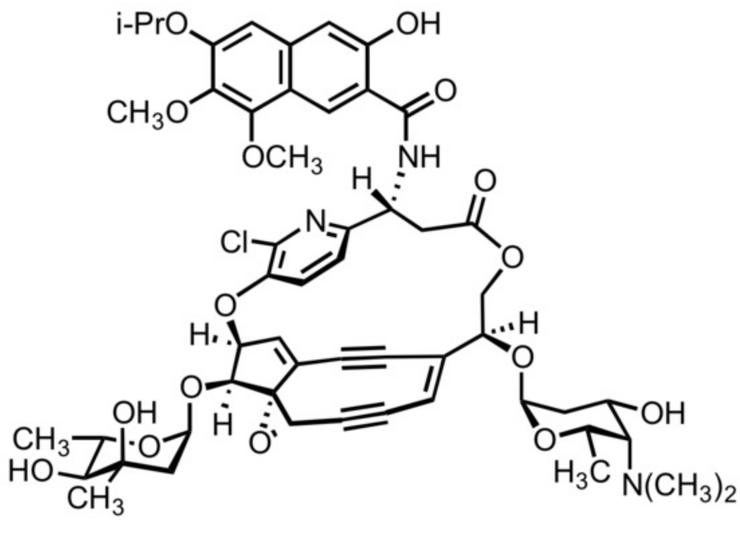

Kedarcidin chromophore
(Revised structure, 2007)

Kedarcidin on a Timeline

Structure Proposed by Leet et al.

1993

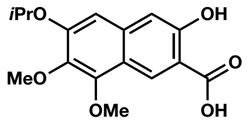

Myers' synthesis of napthoic acid component

1997

Structure Revision by Hirama

Myers' synthesis of revised aglycone

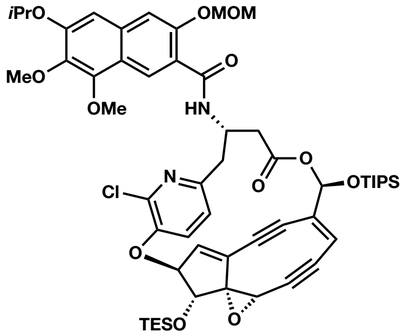

2000

2002

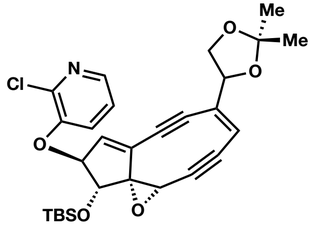

Myers' synthesis of revised core

2007

Hirama' synthesis revised aglycone

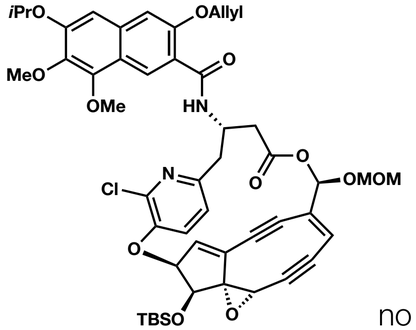

2009

Hirama' synthesis kedarcidin chromophore;
< 3% yield for final step
Product proved to be highly unstable
HRMS spectra matches natural chromophore
no additional characterization data could be obtained

2019

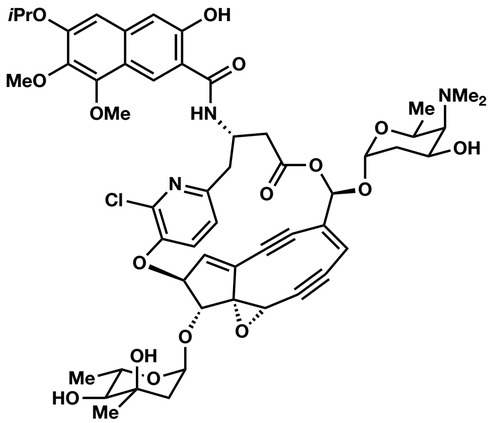

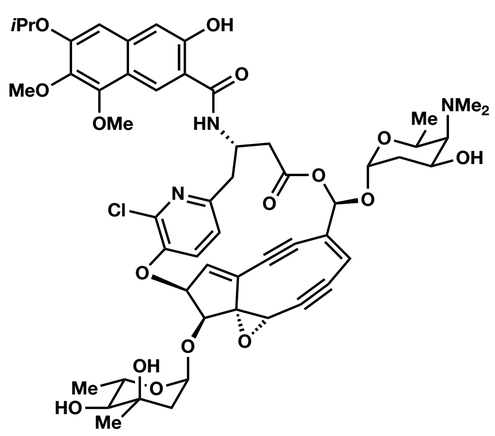

Myers' synthesis of Hirama's proposed Kedarcin:
Call for structural revision

Dynemicin A

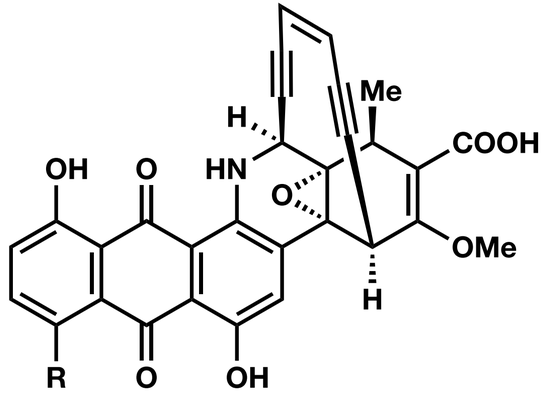

R = OH: dynemicin A

R = H: deoxydynemicin A

Isolated from *Micromonospora chersina*

Dynemicin A

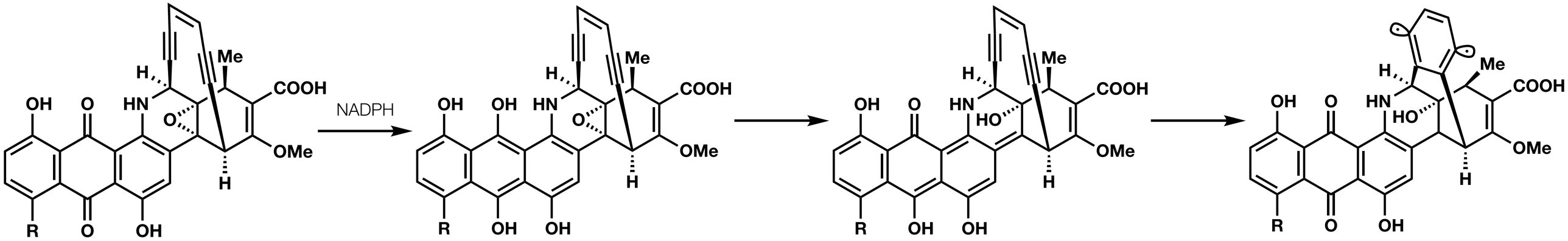

R = OH: dynemicin A

R = H: deoxydynemicin A

NADPH mechanism first proposed by Semmelhack: *Tetrahedron Lett.* **1990**, 31, 1521–1522.

Dynemicin A

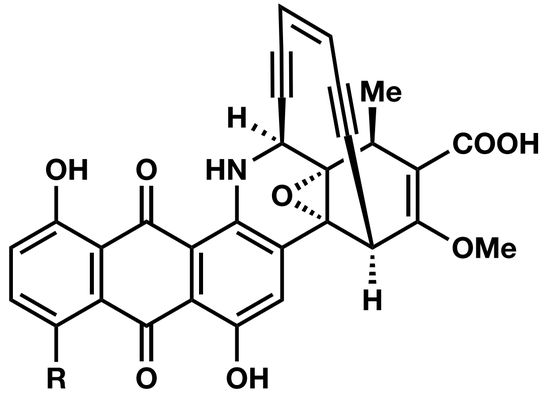

R = OH: dynemicin A

R = H: deoxydynemicin A

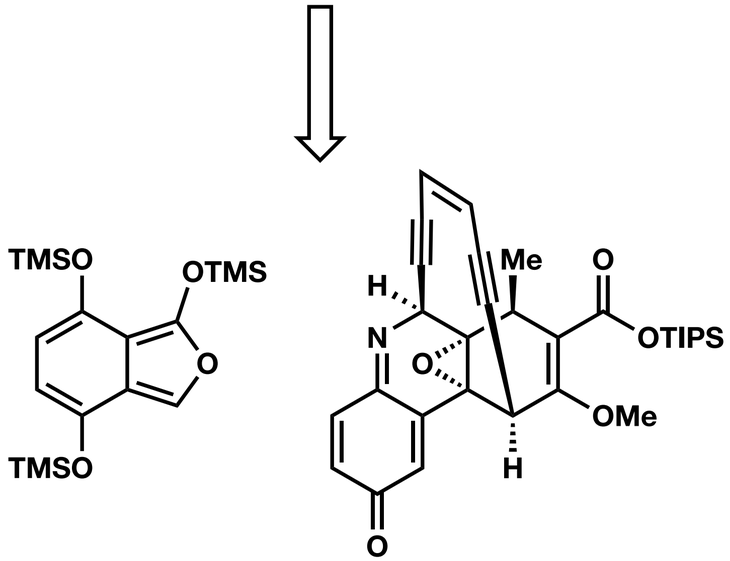

J. Am. Chem. Soc. **1994**,116, 11556-11557

Dynemicin A

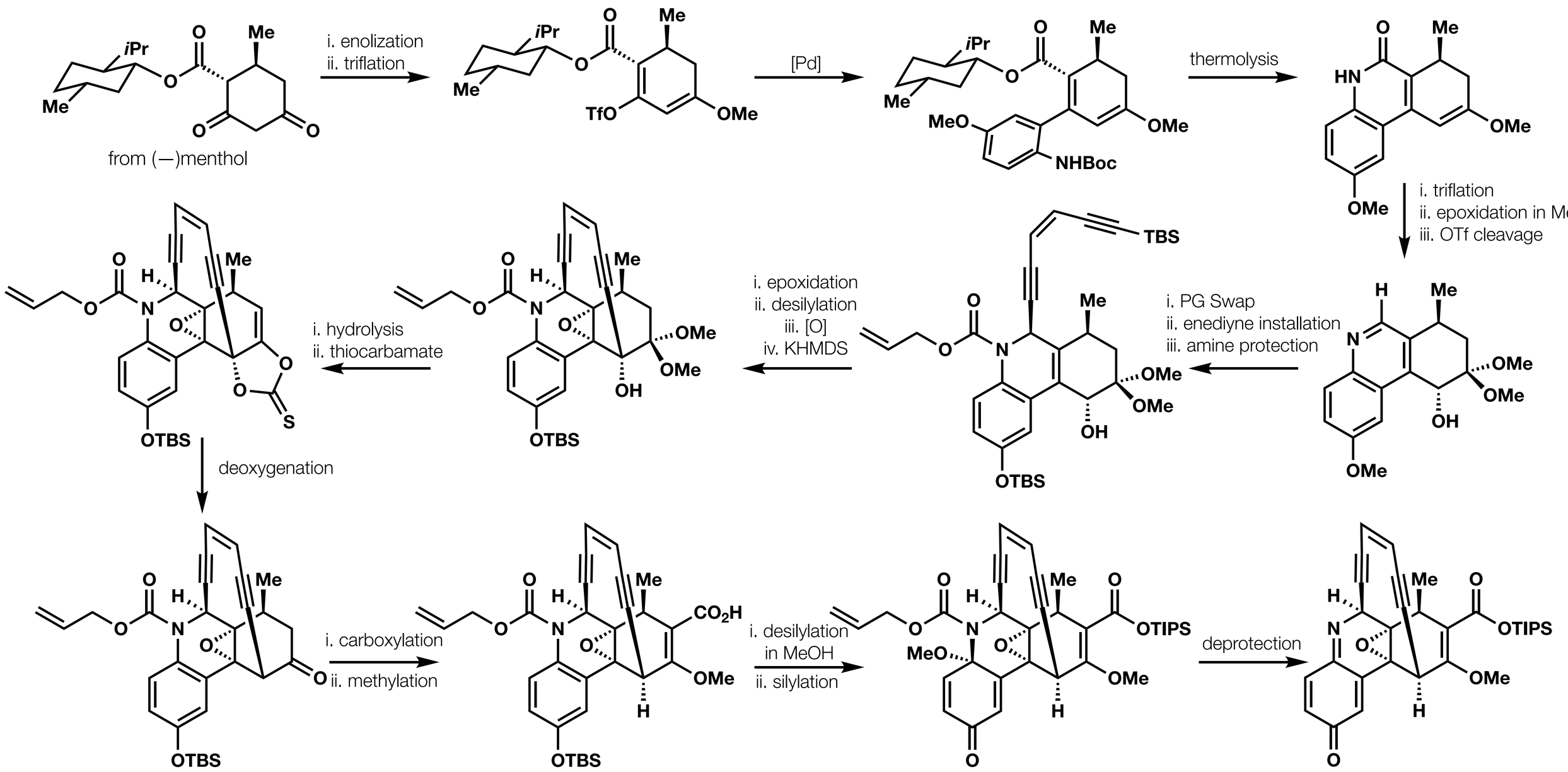
from (—)menthol
i. enolization
ii. triflation
[Pd]
thermolysis
i. triflation
ii. epoxidation in MeOH
iii. OTf cleavage
i. PG Swap
ii. enediyne installation
iii. amine protection
i. epoxidation
ii. desilylation
iii. [O]
iv. KHMDS
i. hydrolysis
ii. thiocarbamate
deoxygenation
i. carboxylation
ii. methylation
i. desilylation
in MeOH
ii. silylation
deprotection

Dynemicin A

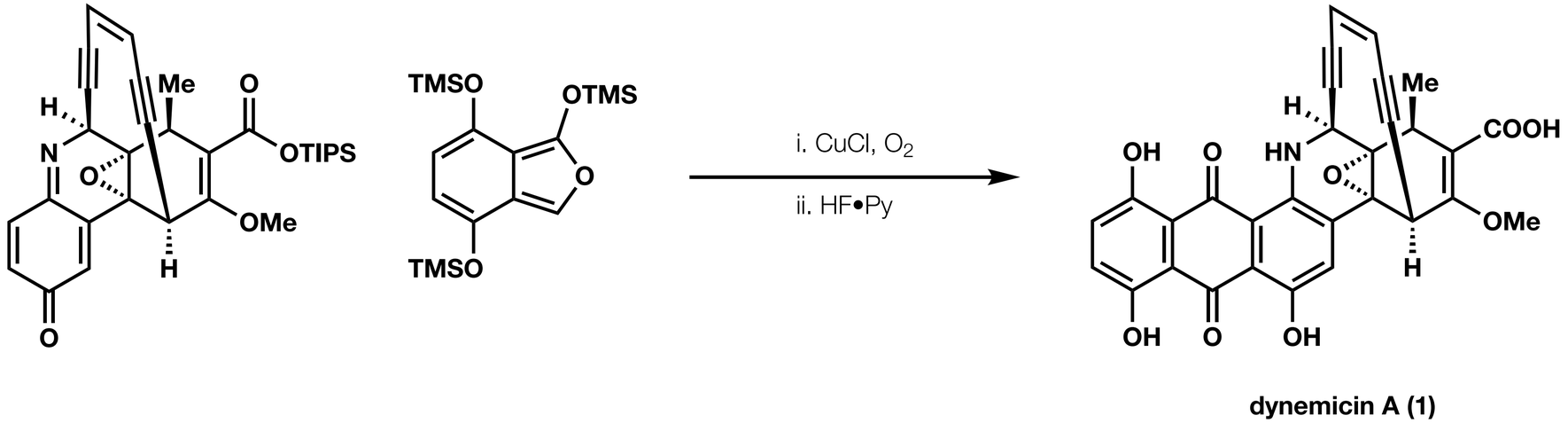

dynemicin A (1)

Chem. Biol. ***1995***, 2, 33–43.

Dynemicin A

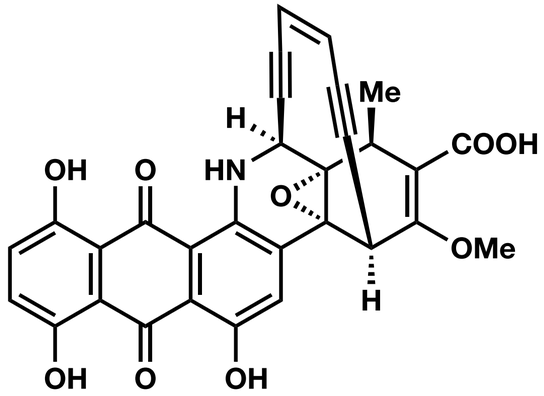

dynemicin A (1)

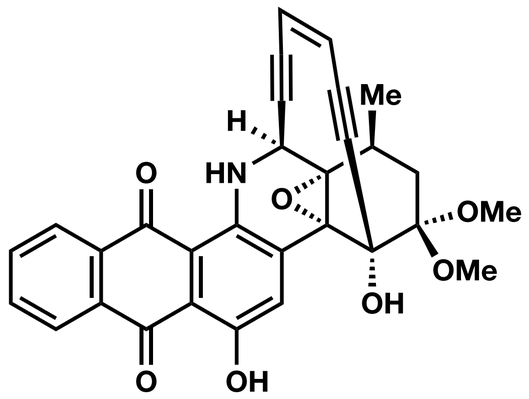

10

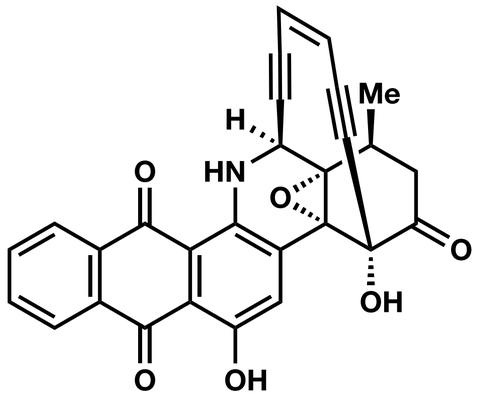

11

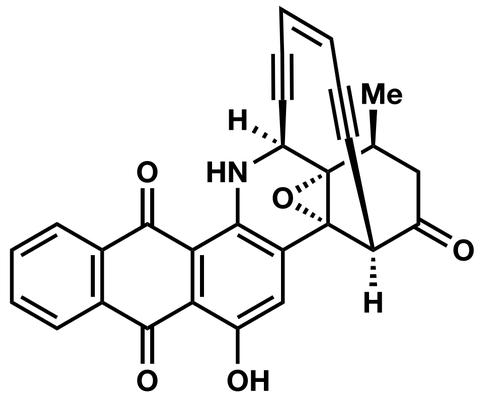

12

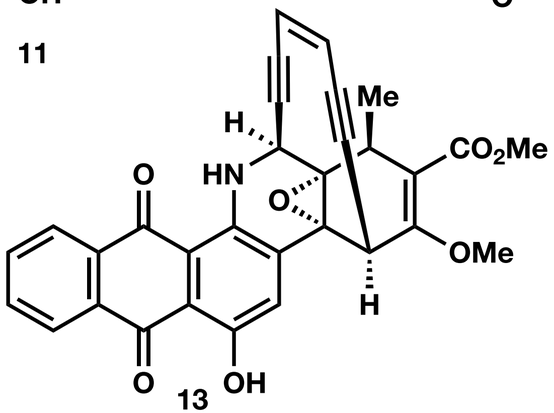

13

Comparison of dynemicin to synthetic analogs
in DNA Cleavage Assays

Key Takeaways

Little sequence specificity for cleavage observed

Different modes of activation result in differences in cleavage efficiencies between analogs

Mechanistically, 10 behaves as a perfect analog of 1

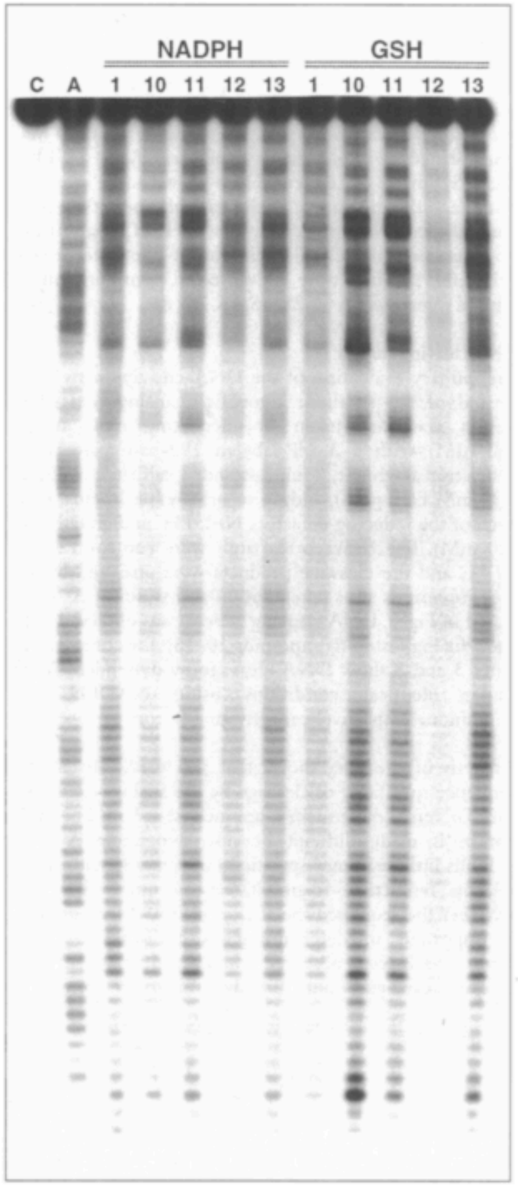

Chem. Biol. ***1995***, 2, 33–43.

Dynemicin A

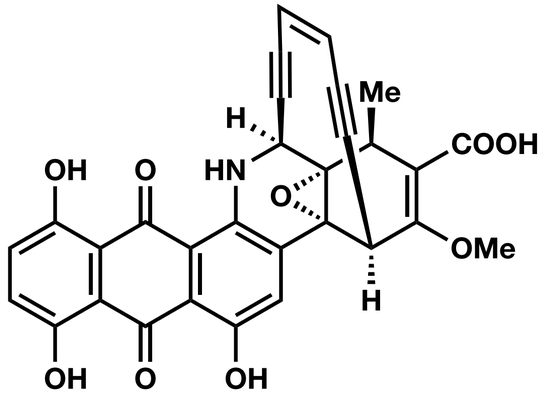

dynemicin A (1)

$K_B = (5\pm2) \times 10^4\ M^{-1}$

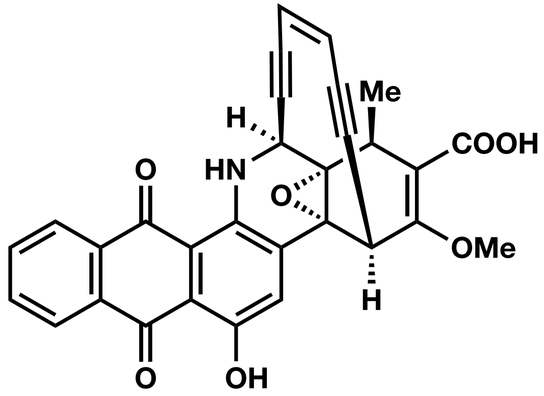

2

$K_B = (6\pm1) \times 10^2\ M^{-1}$

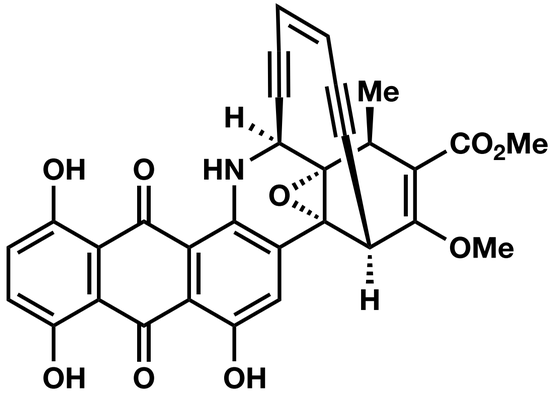

3

$K_B = (8\pm2) \times 10^6\ M^{-1}$

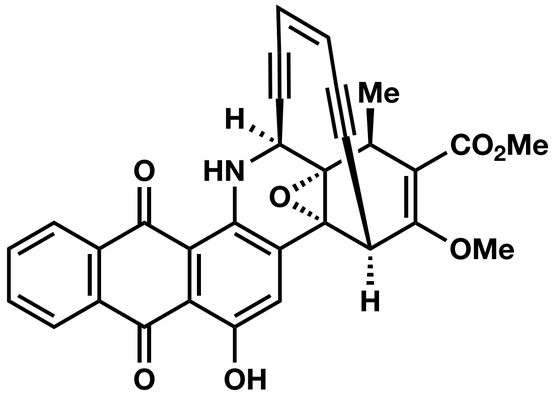

4

$K_B = (5\pm2) \times 10^4\ M^{-1}$

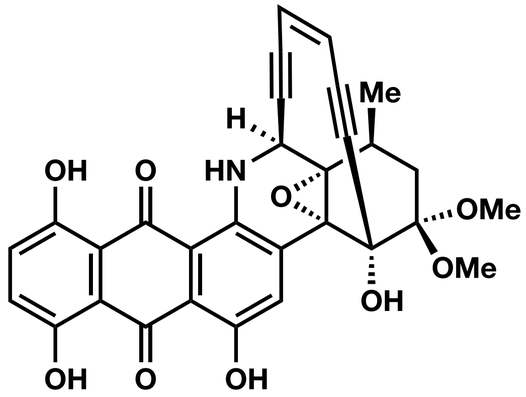

5

$K_B = (4\pm2) \times 10^6\ M^{-1}$

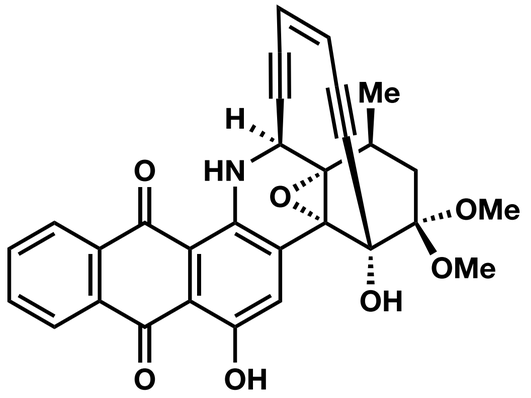

6

$K_B = (4\pm1) \times 10^4\ M^{-1}$

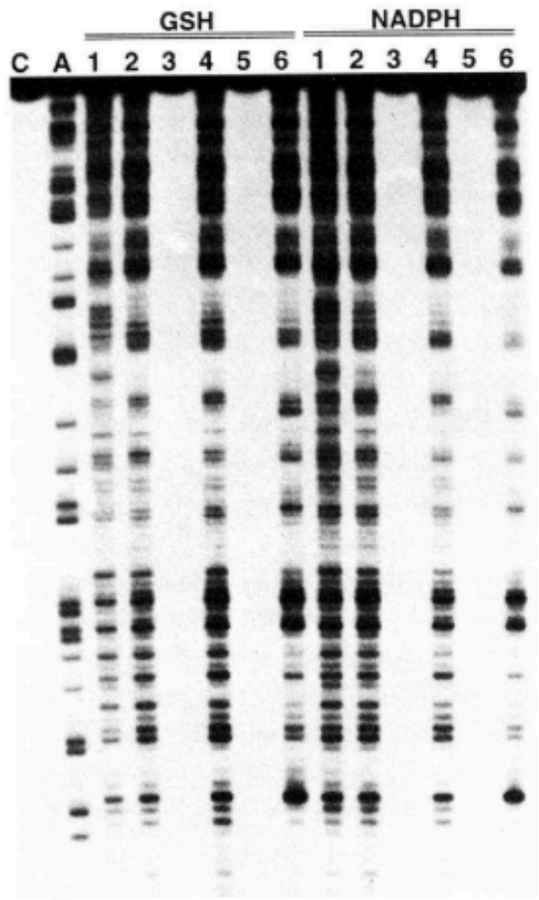

Figure 2. Cleavage of a 5′-^{32}P-labeled 193-base-pair restriction fragment of pBR322 (*Eco*RI/*Ssp*I digests) by **1**−**6** and GSH or NADPH [calf thymus DNA (1.0 mM bp), restriction fragment (~10^5 cpm), tris-HCl buffer (30 mM, pH 7.5), sodium chloride (50 mM), dynemicin A or synthetic anthraquinone (0.05 mM), 37 °C, 12 h]. Reactions initiated by addition of GSH (20 mM) or NADPH (20 mM), as indicated. Lane C: 193-bp restriction fragment alone. Lane A: products from an adenine-specific cleavage reaction (Iverson, B. L.; Dervan, P. B. *Nucleic Acids Res.* **1987**, *15*, 7823).

J. Am. Chem. Soc. **1995**,117, 7574-7575

Dynemicin A

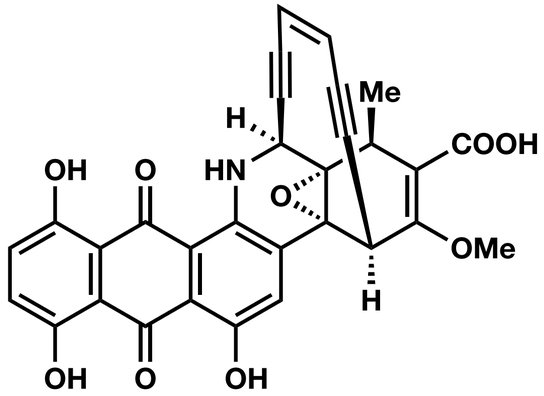

dynemicin A (1)

$K_B = (5\pm2) \times 10^4\ M^{-1}$

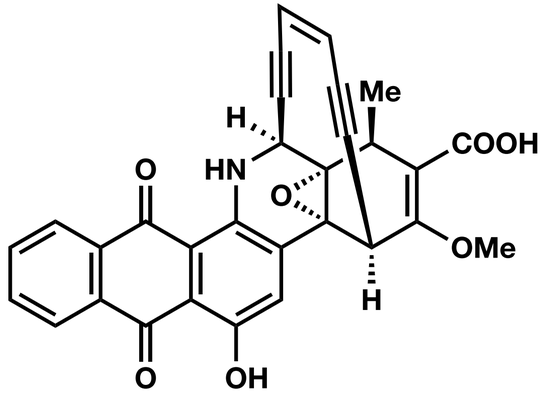

2

$K_B = (6\pm1) \times 10^2\ M^{-1}$

Weakest Binder

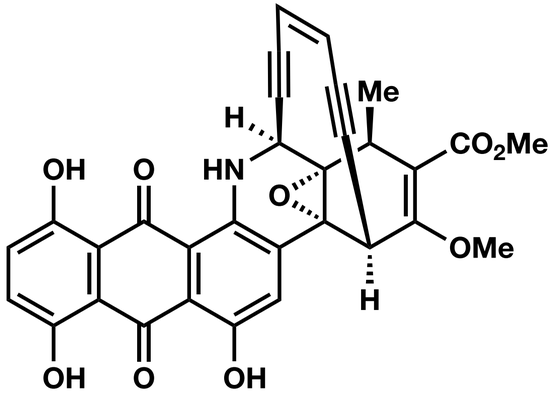

3

$K_B = (8\pm2) \times 10^6\ M^{-1}$

Strong Binder

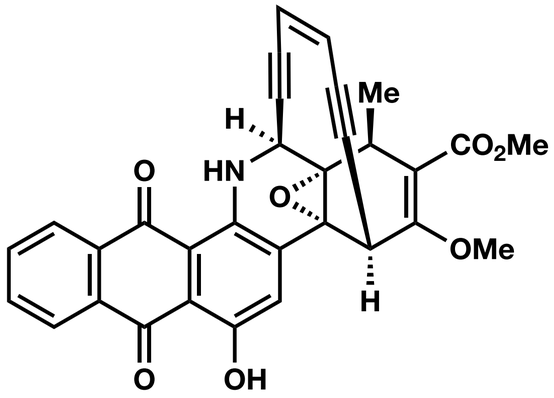

4

$K_B = (5\pm2) \times 10^4\ M^{-1}$

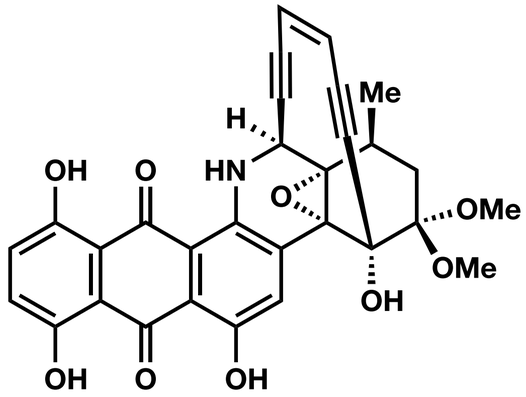

5

$K_B = (4\pm2) \times 10^6\ M^{-1}$

Strong Binder

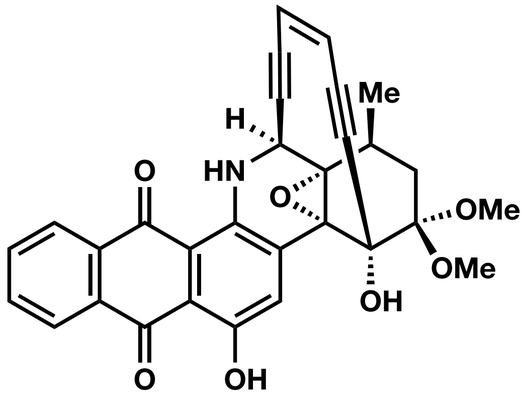

6

$K_B = (4\pm1) \times 10^4\ M^{-1}$

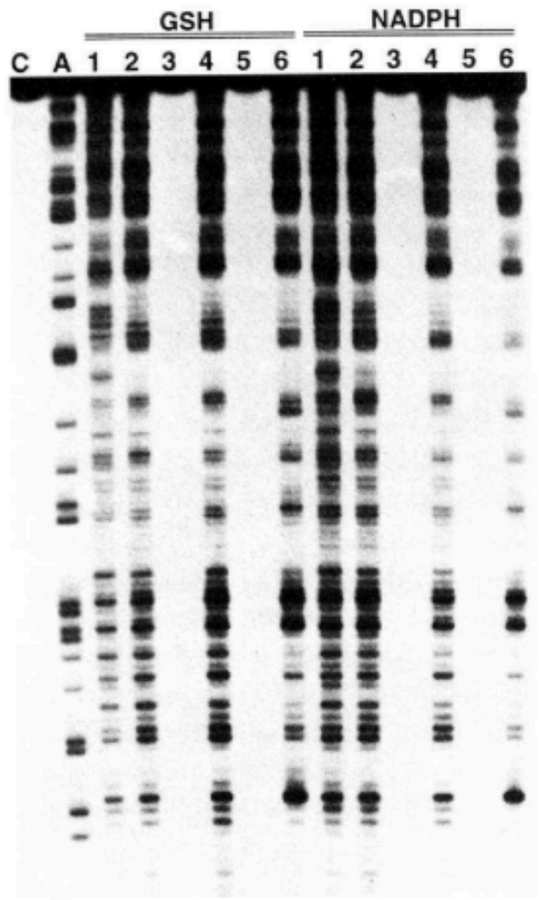

Figure 2. Cleavage of a 5′-^{32}P-labeled 193-base-pair restriction fragment of pBR322 (*Eco*RI/*Ssp*I digests) by **1**−**6** and GSH or NADPH [calf thymus DNA (1.0 mM bp), restriction fragment (~10^5 cpm), tris-HCl buffer (30 mM, pH 7.5), sodium chloride (50 mM), dynemicin A or synthetic anthraquinone (0.05 mM), 37 °C, 12 h]. Reactions initiated by addition of GSH (20 mM) or NADPH (20 mM), as indicated. Lane C: 193-bp restriction fragment alone. Lane A: products from an adenine-specific cleavage reaction (Iverson, B. L.; Dervan, P. B. *Nucleic Acids Res.* **1987**, *15*, 7823).

J. Am. Chem. Soc. **1995**,117, 7574-7575

Dynemicin A

Takeaways

If the DNA-cleaving agent binds too tightly to DNA, activation is prohibitively slow

Weakest binder should be most reactive

Validated experimentally, where **2** is ~50-fold more reactive towards GSH than **1**

However, at lower concentrations of DNA, **2** has decreased efficiency of cleaving DNA compared to **1**

Thus, the natural product, **1**, seems to strike an optimal balance (evolutionary?) between

i. Rate of Reaction with Nucleophile - where weak binding is advantageous

and

ii. Cleavage - where tight binding is advantageous

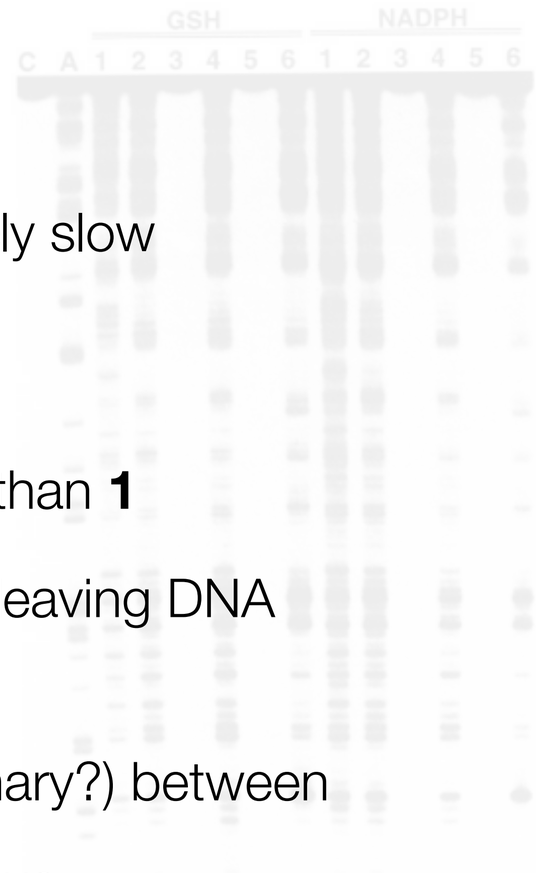

Figure 2. Cleavage of a 5′-^{32}P-labeled 193-base-pair restriction fragment of pBR322 (*Eco*RI/*Sty*I digests) by **1**−**6** and GSH or NADPH [calf thymus DNA (1.0 mM bp), restriction fragment (~10^5 cpm), tris-HCl buffer (30 mM, pH 7.5), sodium chloride (50 mM), dynemicin A or synthetic anthraquinone (0.05 mM), 37 °C, 12 h]. Reactions initiated by addition of GSH (20 mM) or NADPH (20 mM), as indicated. Lane C: 193-bp restriction fragment alone. Lane A: products from an adenine-specific cleavage reaction (Iverson, B. L.; Dervan, P. B. *Nucleic Acids Res.* **1987**, *15*, 7823).

J. Am. Chem. Soc. **1995**,117, 7574-7575

Ene-diynes

neocarzinostatin chromophore

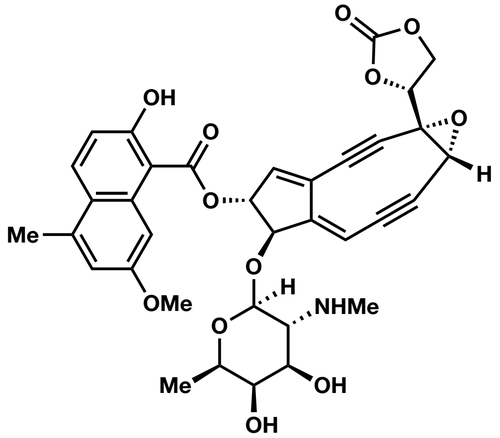

dynemicin A

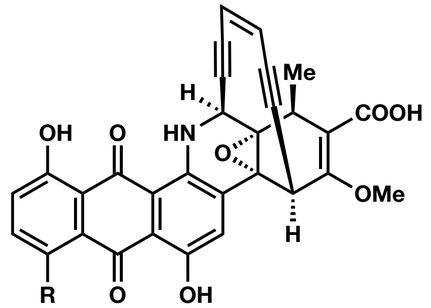

kedarcidin chromophore

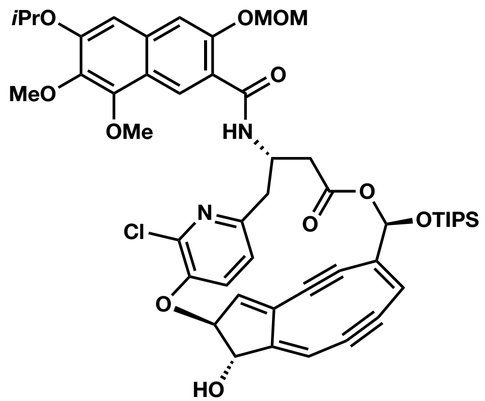

N1999A2

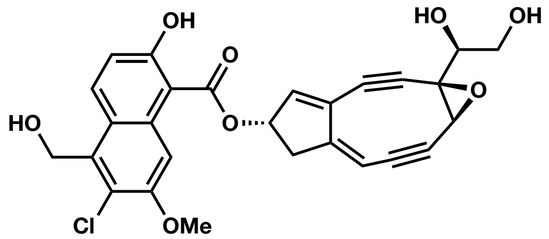

Ene-diynes

Overarching Research Theme

Utilize convergent syntheses of complex molecules for

1) the interrogation of biological mechanisms

2) structural elucidation

3) Unsuccessful (so far) in synthesizing unnatural analogs for improvement of bioactivity

neocarzinostatin chromophore

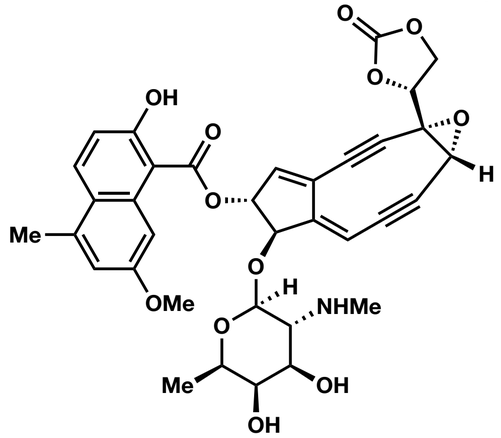

dynemicin A

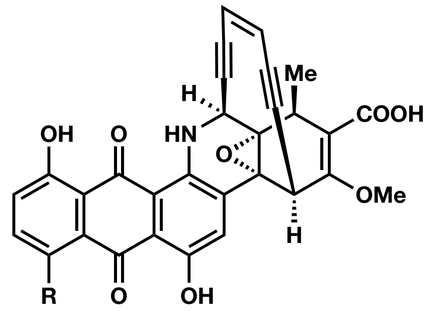

kedarcidin chromophore

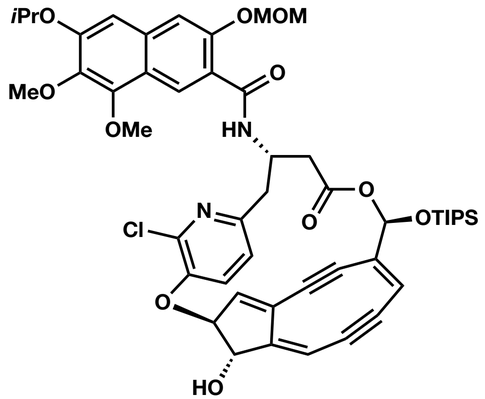

N1999A2

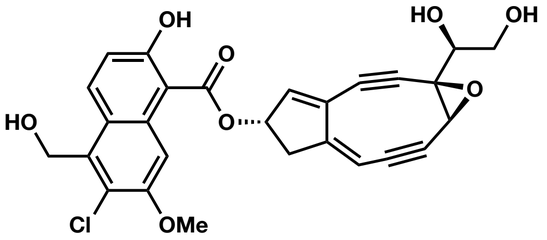

DNA Alkylaters

(—)-saframycin

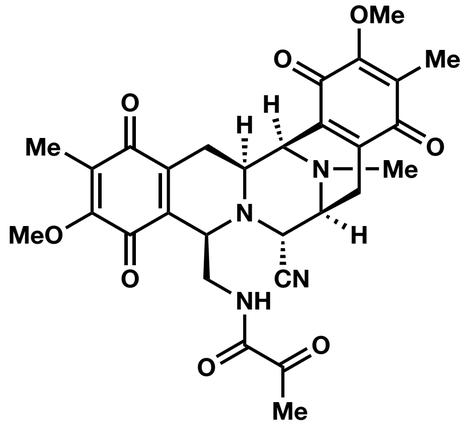

trioxacarcins

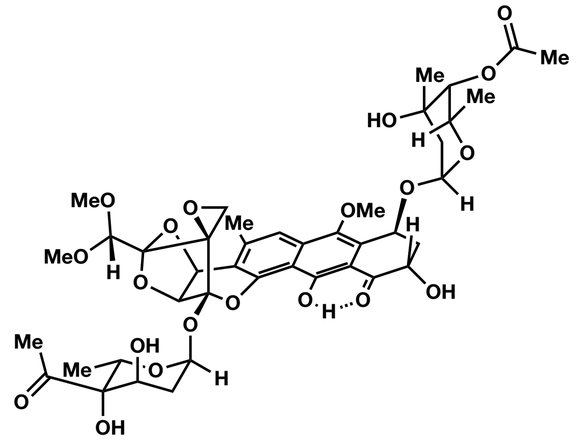

DNA Alkylaters

Mechanism of Action

Nucleophiles or reductants trigger aromatization of quinone, facilitating intercolation

Protons promote iminium formation, which can be attacked by N2 of Guanine, resulting in DNA alkylation

(—)-saframycin

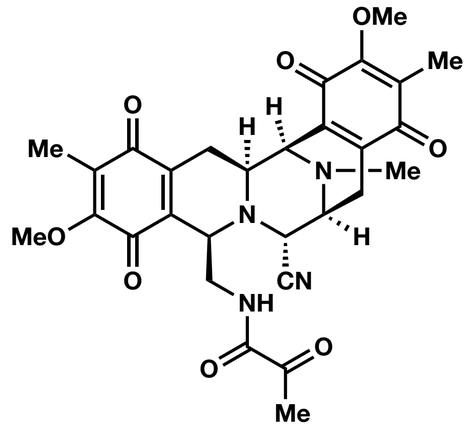

Mechanism of Action

Crescent shape facilitates binding to the minor groove of DNA (GC-rich sequences)

Spiroepoxide is susceptible to attack by N7 of Guanine, resulting in DNA alkylation

trioxacarcins

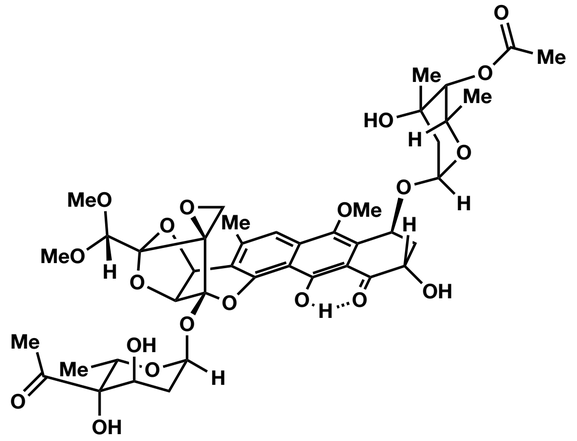

DNA Alkylaters

Related Natural Product: ET-743
(Yondelis, FDA-approved in 2015)

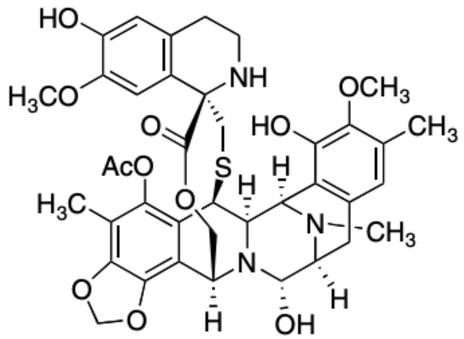

ET-743 (2)

For the treatment of advanced soft tissue sarcoma such as liposarcoma and leiomyosarcoma

(—)-saframycin

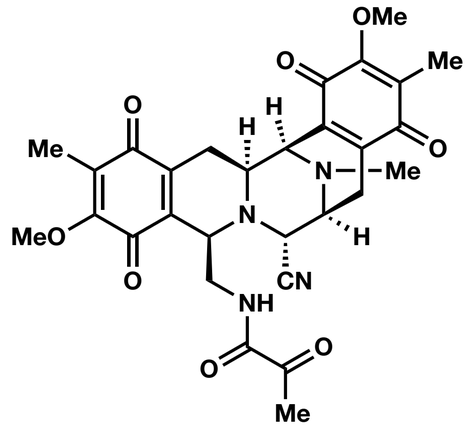

trioxacarcins

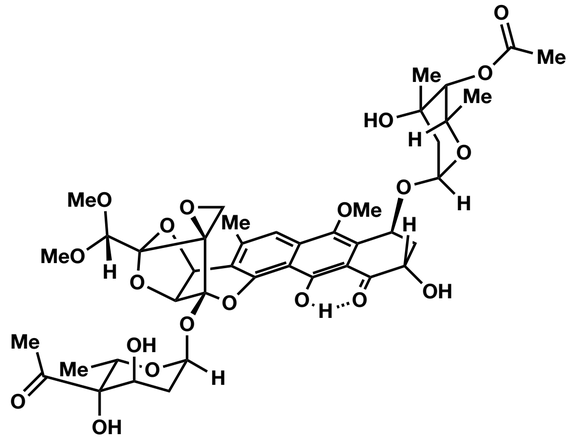

Synthesis of Saframycin

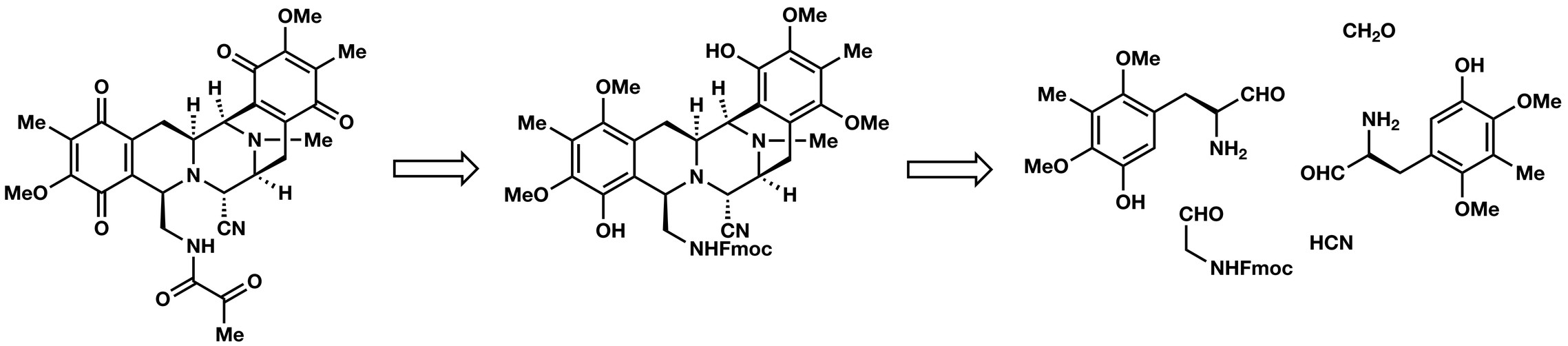

(—)-saframycin

JACS **1999**; 121(36): 8401–8402.
JACS **1999**; 121(46): 10828–10829.

Synthesis of Saframycin

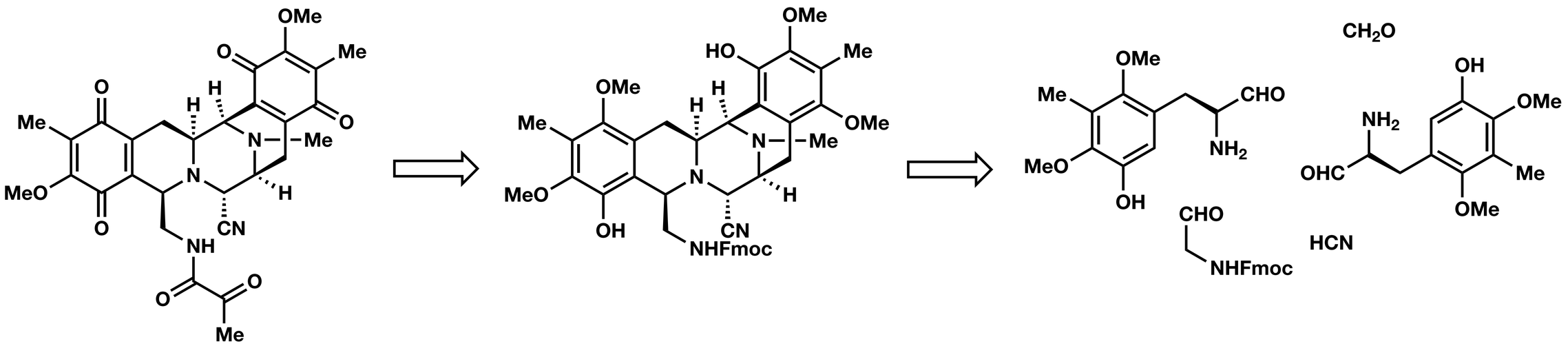

(—)-saframycin

Key Method: "*C*-protected" α-amino aldeydes

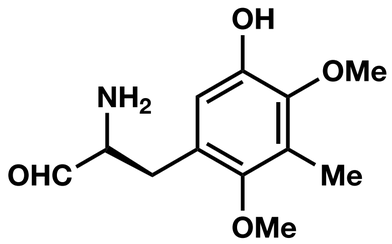

≡

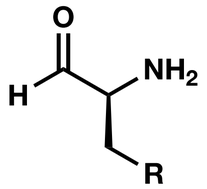

prone to epimerization

See: *J. Am. Chem. Soc.* **2000**, 122, 3236-3237

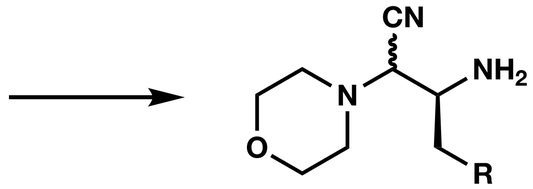

Stable to silica gel and mild acids

Minimal epimerization observed during formation and subsequent manipulations (i.e. mannich, reduction, pictet-spenger)

JACS **1999**; 121(36): 8401–8402.

JACS **1999**; 121(46): 10828–10829.

Synthesis of Saframycin

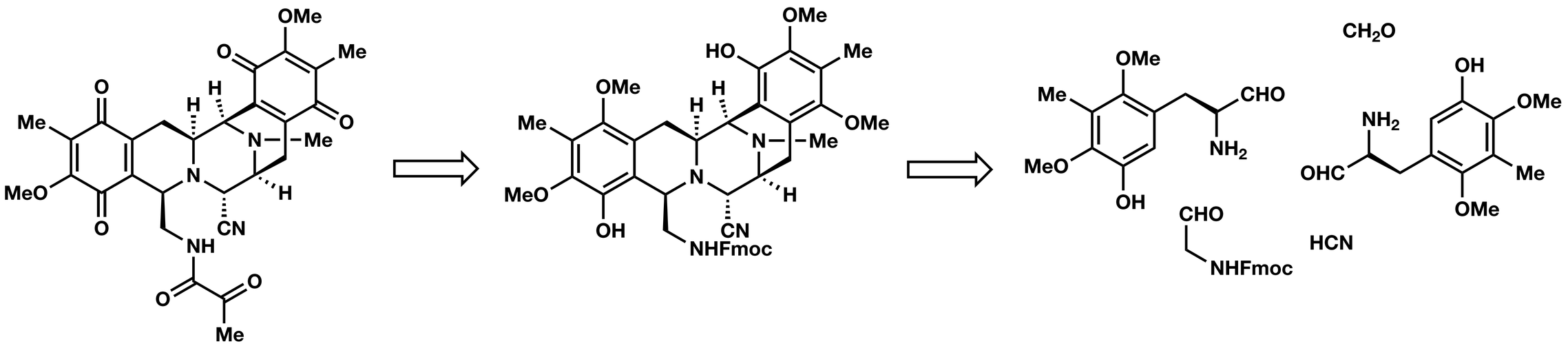

(—)-saframycin

Key Method: "*C*-protected" α-amino aldeydes

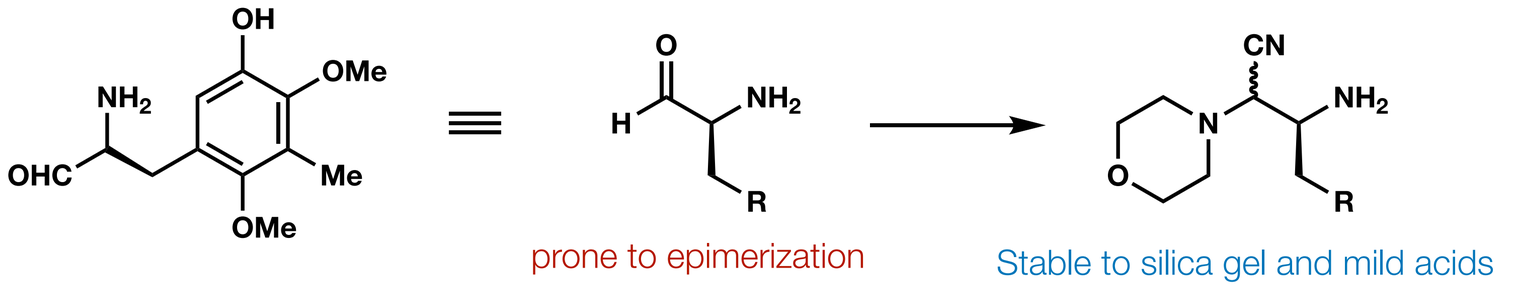

prone to epimerization

See: *J. Am. Chem. Soc.* **2000**, 122, 3236-3237

Stable to silica gel and mild acids

Minimal epimerization observed during formation and subsequent manipulations (i.e. mannich, reduction, pictet-spenger)

JACS **1999**; 121(36): 8401–8402.

JACS **1999**; 121(46): 10828–10829.

Similar strategy was applied towards the synthesis of

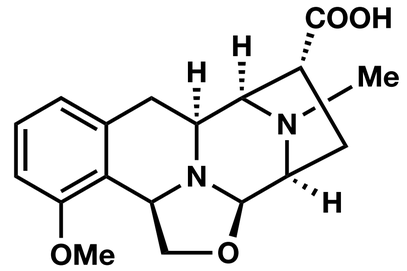

(—)-quinocarcin

JACS **2005**; 127(48): 16796–16797.

Synthesis of Saframycin

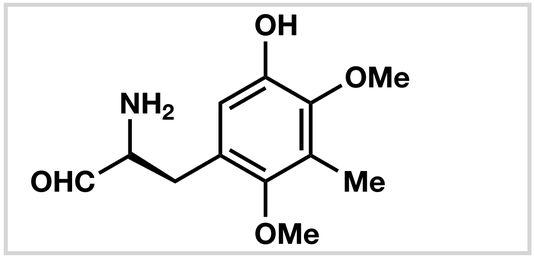

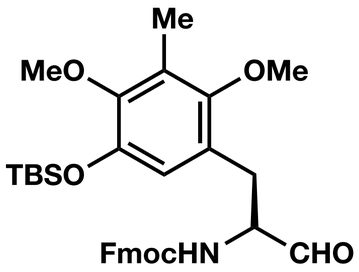

N-protected
96% ee

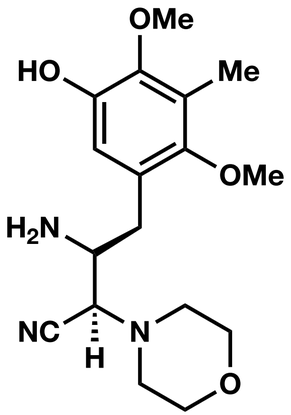

C-protected
92% ee

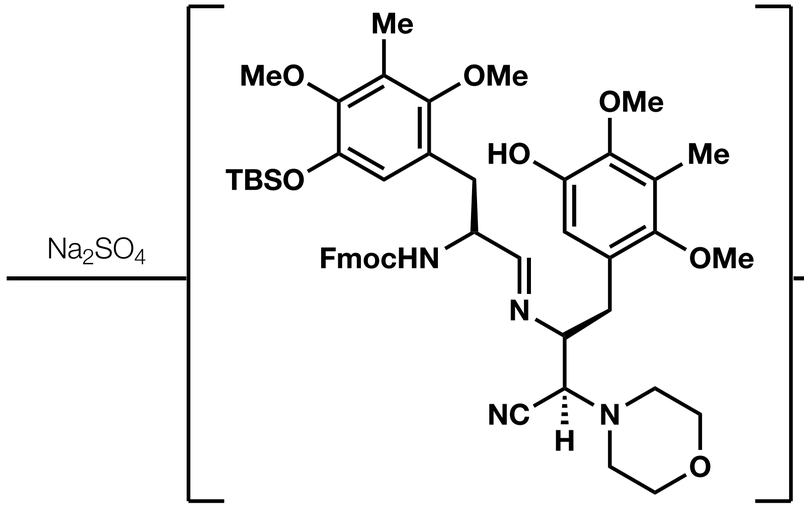

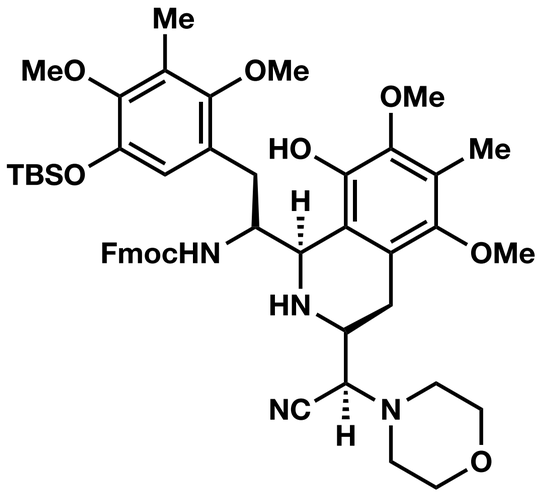

99% ee

JACS **1999**; 121(46): 10828–10829.

Synthesis of Saframycin

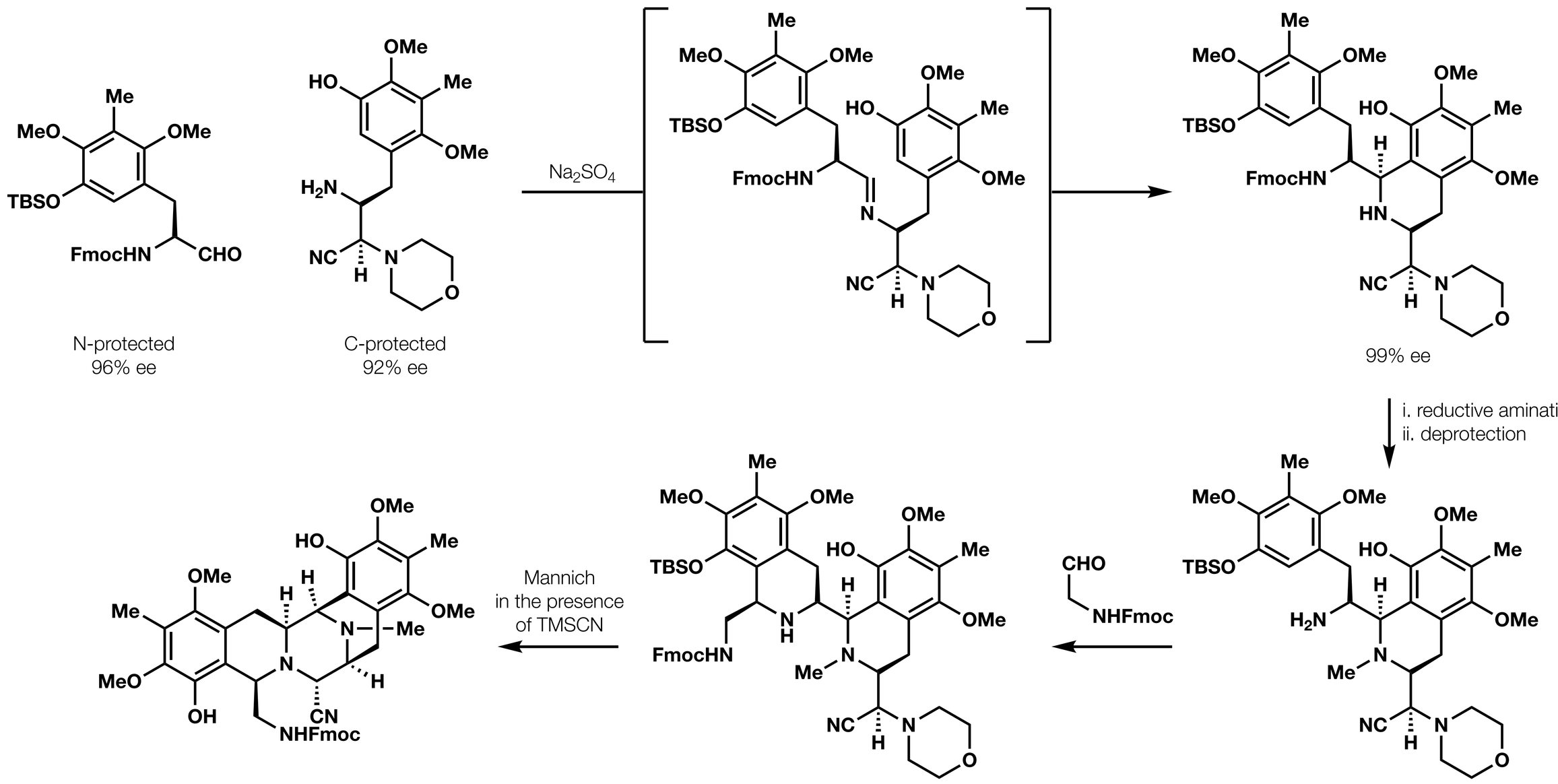

JACS **1999**; 121(46): 10828–10829.

Synthesis of Saframycin

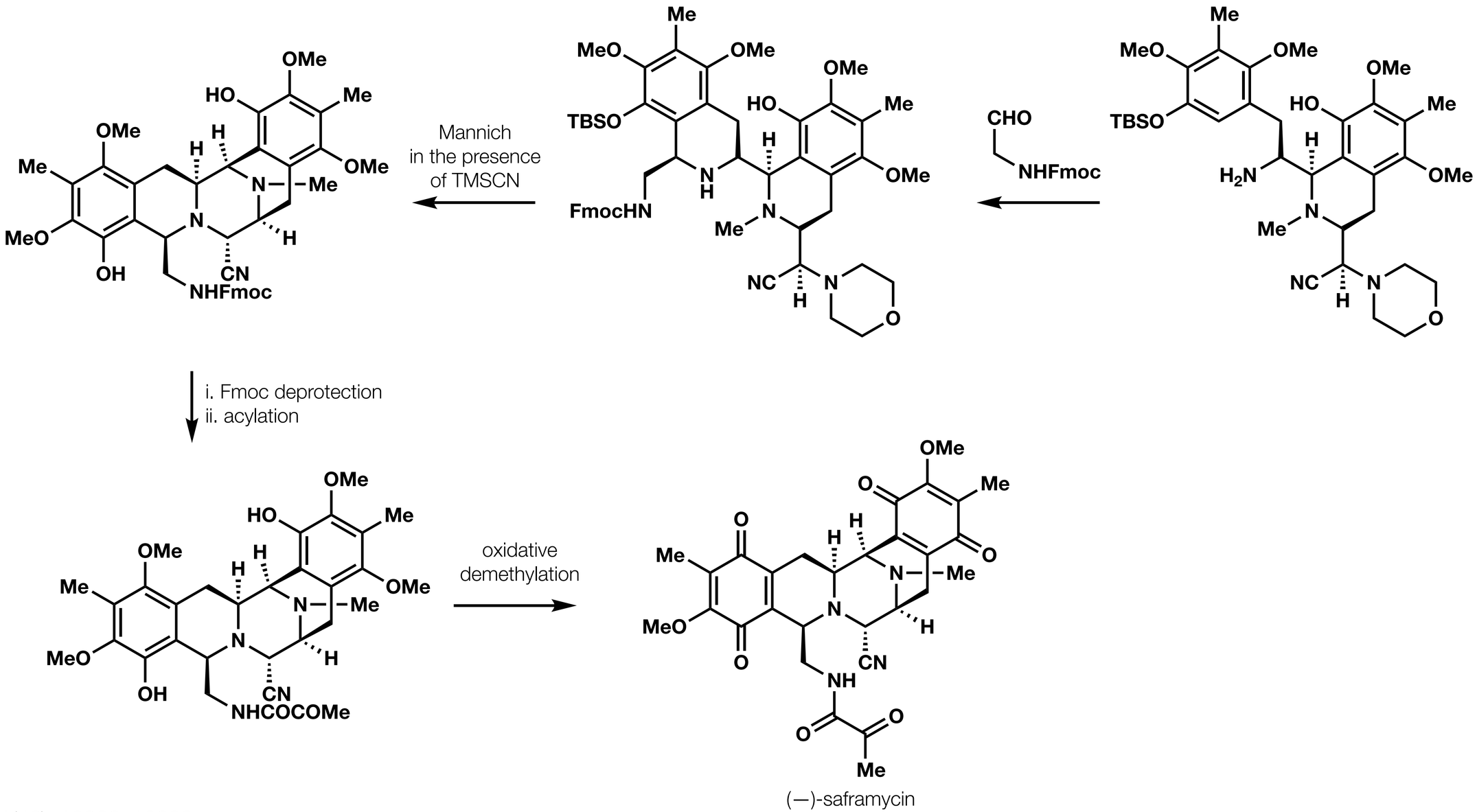

JACS **1999**; 121(46): 10828–10829.

Saframycin Analogs and Antiproliferative Activities

Prior to approval of Yondelis, Saframycin derivatives were studied as a potential alternative that mitigates side effects such as body weight loss and hepatic toxicity.

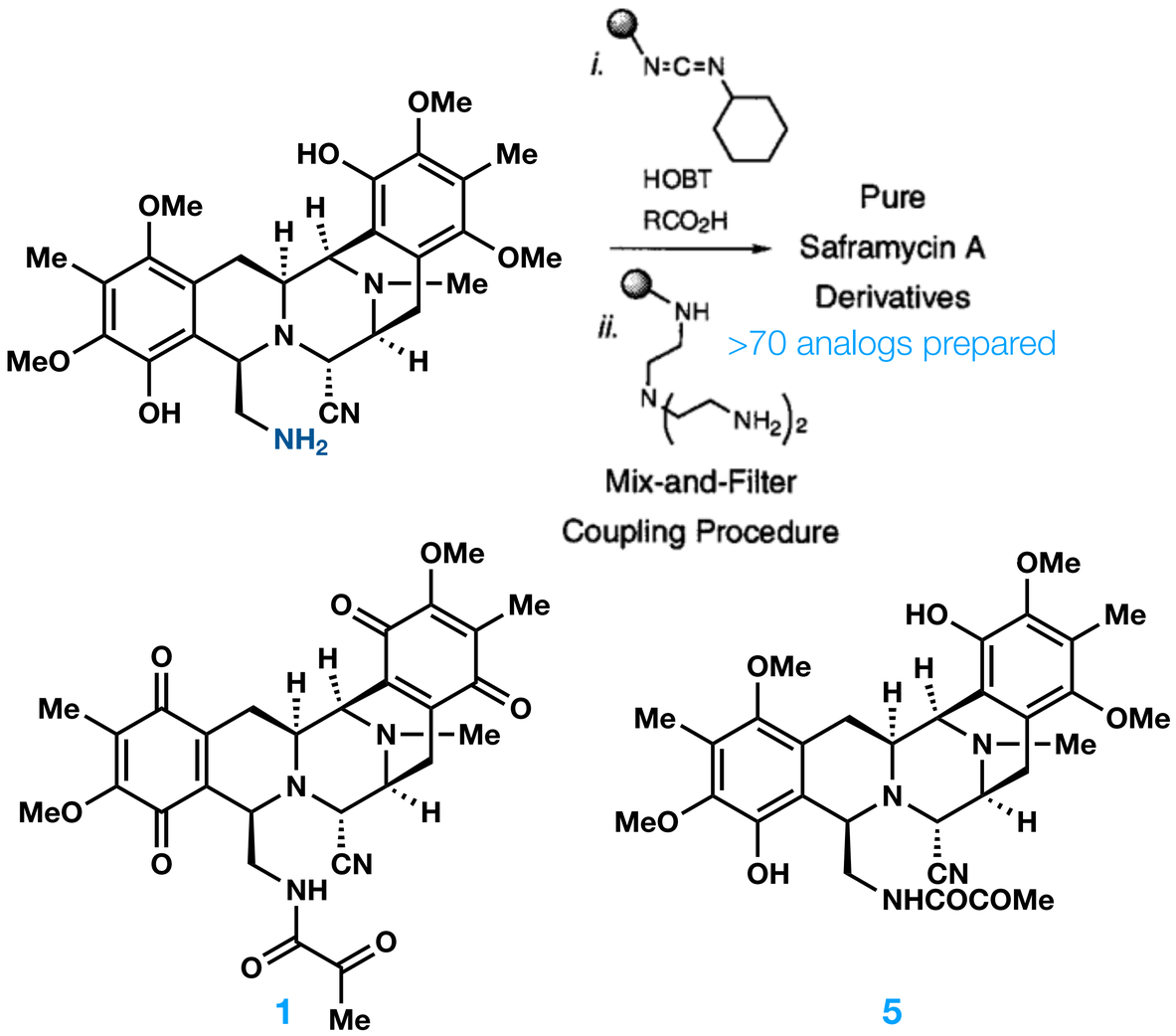

Table 1. Some of the Most Potent Bishydroquinone Derivatives of Saframycin A and Their Antiproliferative Activities

N =	IC_{50}, nM A375	IC_{50}, nM A549
Saframycin A (**1**)	5.3	133
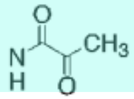 (**5**)	4.5	160
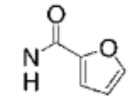	13	290
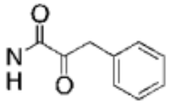	2.4	39
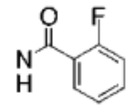	2.5	37
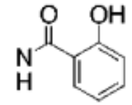 (**7**)	1.4	14
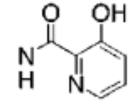 (**8**)	1.2	11
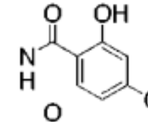 (**9**)	1.2	6.5
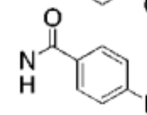	1.7	25
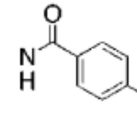	1.9	37

N =	IC_{50}, nM A375	IC_{50}, nM A549
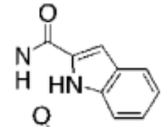	2.7	31
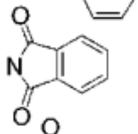 (**10**)	1.7	9.2
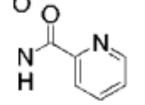	3.3	40
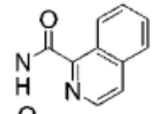	2.5	32
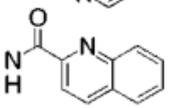 (**11**)	1.3	4.4
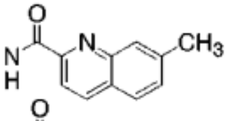 (**12**)	1.4	4.6
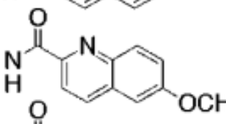 (**13**)	2.0	3.5
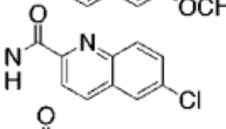 (**14**)	1.5	4.1
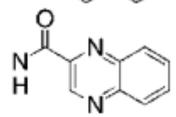 (**15**)	1.2	4.7
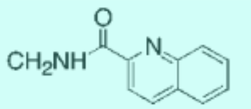 (**16**)[10]	3.6	78

A375 melanoma and A549 lung carcinoma

JACS **2001**; 123(21): 5114–5115.

Saframycin Analogs and Antiproliferative Activities

Table 1. GI50 values for the in vitro growth inhibitory effects of reference compound **3** in tumor cells from different tissues

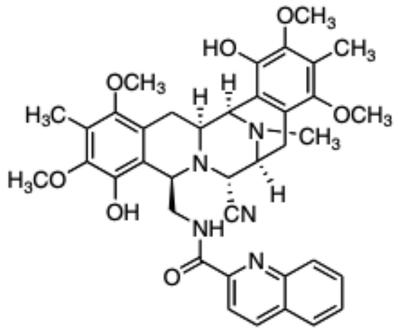

3

Cell type	Histology	GI50[a] (nM)
DLD-1	Colon	8.1
HCT-116		5.8
HT-29		7.5
CWR 22Rv1	Prostate	1.1
DU145		6.9
PC-3		6.2
A549	Lung	10.7
H1299		6.2
MDA-MB-231	Breast	4.5
HeLa-S3	Cervical	6.6
HT-1080	Fibrosarcoma	5.0
BxPC-3	Pancreatic	5.8
Nalm-6	B-cell leukemia[b]	0.6
P12	T-cell leukemia[b]	1.9

[a] Cells were grown in culture to a specific cell density and treated with compound for a period equal to two cell doubling times.
[b] Ref. 13.

Table 2. GI50 values for the growth inhibitory effects of saframycin analogs in tumor cells

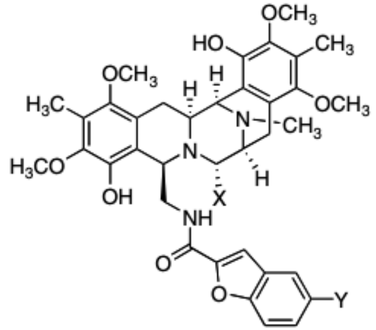

5

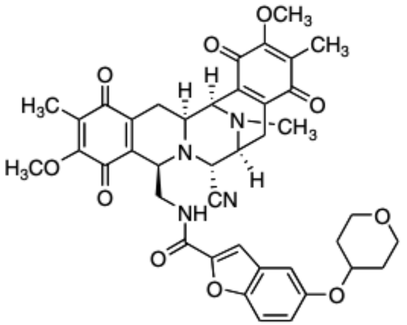

6

	X	Y	Yield (%)	GI50 (nM)			
				HCT-116	DLD-1	PC-3	A549
5a	CN	H	72	5.5	ND[b]	ND[b]	ND[b]
5b	CN	Tetrahydropyran-4-yloxy	60	3.2	8.3	2.7	18.9
5c	CN	2-(*N*-Morpholino)-ethoxy	ND[a]	8.1	22.4	11.7	57.5
5d	OH	Tetrahydropyran-4-yloxy	58	5.5	10.4	5.0	20.6
5e	H	Tetrahydropyran-4-yloxy	45	>300	ND[b]	ND[b]	ND[b]
6			44	17.3	26.5	16.5	ND[b]

[a]Yield of last step not determined; [b]GI50 value not determined.

DNA Alkylaters

(—)-saframycin

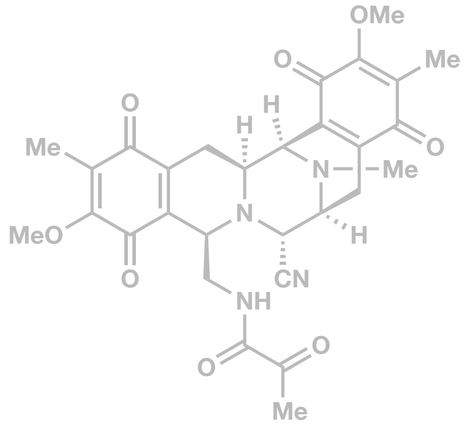

trioxacarcins

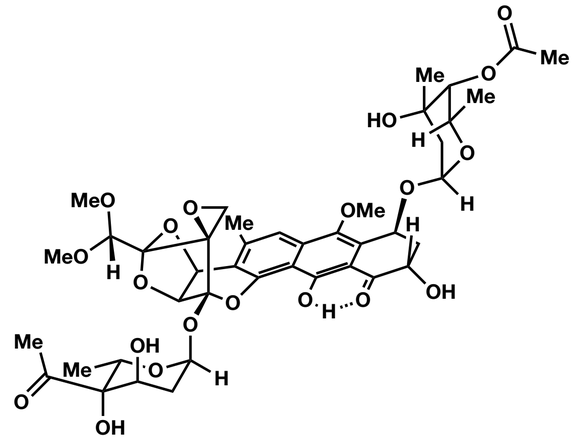

Trioxacarcins

DC-45-A1

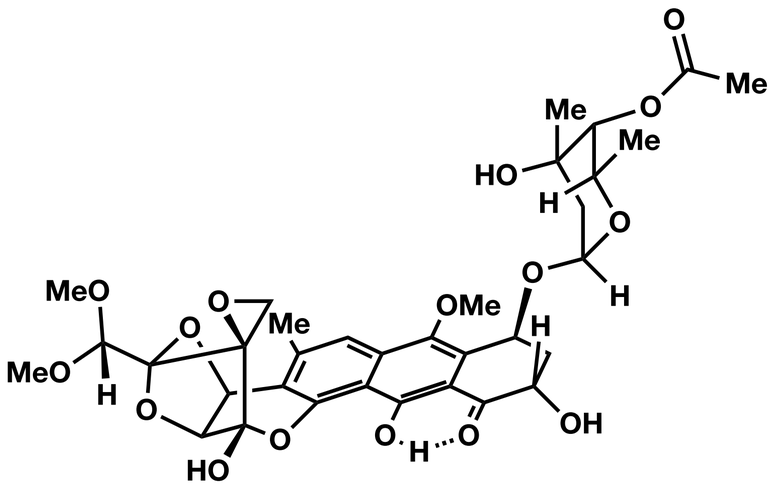

LL-D49194α1

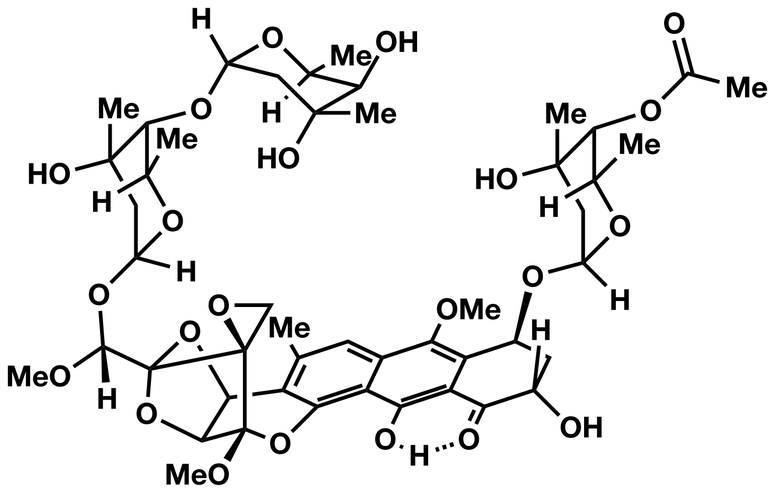

Trioxacarcin A

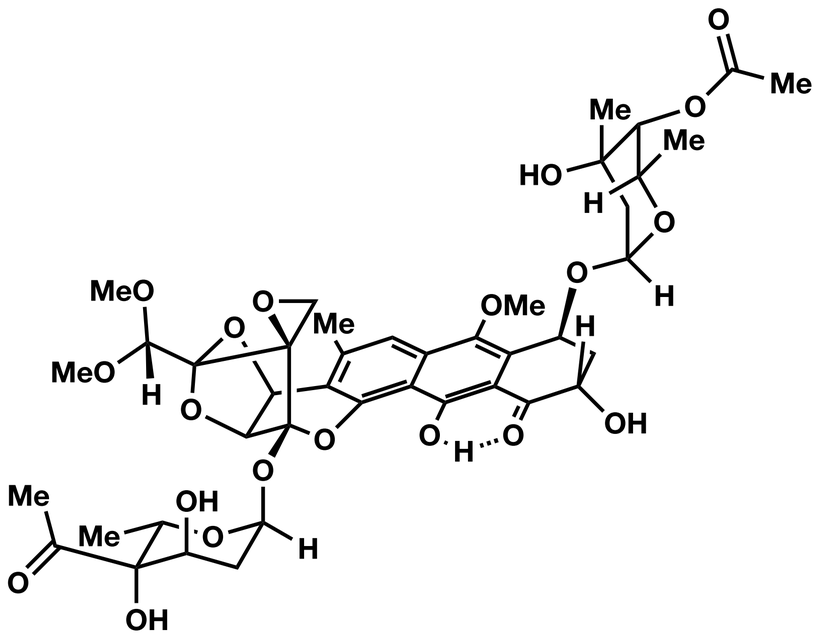

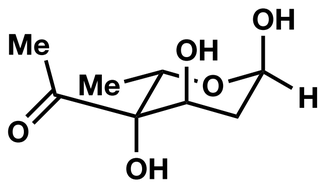

α-Trioxacarcinose B

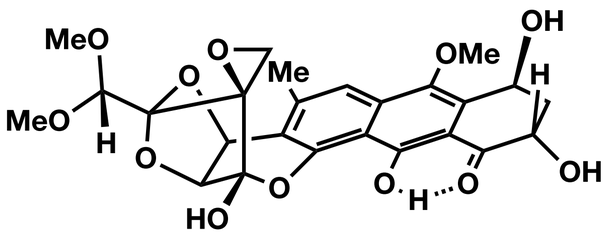

DC-45-A2

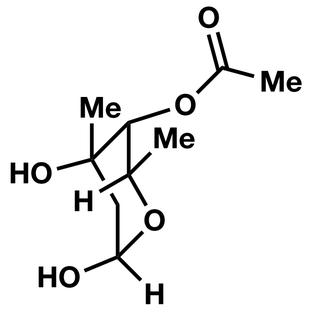

α-Trioxacarcinose A

PNAS U.S.A. **2011**, 108, 6709–6714.

Trioxacarcins

DC-45-A1

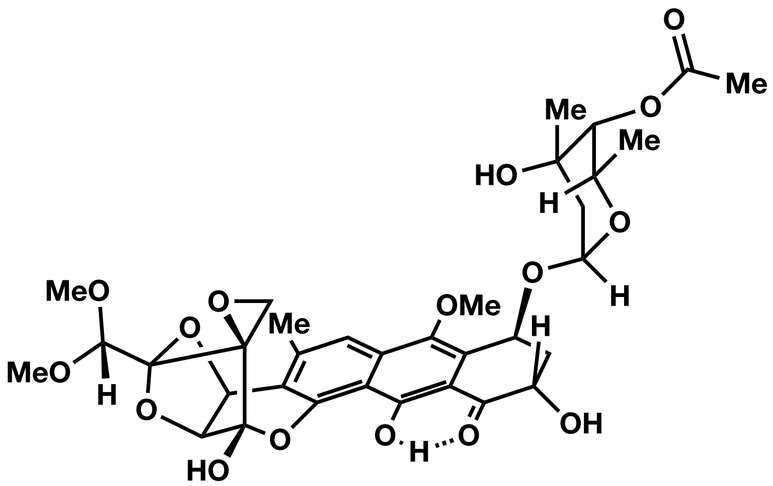

LL-D49194α1

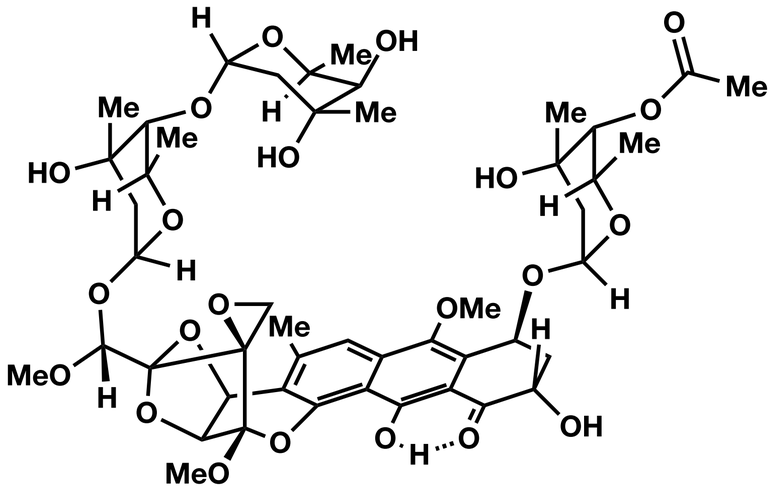

Trioxacarcin A

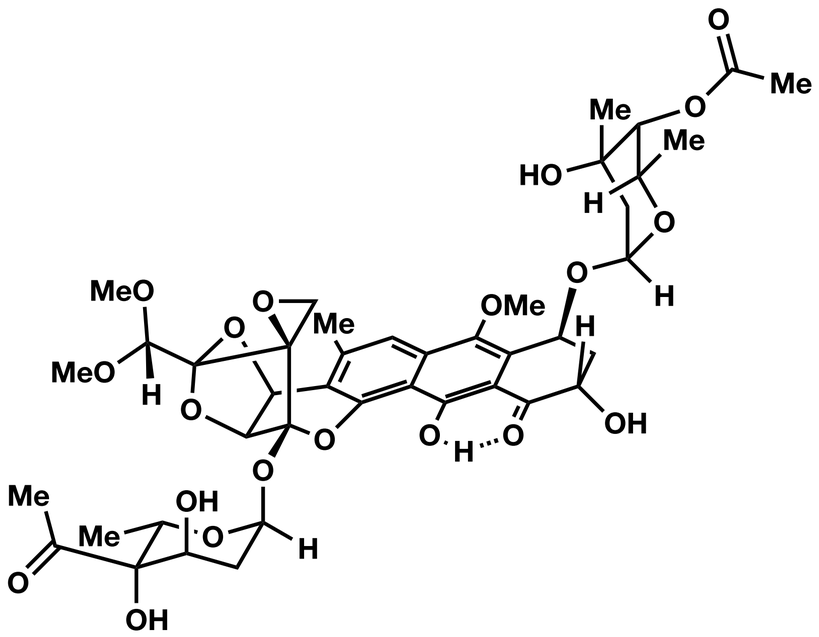

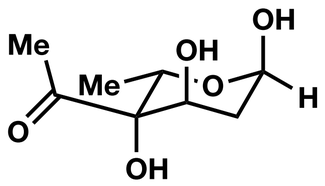

α-Trioxacarcinose B

DC-45-A2

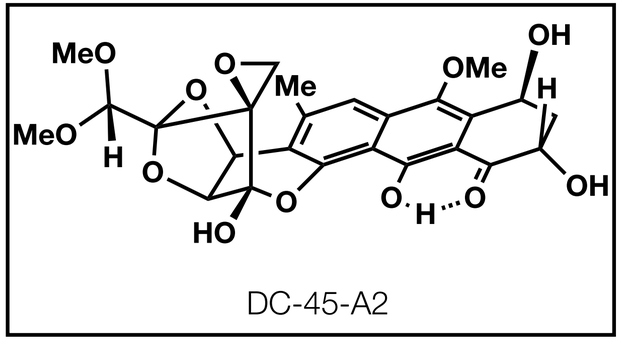

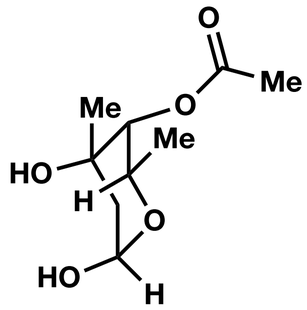

α-Trioxacarcinose A

PNAS U.S.A. **2011**, 108, 6709–6714.

Trioxacarcins

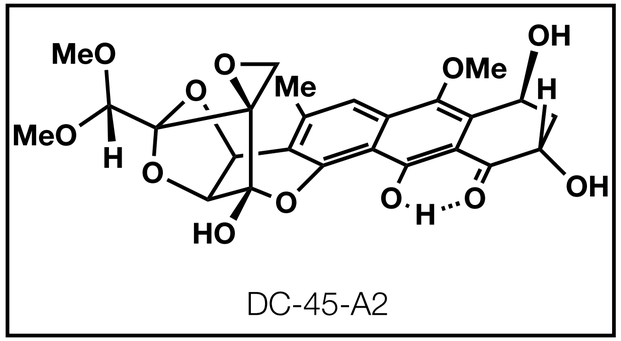

DC-45-A2

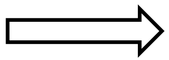

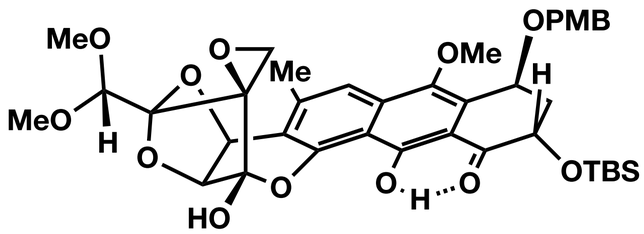

Key Synthetic Precursor:
Orthogonally Protected DC-45-A2

PNAS U.S.A. **2011**, 108, 6709–6714.

Trioxacarcins

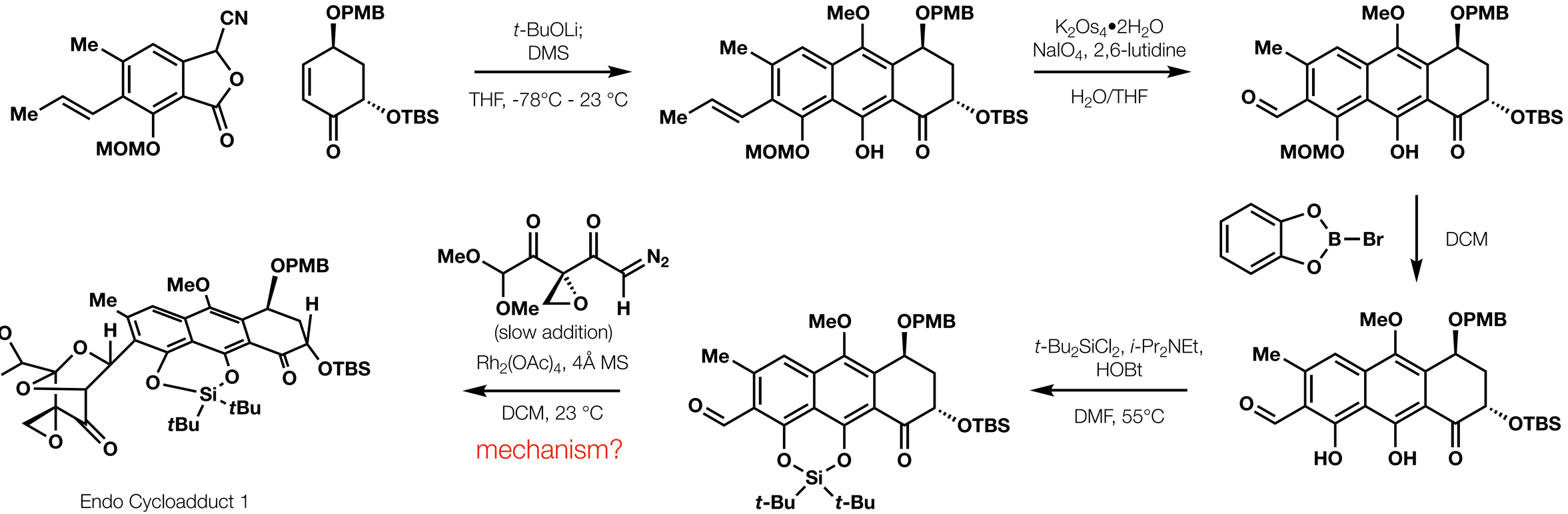

Trioxacarcins

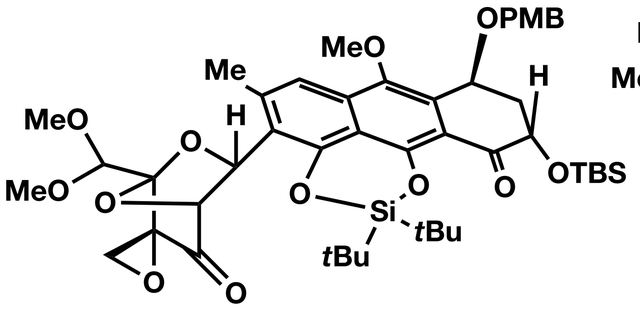

Endo Cycloadduct 1

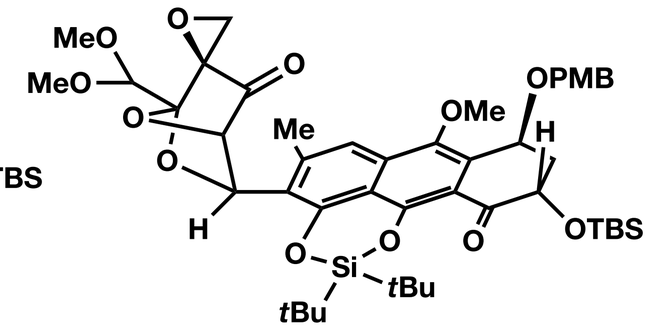

Endo Cycloadduct 2

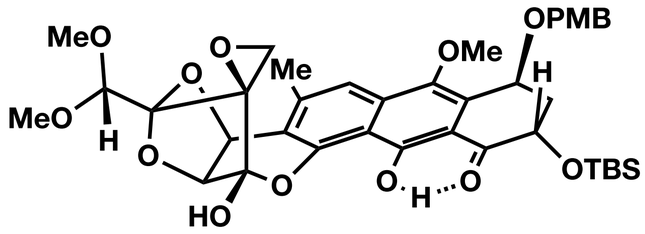

Key Synthetic Precursor:
Orthogonally Protected DC-45-A2

i. DDQ
ii. $Et_3N•3HF$

DC-45-A2

$Et_3N•3HF$

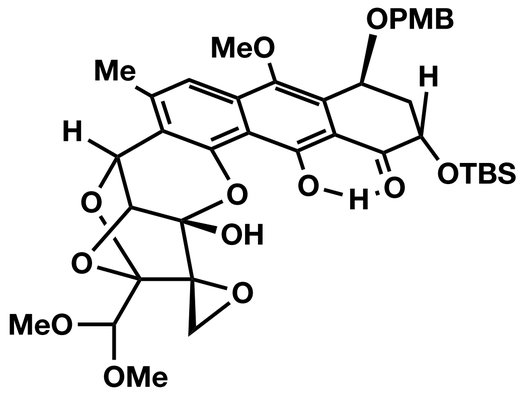

iso-precursor

i. DDQ
ii. $Et_3N•3HF$

iso-DC-45-A2

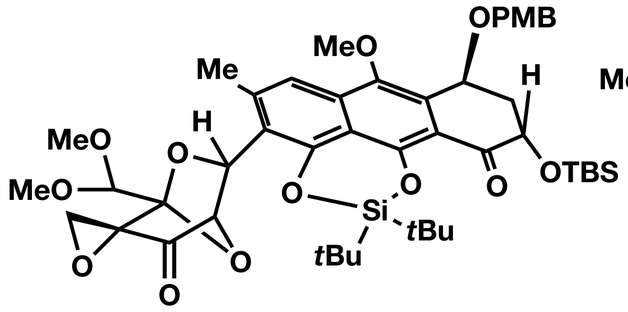

Exo Cycloadduct 1

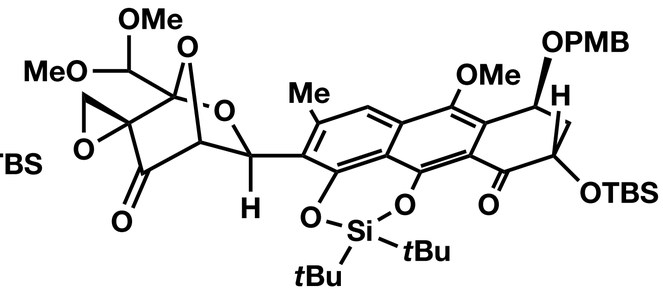

Exo Cycloadduct 2

Trioxacarcins

Analogs of DC-A5-42

dideoxy-DC-A5-42 (**1**) is more potent than DC-45-A2 (**26**)

iso-DC-45-A2 (**25**) is inactive

1 and **26** are shown to modify a short DNA duplex (12 base pairs) with a single guanine (G) in the center.

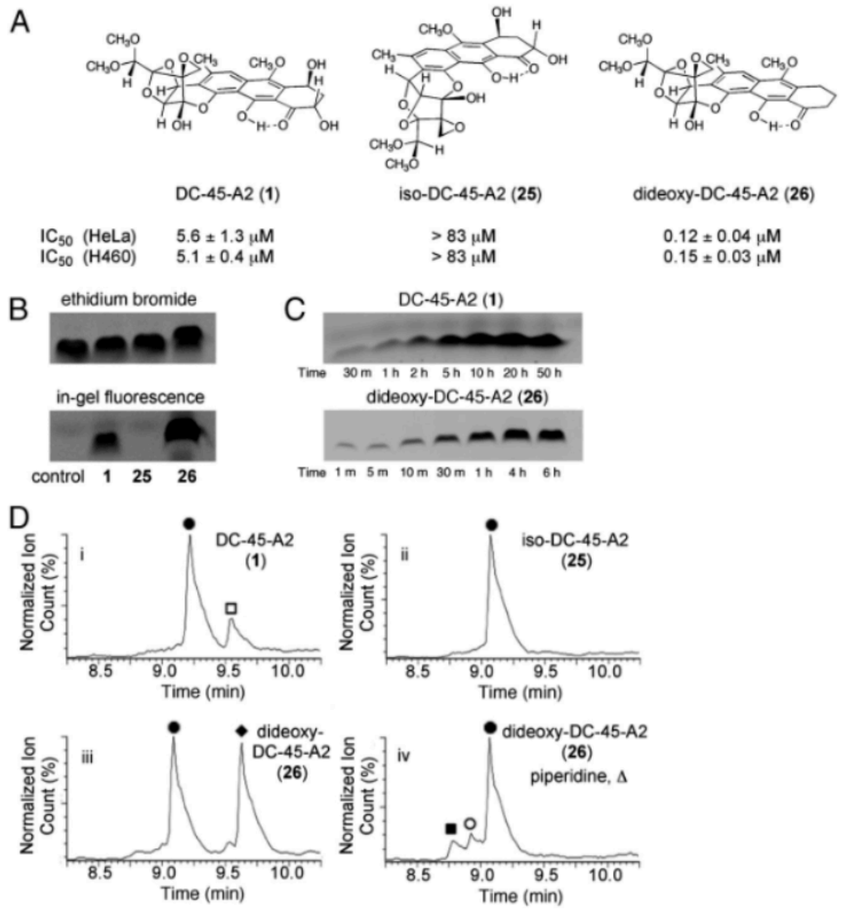

Fig. 4. Synthetic nonglycosylated trioxacarcins, their antiproliferative activities in cultured human cancer cells, and DNA-modifying effects. (*A*) IC_{50} values for DC-45-A2, iso-DC-45-A2, and dideoxy-DC-45-A2 measured in HeLa (cervical cancer) and H460 (lung cancer) cells lines. (*B*) Images of TBE 20% polyacrylamide gels of the products of the reaction of the self-complementary duplex 12-mer d(AATTACGTAATT) (100 μM) with DC-45-A2 (lane 2, 100 μM), iso-DC-45-A2 (lane 3, 100 μM), or dideoxy-DC-45-A2 (lane 4, 100 μM) for 2 h at 23 °C; visualized with ethidium bromide and by in-gel fluorescence. (*C*) Images of TBE gels of the products of the reaction of the self-complementary duplex 12-mer d(AATTACGTAATT) (100 μM) with DC-45-A2 or dideoxy-DC-45-A2 (25 μM) at 23 °C for the indicated times; visualized by in-gel fluorescence. (*D*) LC-MS chromatograms of reaction mixtures of the self-complementary duplex 12-mer d(AATTACGTAATT) (100 μM) and (*i*) DC-45-A2 (100 μM), (*ii*) iso-DC-45-A2 (100 μM), or (*iii*) dideoxy-DC-45-A2 (100 μM) after 24 h at 23 °C; *iv* depicts the LC-MS chromatogram of the reaction mixture of the self-complementary duplex 12-mer d(AATTACGTAATT) (100 μM) and dideoxy-DC-45-A2 (100 μM) after 24 h at 23 °C followed by the addition of piperidine (1 M) and heating for 30 min at 95 °C; ●, (AATTACGTAATT); □, (AATTACGTAATT • **1**); ◆, (AATTACGTAATT • **26**); ■, (pTAATT); ○= (AATTACp).

PNAS U.S.A. **2011**, 108, 6709–6714.

Trioxacarcins - Glycosyidic Analogs

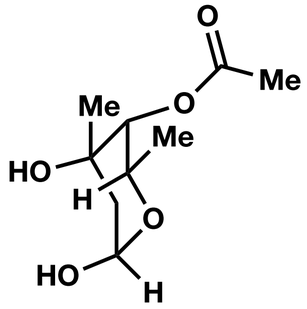

α-Trioxacarcinose A

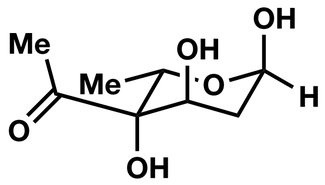

α-Trioxacarcinose B

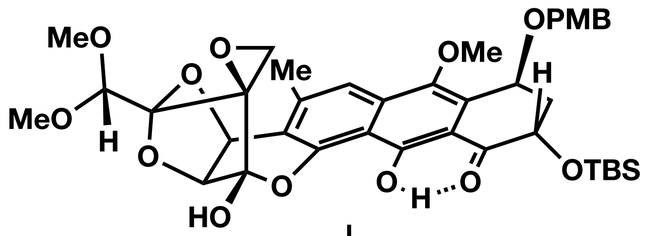

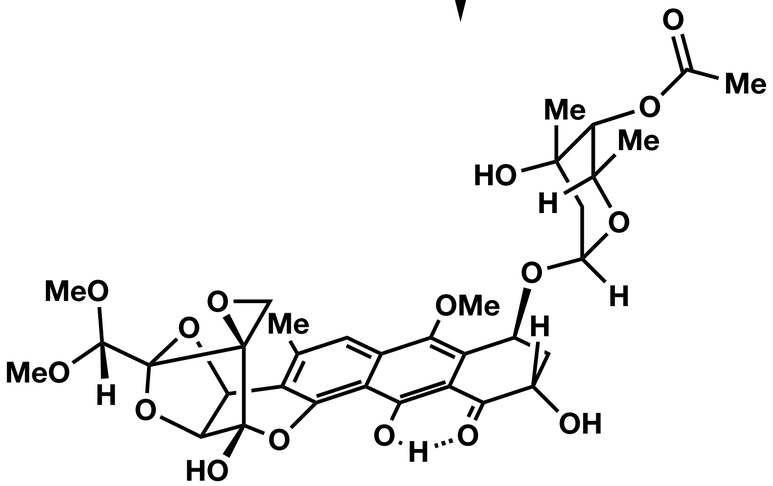

DC-45-A1

GI_{50} = 37 ± 7 nM

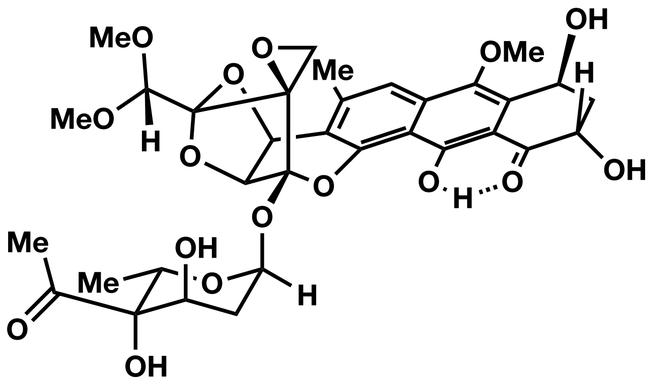

monoglycoside (trioxacarcinose B containing)

GI_{50} = 767 ± 74 nM

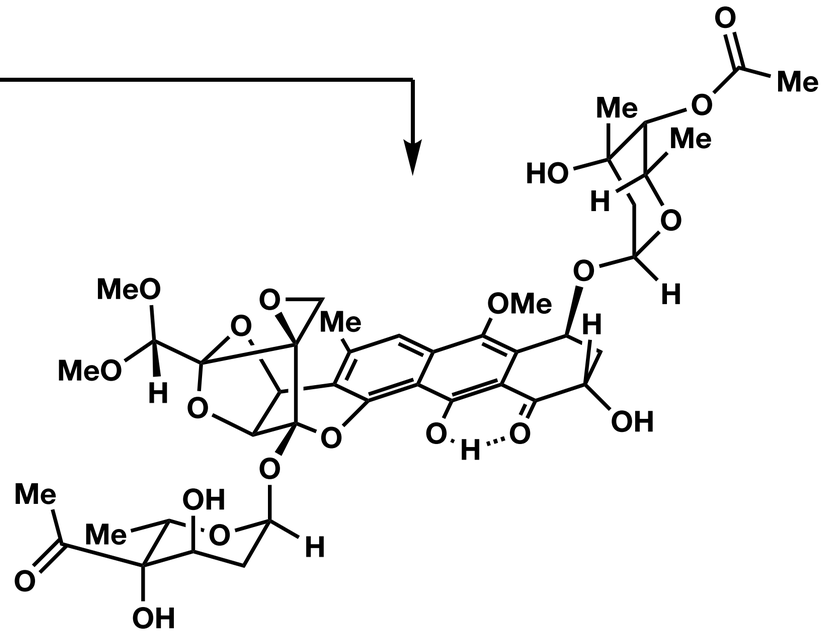

Trioxacarcin A

GI_{50} = 0.85 ± 0.36 nM

Organic Letters. **2011**; 13(20): 5584–5587. *Organic Letters.* **2012**; 14(7): 1812–1815. *Nature Chemistry*. **2013**; 5(10): 886–893.

Trioxacarcins - Glycosyidic Analogs

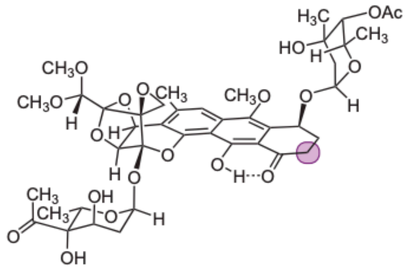

25

GI_{50} (H460) 4.5 ± 2.0 nM

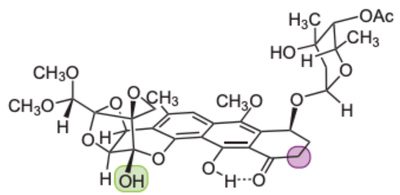

26

17 ± 2 nM

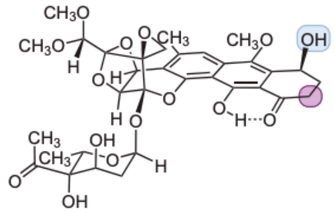

27

206 ± 70 nM

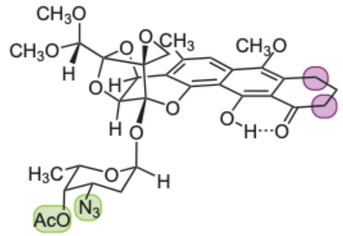

30

GI_{50} (H460) 102 ± 3 nM

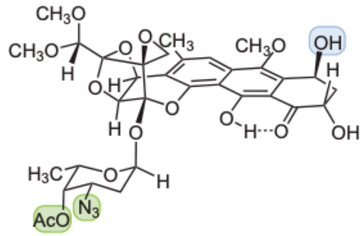

31

397 ± 82 nM

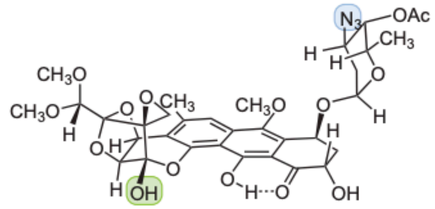

32

225 ± 26 nM

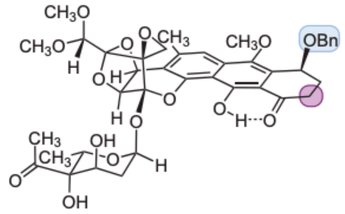

28

GI_{50} (H460) 315 ± 58 nM

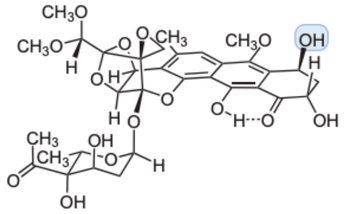

9

767 ± 74 nM

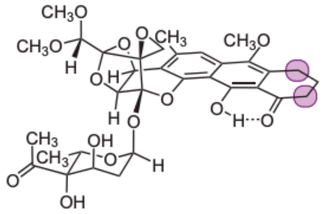

29

19 ± 7 nM

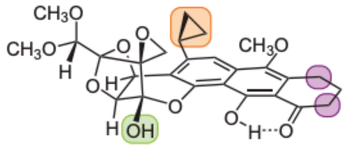

33

GI_{50} (H460) 374 ± 87 nM

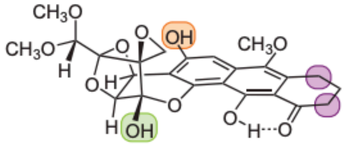

34

>2,500 nM

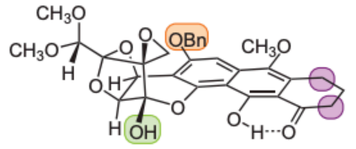

35

>2,500 nM

No SAR discussed, but synthetic strategy is clearly effective at generating a variety of analogs

Trioxacarcins - Evidence for Mechanism of Action

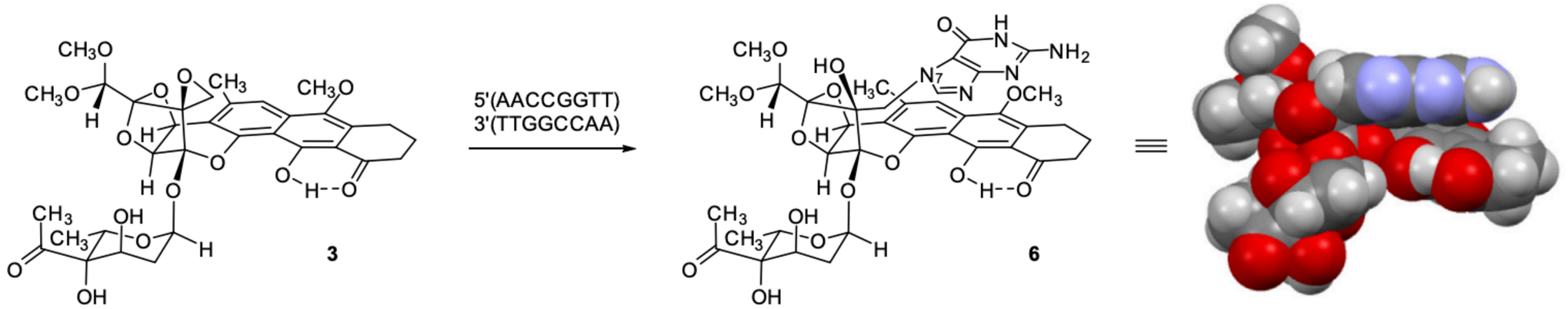

Scheme 1. Formation of guanine adduct **6** from the fully synthetic trioxacarcin analog **3**.

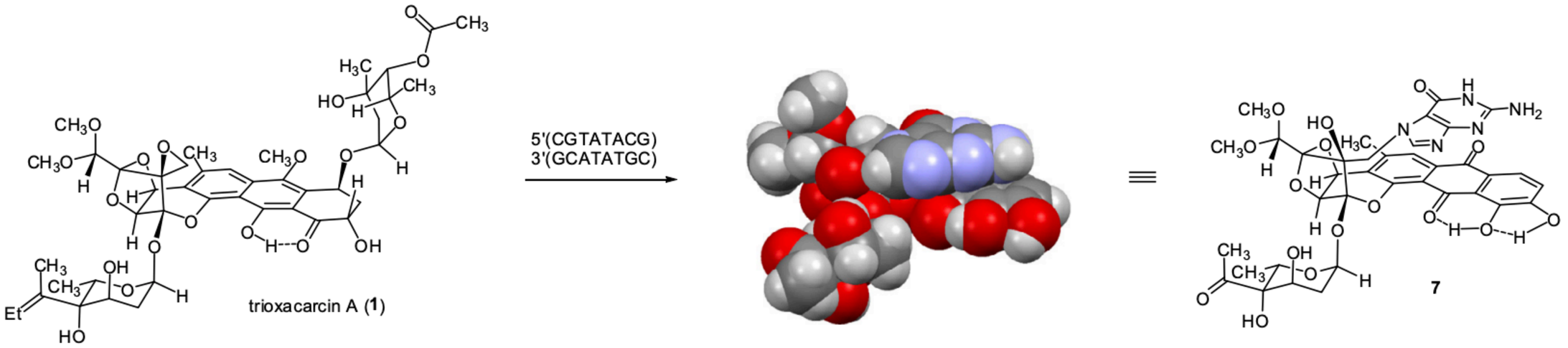

Trioxacarcins - Evidence for Mechanism of Action

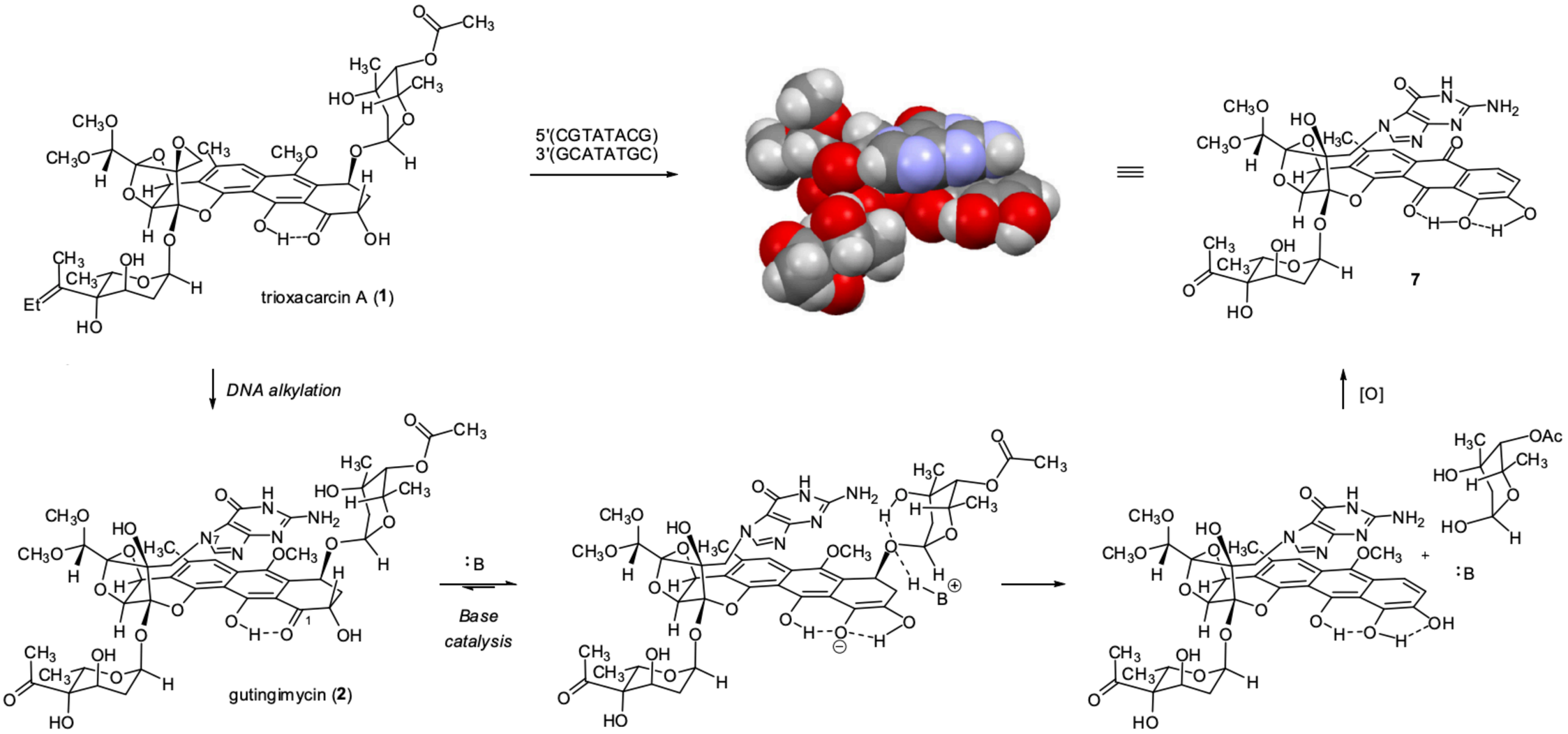

Combatting Antibiotic Resistance

Perhaps Myers' Most Impactful Work

Tetracyclines

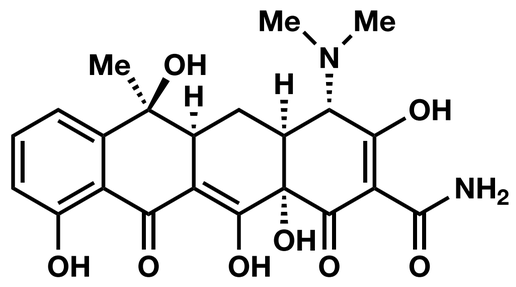

(—)-tetracycline

Macrolides

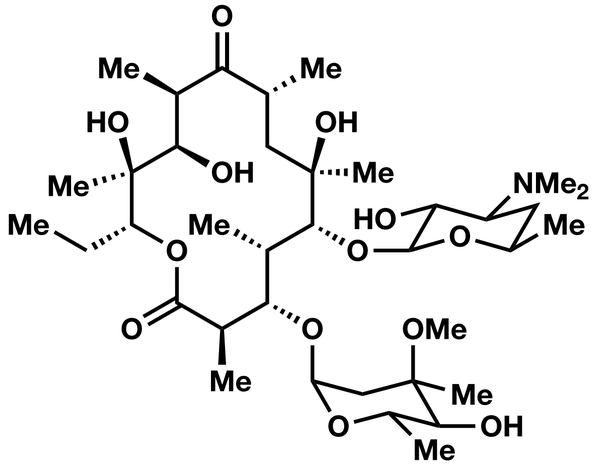

Erythromycin

Lincosamides

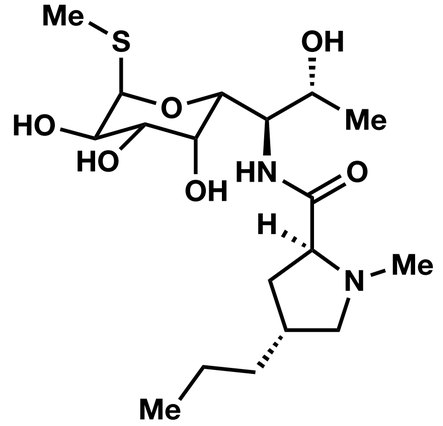

Lincomycin

Overarching Research Theme

Convergent Routes with High Modularity

↓

SAR Exploration

↓

Identification of Clinically Relevant Targets

Tetracyclines

Widely prescribed class of antibiotics since the 1950s

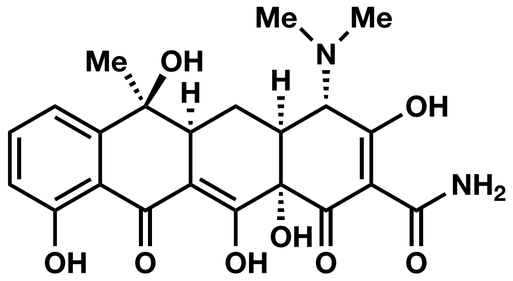

(—)-tetracycline

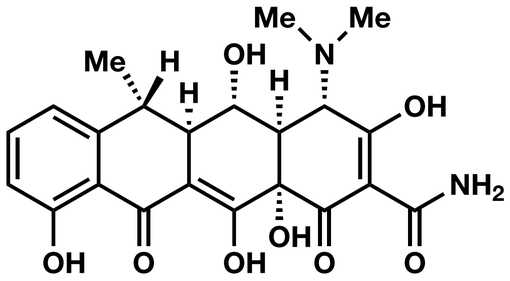

(—)-doxycycline

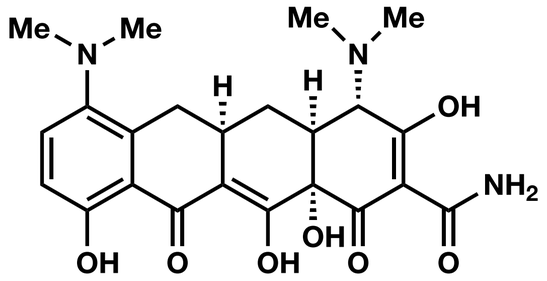

(—)-minocycline

natural product produced on large scale by fermentation

both are non-natural antibiotics and are manufactured by semisynthesis

Commonly prescribed for

- respiratory infections
- STIs
- UTIs
- Lyme disease
- Other systematic bacterial infections

- acne
- rosacea

Science. **2005**; 308(5720): 395–398.

Tetracyclines - Convergent Synthesis

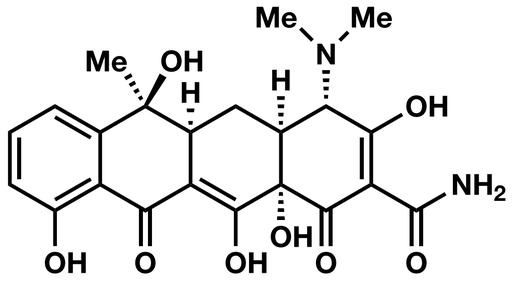

(—)-tetracycline

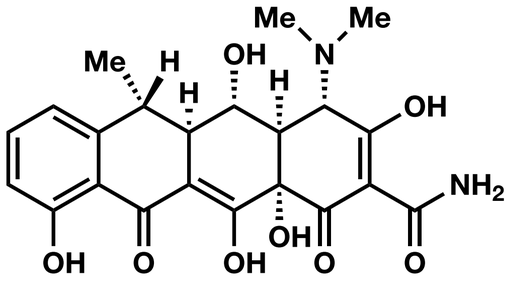

(—)-doxycycline

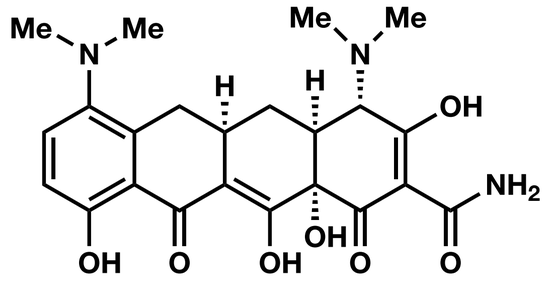

(—)-minocycline

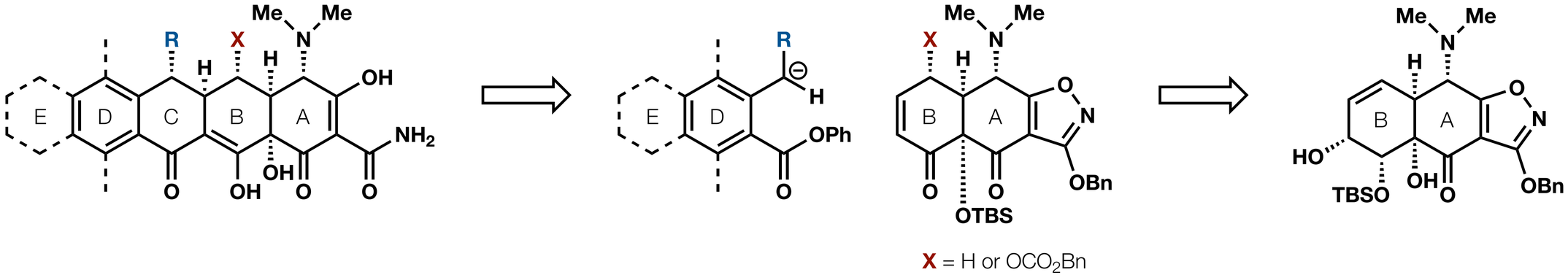

X = H or OCO_2Bn

Tetracyclines - Convergent Synthesis

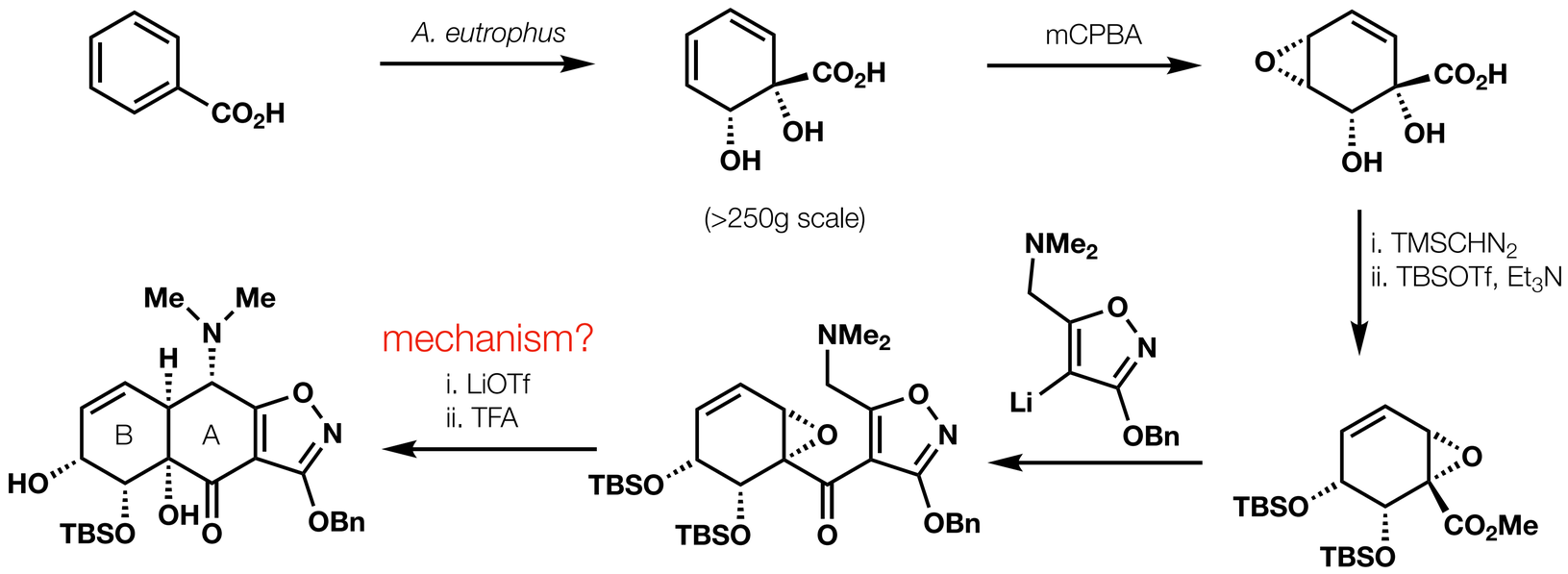

Tetracyclines - Convergent Synthesis

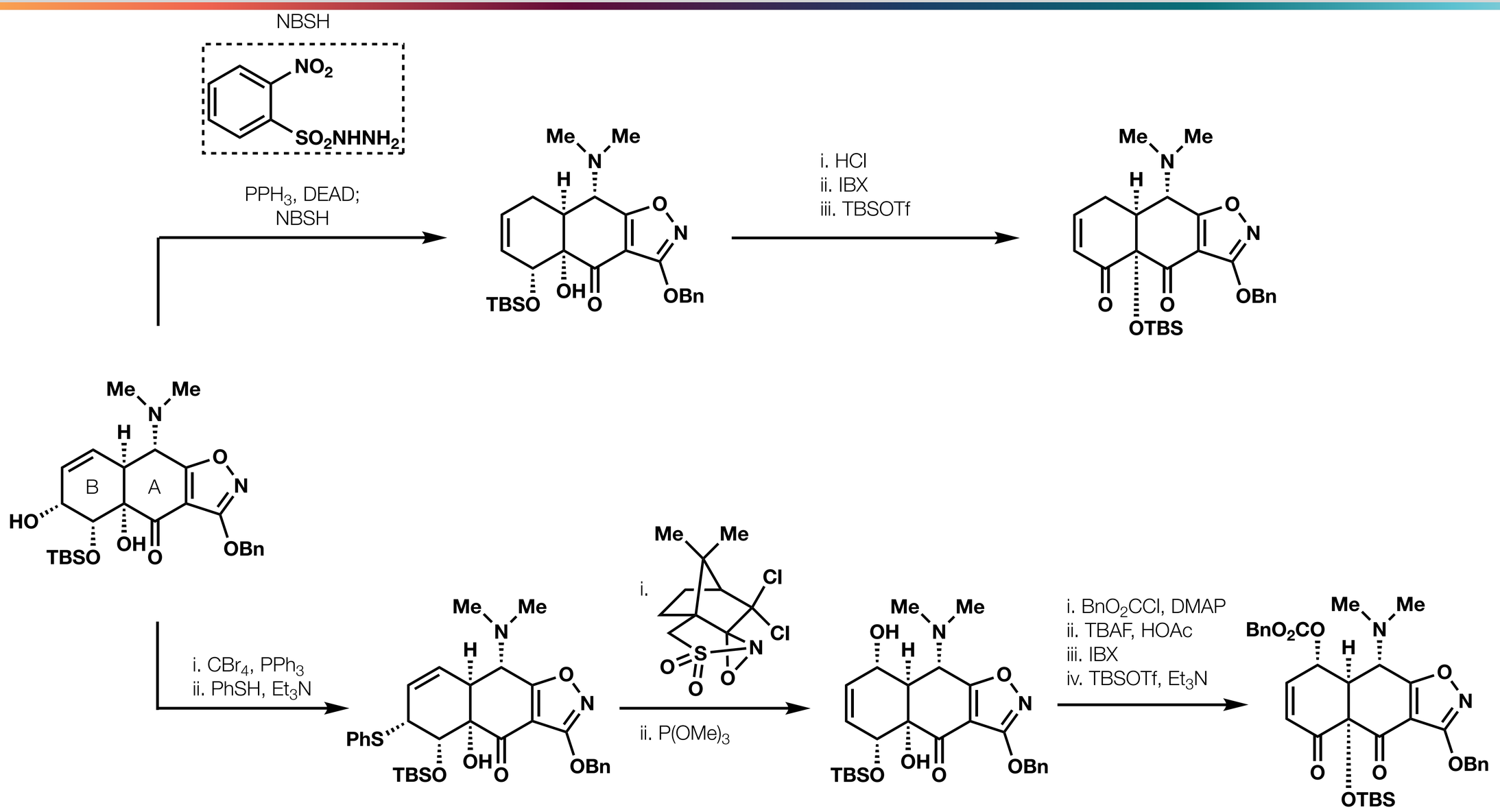

Science. **2005**; 308(5720): 395–398.

Tetracyclines - Convergent Synthesis

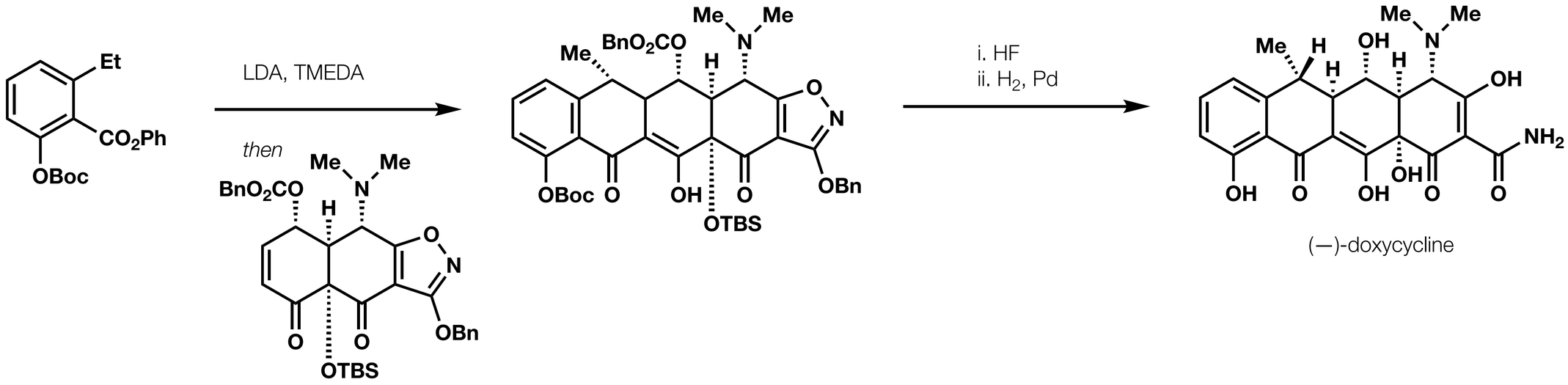

(—)-doxycycline

Science. **2005**; 308(5720): 395–398.

Tetracyclines - Convergent Synthesis

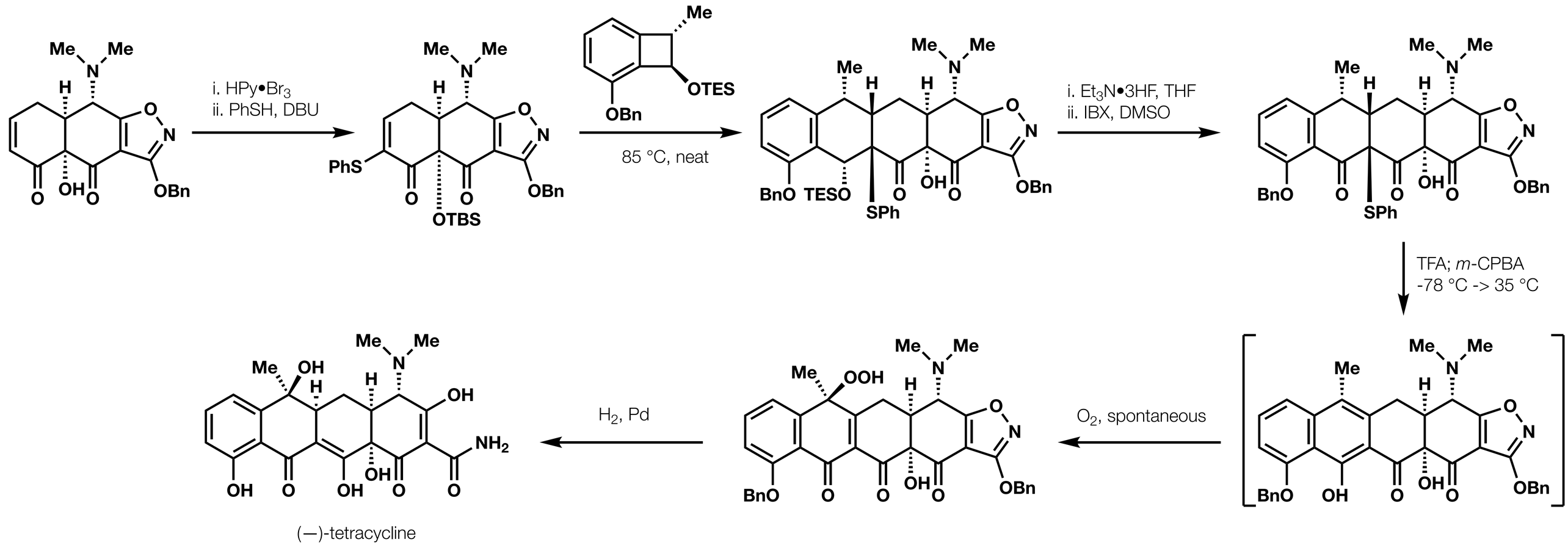

Tetracyclines - Convergent Synthesis

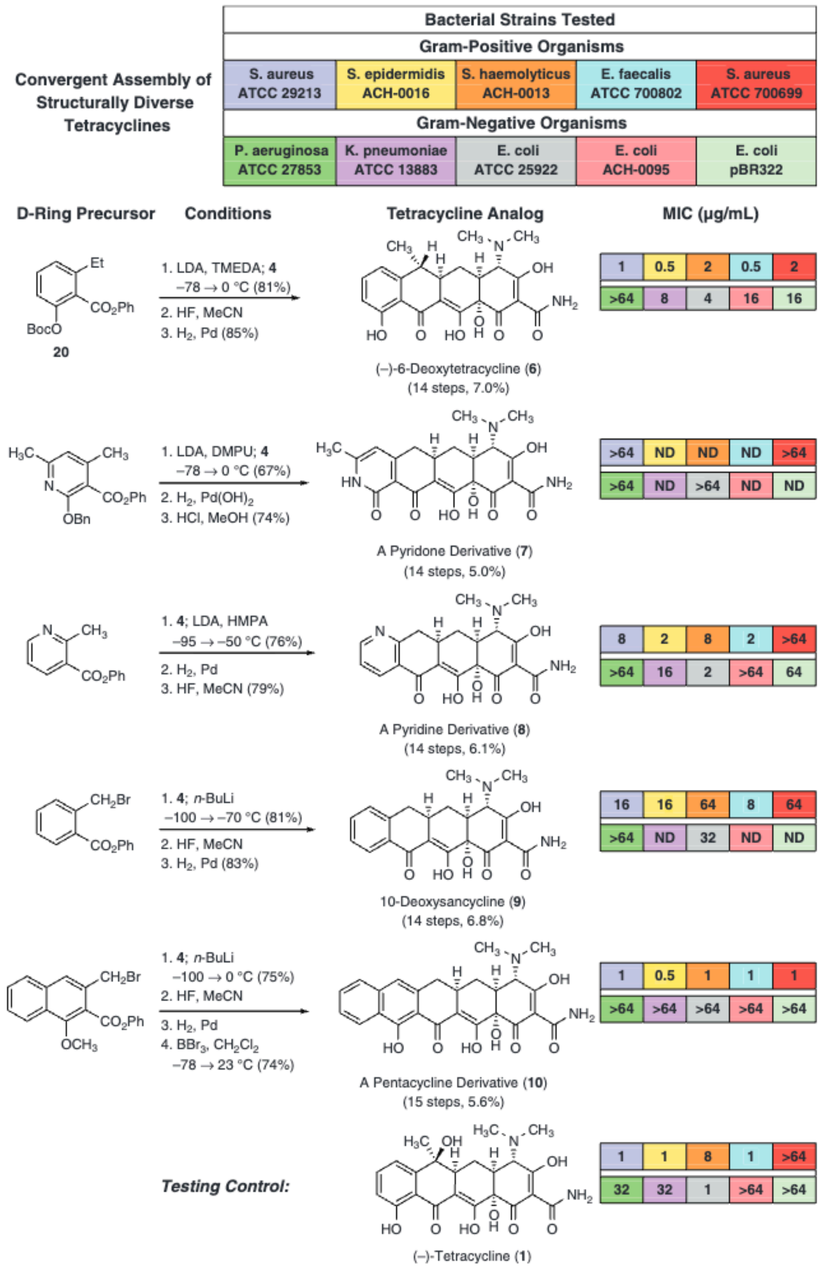

Initiated a platform that allowed for the synthesis of more than 3000 tetracycline analogs

Science. **2005**; 308(5720): 395–398.

Identification of Most Potent Analog

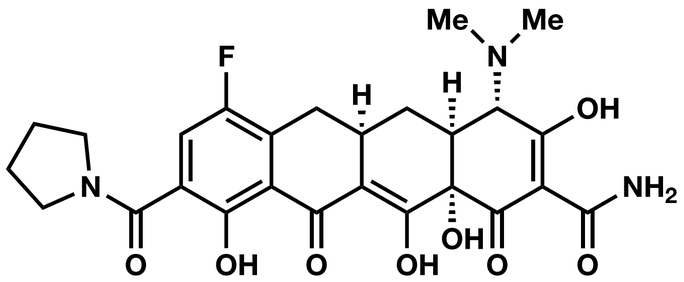

TP-434 (eravacycline)

Systematic exploration of analogs led to identification of TP-434 as a lead target

MIC90 values of ≤2 μg/ml against panels of all major bacterial species (Both Gram-positive and Gram-negative) except for *Pseudomonas aeruginosa* and *Burkholderia cenocepacia*

Tetraphase Pharmaceuticals (founded by Myers) began advancing TP-434 in preclinical development in 2008

FDA approved eravacycline (Xerava) for complicated intra-abdominal infections in 2018

Antimicrob. Agents Chemother. **2013,** 57, 5548–5558

Combatting Antibiotic Resistance

Perhaps Myers' Most Impactful Work

Tetracyclines

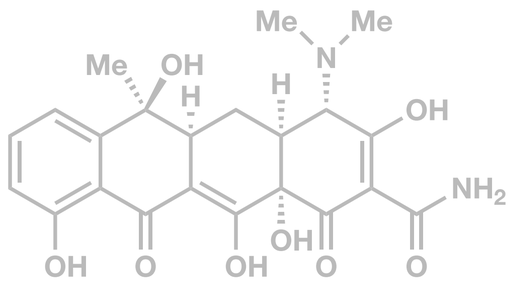

(—)-tetracycline

Macrolides

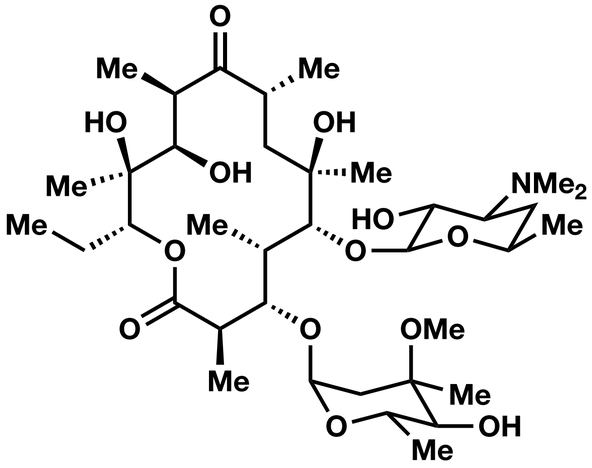

Erythromycin

Lincosamides

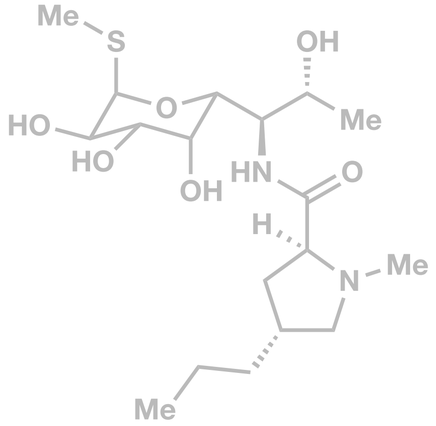

Lincomycin

Overarching Research Theme

Convergent Routes with High Modularity

↓

SAR Exploration

↓

Identification of Clinically Relevant Targets

Macrolides - Dependency on Semisynthesis

Nature. **2016**: 533(7603): 338–345.

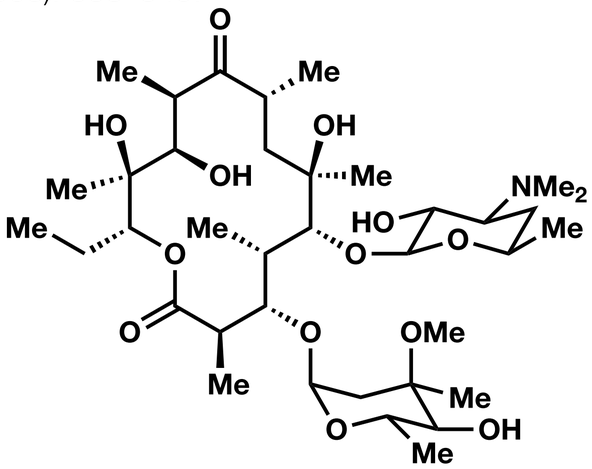

Erythromycin (Fermentation product)

US FDA appoval 1952

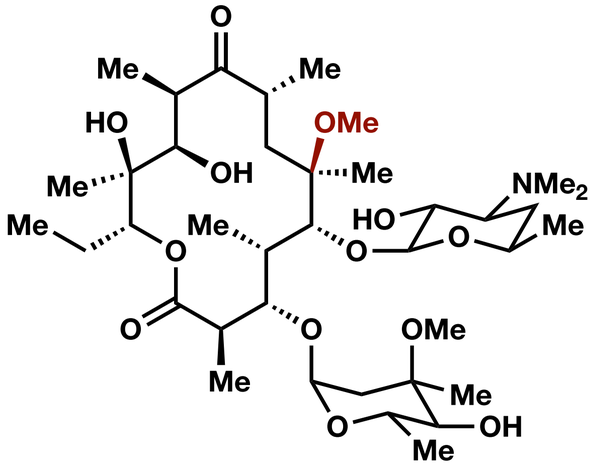

Clarithromycin (**6** steps from erythromycin)

1991

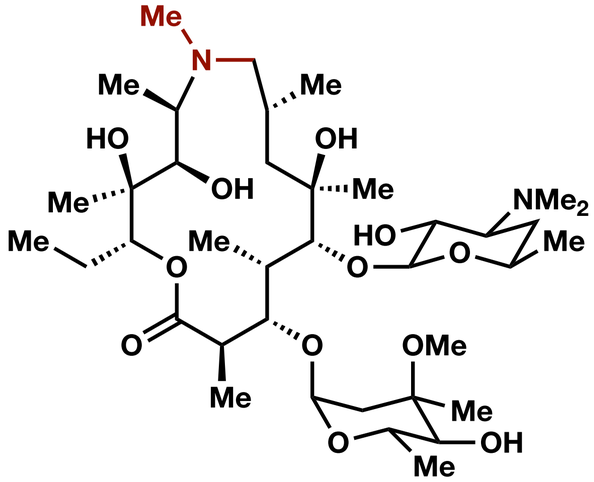

Azithromycin (**4** steps from erythromycin)

1991

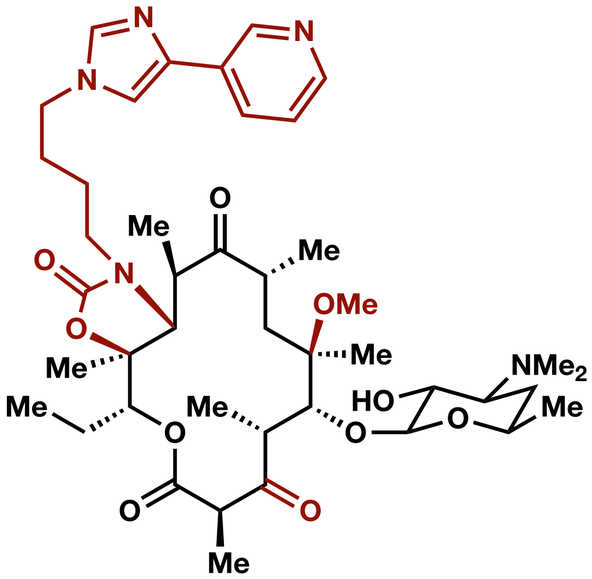

Telithromycin (**12** steps from erythromycin)

US FDA appoval 2004

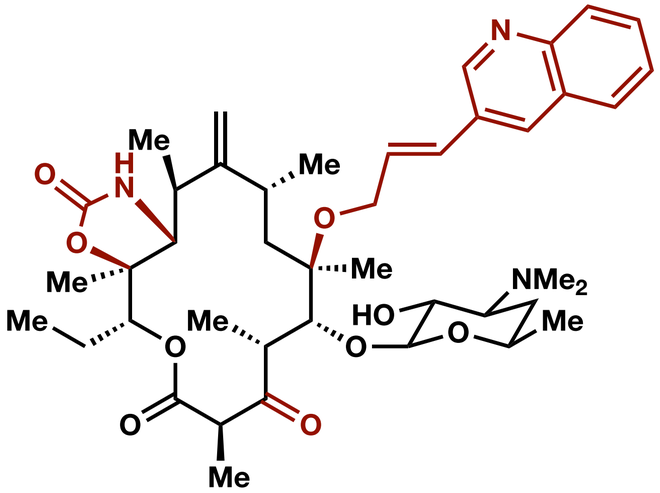

Cethromycin (**9** steps from erythromycin)

Former clinical candidate

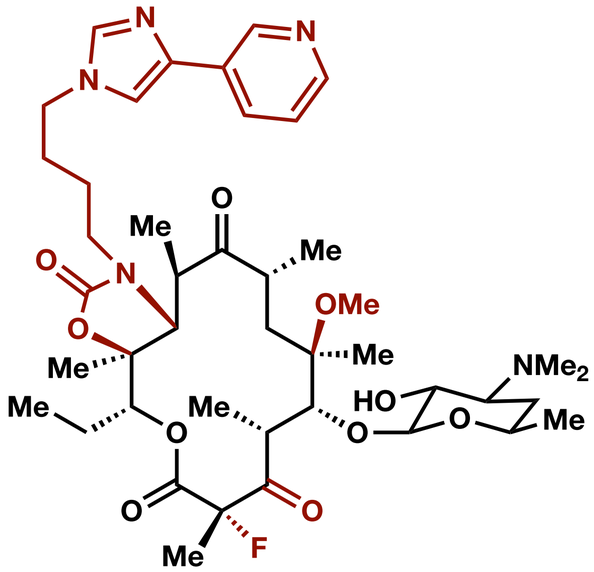

Solithromycin (**16** steps from erythromycin)

Former clinical candidate

Macrolides - Convergent Strategy

Nature. **2016**: 533(7603): 338–345.

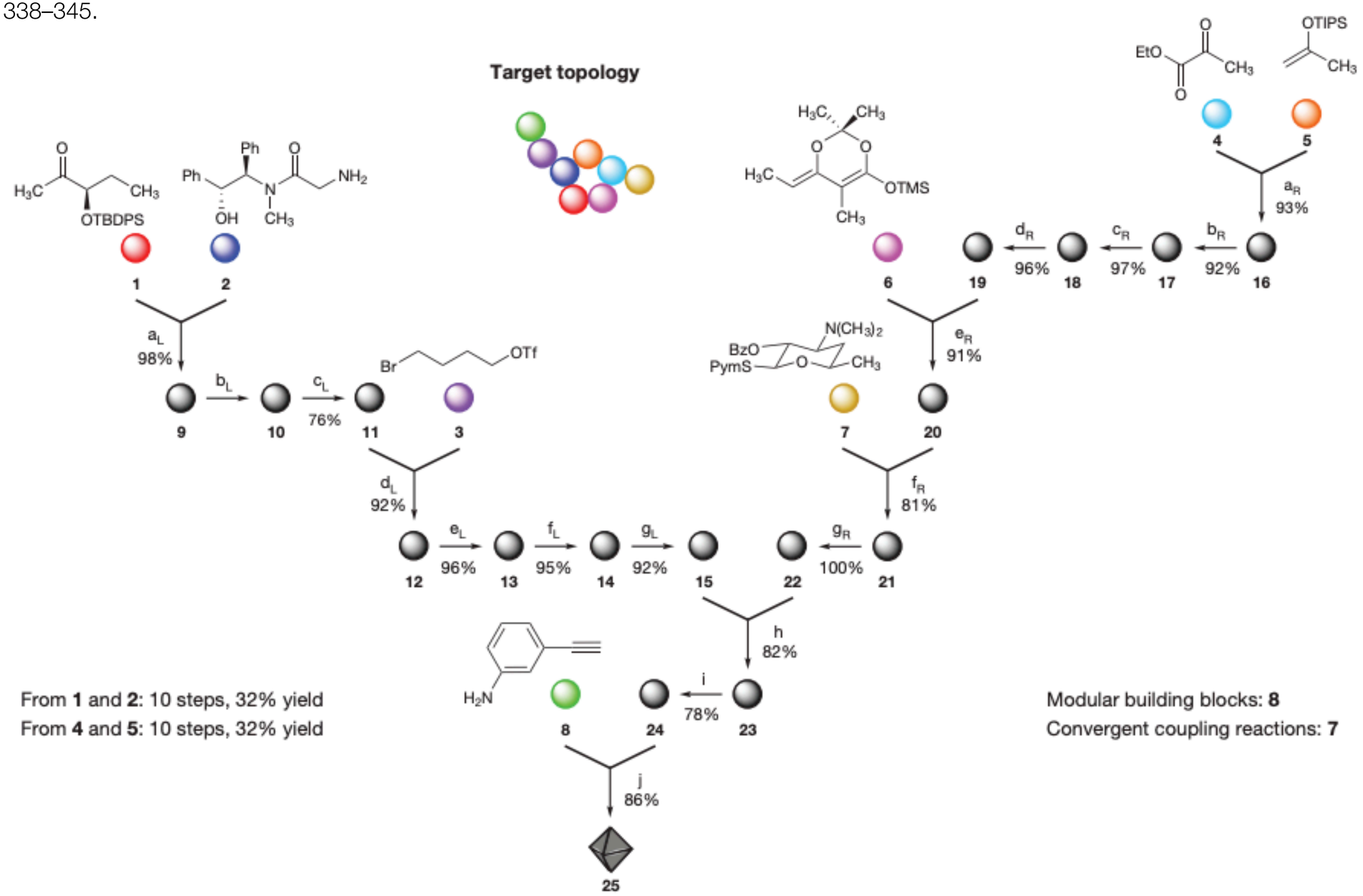

Macrolides - Convergent Strategy

Nature. **2016**: 533(7603): 338–345.

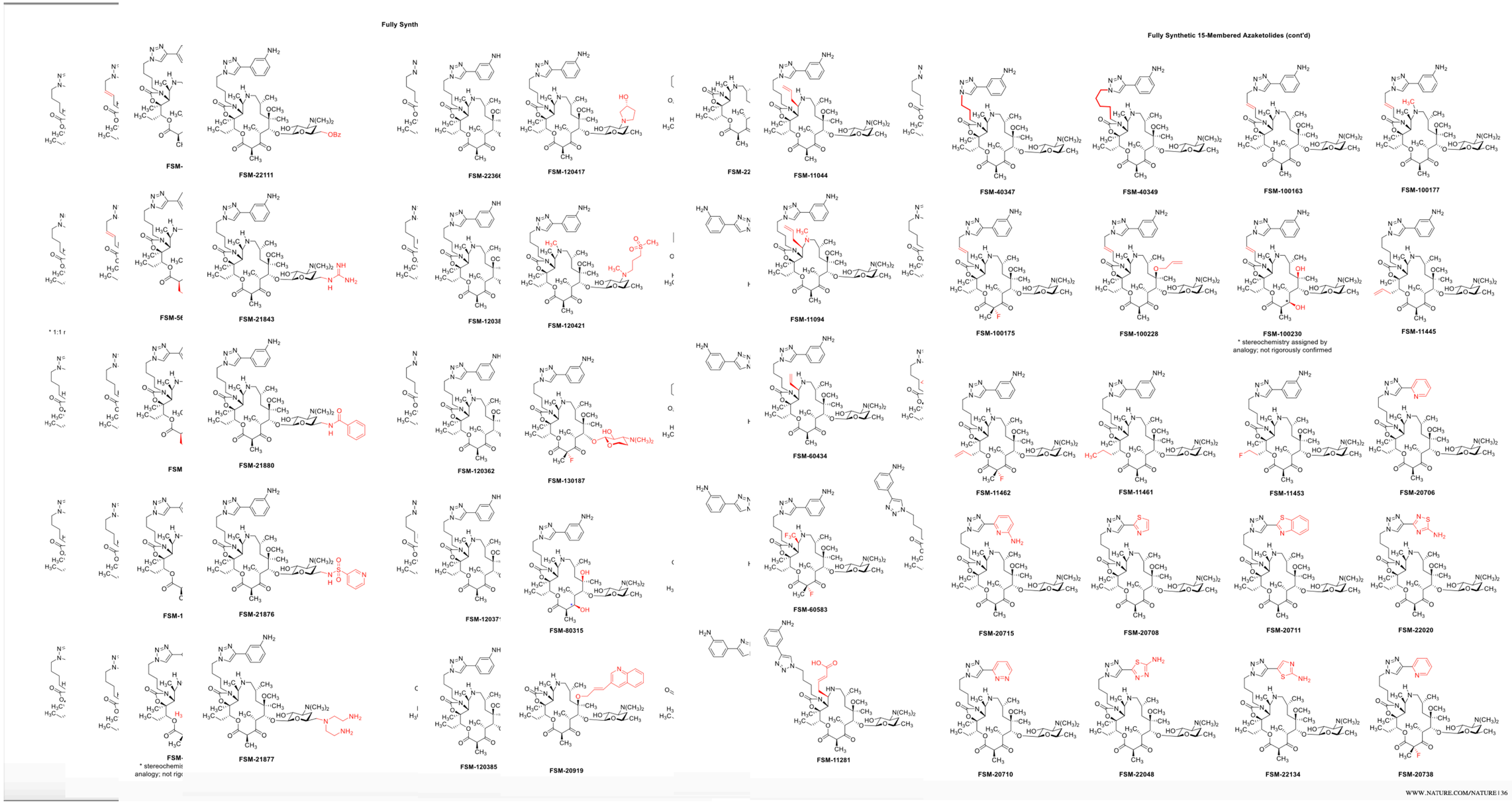

Macrolides - Convergent Strategy

Nature. **2016**: 533(7603): 338–345.

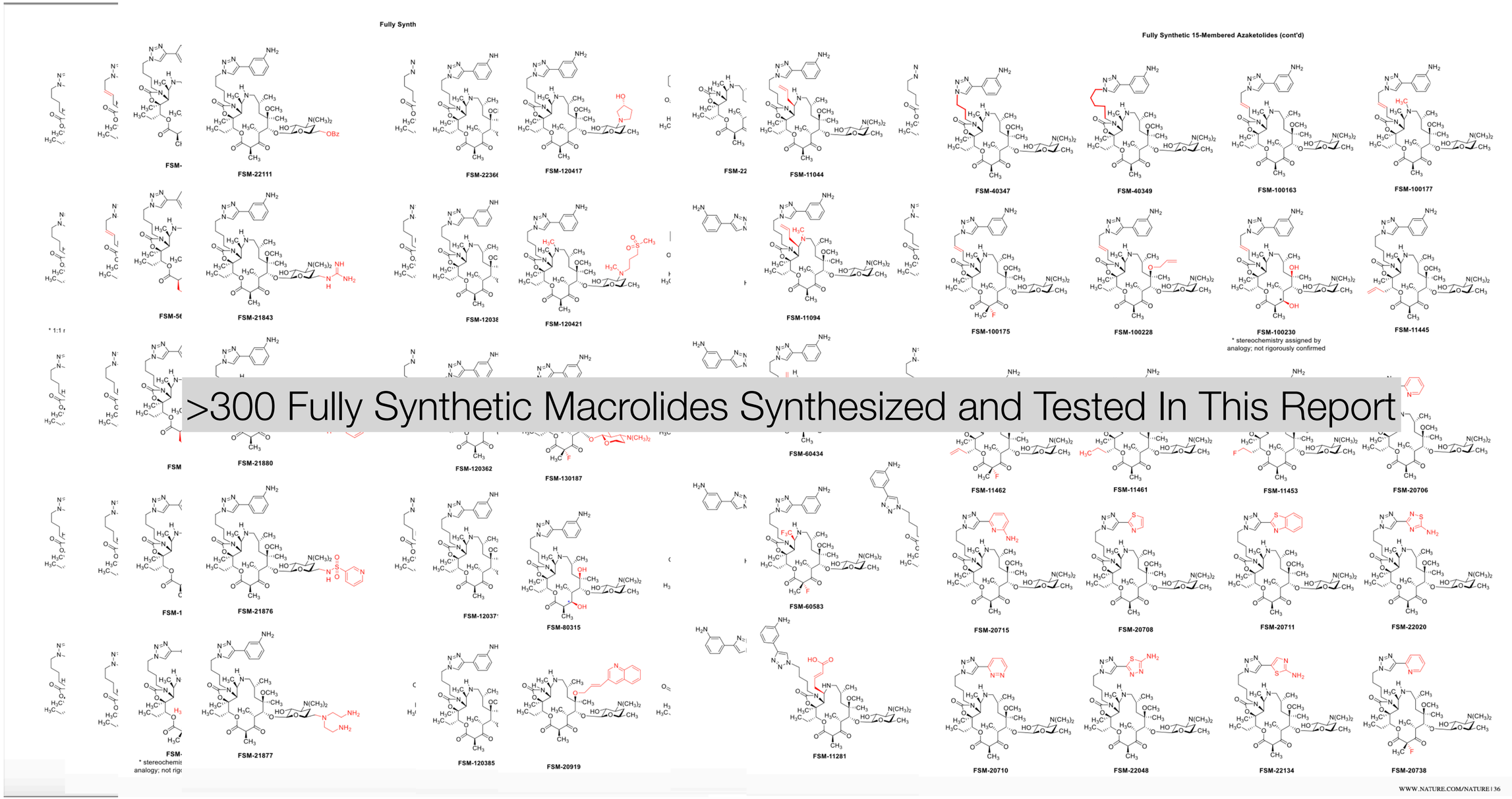

Macrolides - Convergent Strategy

As of 2021, more than 2500 macrolides have been prepared using Myers' strategy

This huge library has enabled correlation of physicochemical properties to enhanced activity, especially towards the development of antibiotics for Gram-negative bacteria

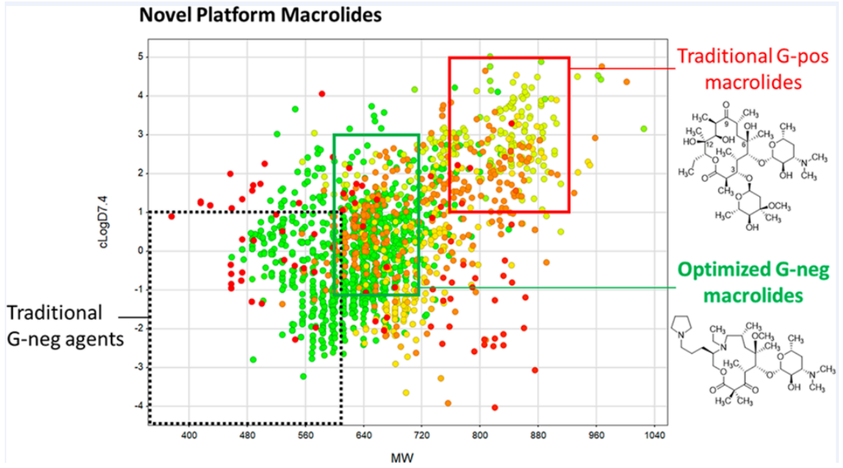

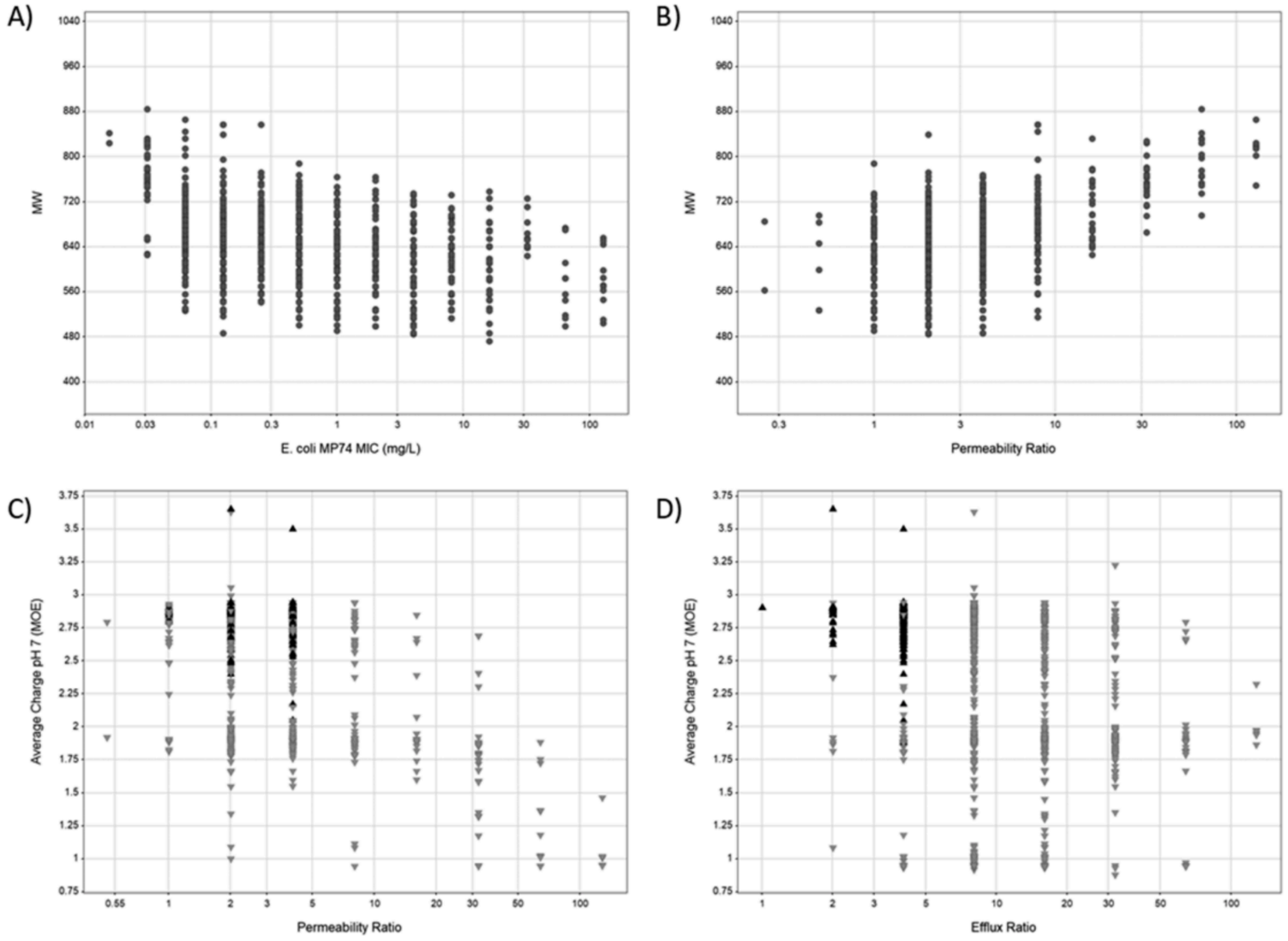

Figure 5. Correlation of physicochemical properties with target engagement, permeability, and efflux: (A) *E. coli* MP-74 MIC vs MW, (B) permeability ratio vs MW, (C) permeability ratio vs average charge at pH 7, and (D) efflux ratio vs average charge at pH 7. ▲, compounds with permeability and efflux ratios ≤4; ▼, compounds with permeability or efflux ratios >4.

Acc. Chem. Res. **2021**, 54, 1635-1645

Combatting Antibiotic Resistance

Perhaps Myers' Most Impactful Work

Tetracyclines

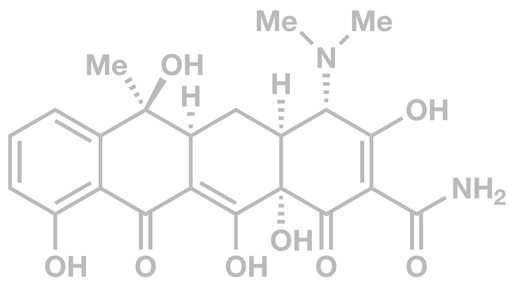

(—)-tetracycline

Macrolides

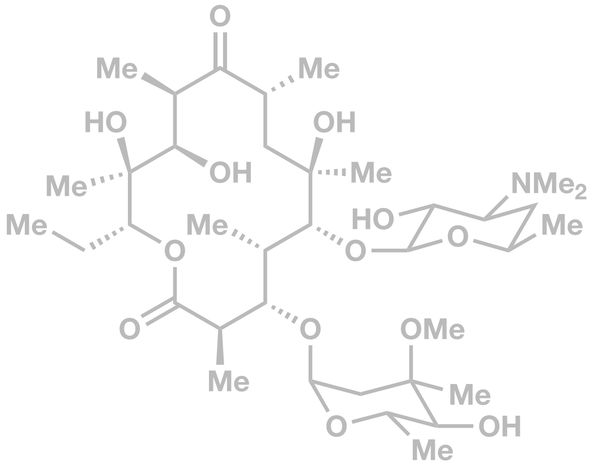

Erythromycin

Lincosamides

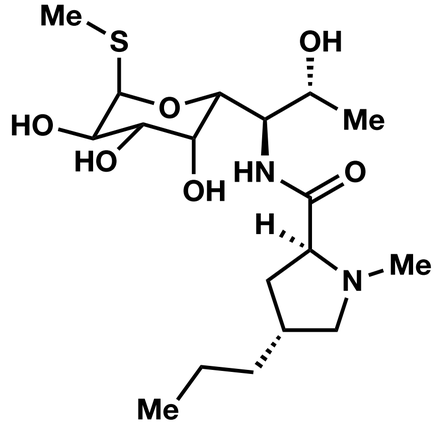

Lincomycin

Overarching Research Theme

Convergent Routes with High Modularity

↓

SAR Exploration

↓

Identification of Clinically Relevant Targets

Lincosamides

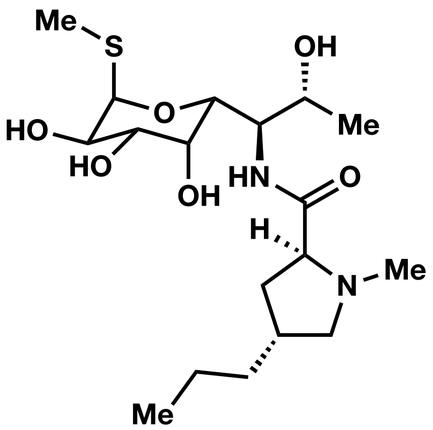

Lincomycin

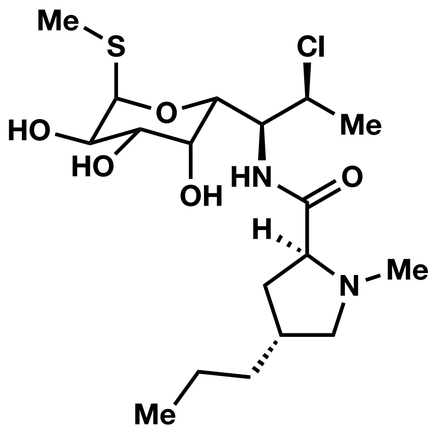

Clindamycin

FDA Approved in 1970

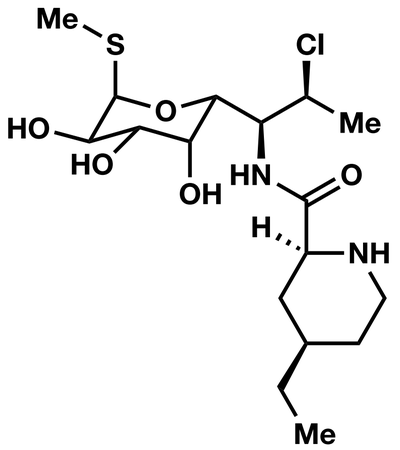

Pirlimycin (Pirsue)

Lincosamides

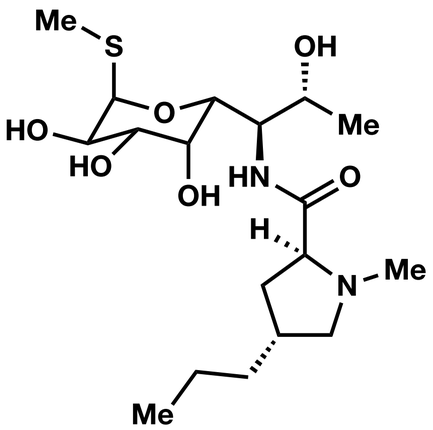

Lincomycin

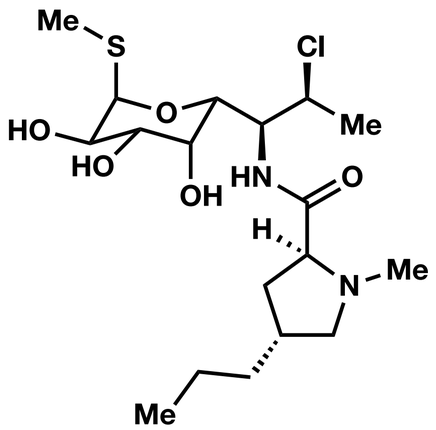

Clindamycin

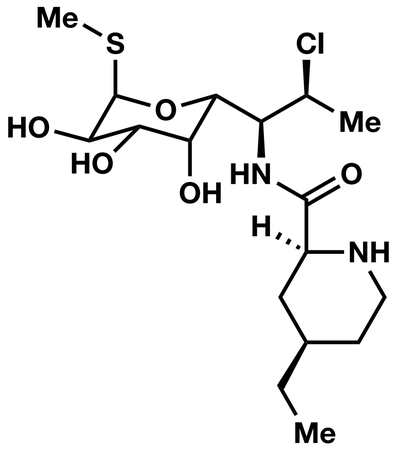

Pirlimycin (Pirsue)

⇩ de novo synthesis needed!

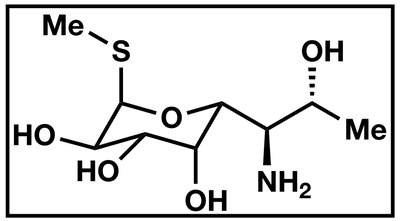

Methylthiolincosamine (MTL)

J. Am. Chem. Soc. **2021**, 143, 6829–6835

Lincosamides

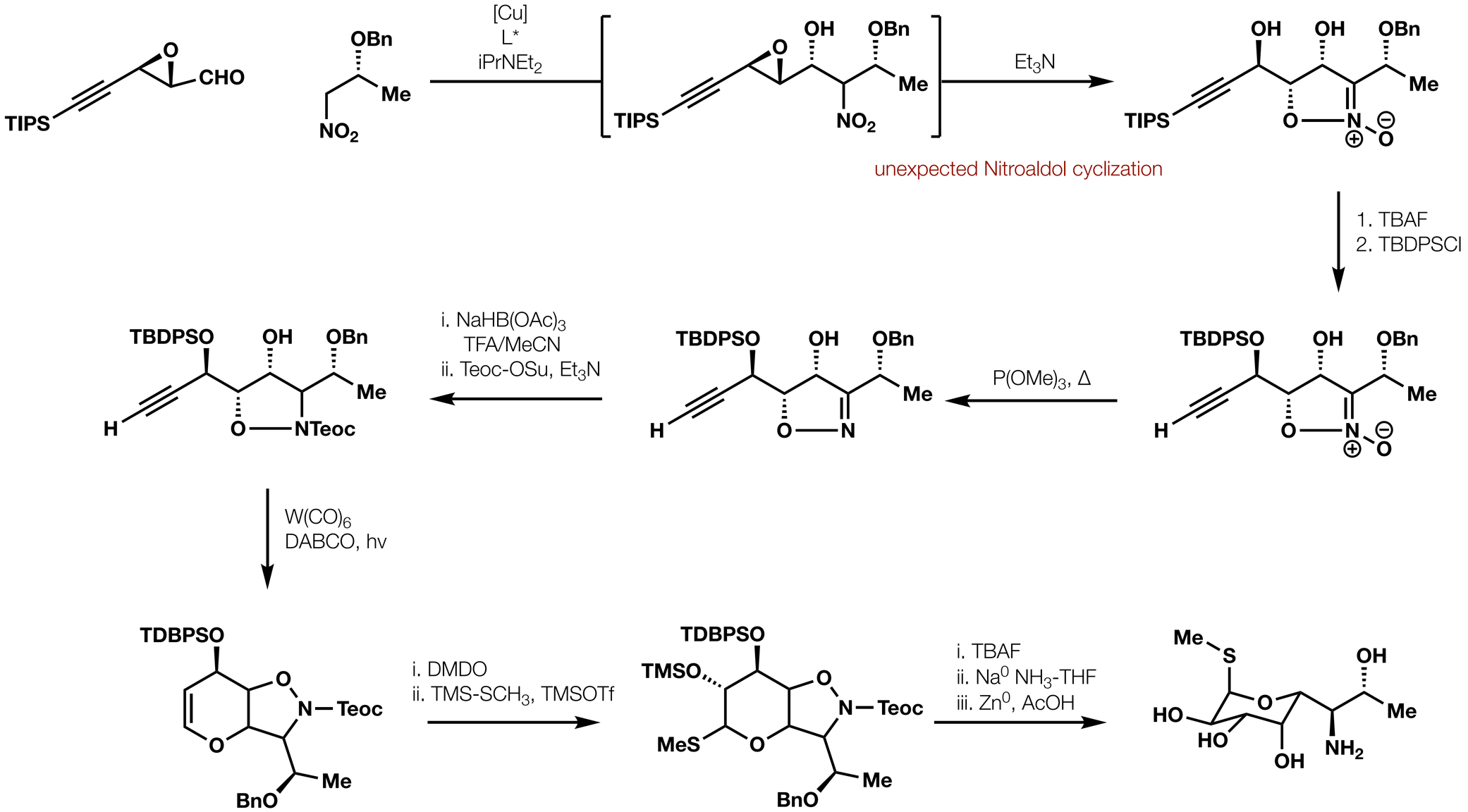

J. Am. Chem. Soc. **2021**, 143, 6829–6835

Lincosamides

Table 1. Structures and Minimum Inhibitory Concentrations (μg/mL) of Selected Lincosamides Prepared by the Route Described

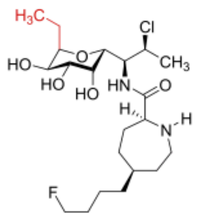

37
(20 LLS)

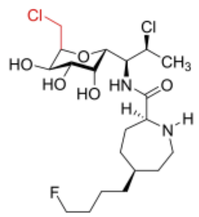

43
(24 LLS)

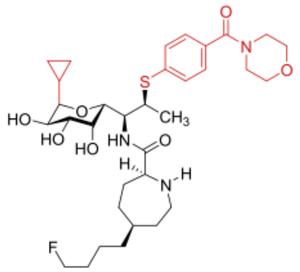

44
(23 LLS)

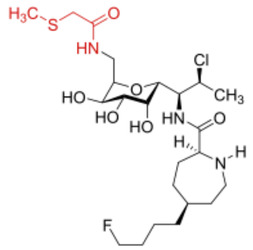

45
(24 LLS)

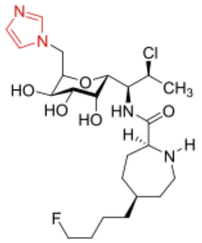

46
(24 LLS)

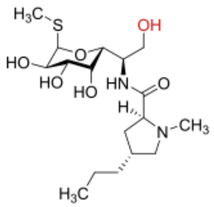

42
(16 LLS)

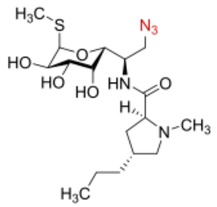

47
(20 LLS)

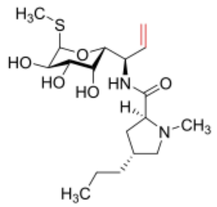

48
(19 LLS)

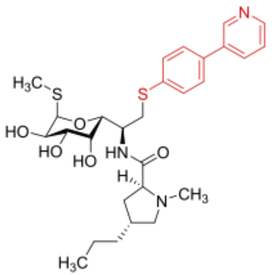

49
(18 LLS)

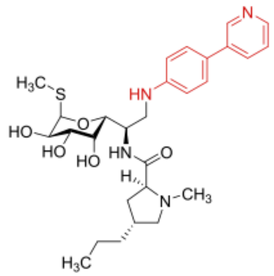

50
(19 LLS)

	Species	Description	Linco	Clinda	5	37	43	44	45	46	42	47	48	49	50
Gram +	*S. aureus*	ATCC 29213	1	0.25	≤0.06	≤0.06	16	8	>64	>64	32	8	8	0.5	32
	S. aureus	BAA 977; i-*ermA*	1	0.25	≤0.06	≤0.06	4	8	>64	>64	NT	NT	8	NT	NT
	S. pneumoniae	ATCC 49619	0.5	0.12	≤0.06	≤0.06	1	0.12	2	8	4	4	2	0.25	8
	S. pneumoniae	MMX 3028; c-*ermB*	>64	>64	8	64	>64	16	>64	>64	NT	>64	NT	>64	>64
	S. pneumoniae	MMX 3031; c-*mefA*	0.25	0.06	≤0.06	≤0.06	1	0.12	4	8	NT	0.12	NT	0.25	32
	S. pyogenes	ATCC 19615	≤0.06	0.06	≤0.06	≤0.06	4	≤0.06	2	4	8	2	2	≤0.06	8
	S. pyogenes	MMX 946; MLS_B	>64	>64	4	64	>64	4	>64	>64	NT	>64	NT	>64	>64
	E. faecalis	ATCC 29212	32	16	≤0.06	>64	>64	>64	>64	>64	64	>64	NT	>64	>64
Gram −	*K. pneumnoniae*	ATCC 10031	NT	8	0.5	1	NT	NT	NT	NT	NT	NT	>64	NT	NT
	E. coli	ATCC 25922	>64	>64	4	32	>64	>64	>64	>64	>64	>64	>64	>64	>64
	P. aeruginosa	ATCC 27853	>64	>64	>64	>64	>64	>64	>64	>64	NT	NT	NT	NT	NT
	H. influenzae	ATCC 49247	32	16	0.25	1	>64	>64	>64	>64	NT	NT	NT	NT	NT

MIC Color Scale (μg/mL) ≤0.06 | 0.12 | 0.25 | 0.5 | 1 | 2 | 4 | 8 | 16 | 32 | 64 | >64

J. Am. Chem. Soc. **2021**, 143, 6829–6835

Lincosamides - Iboxamycin

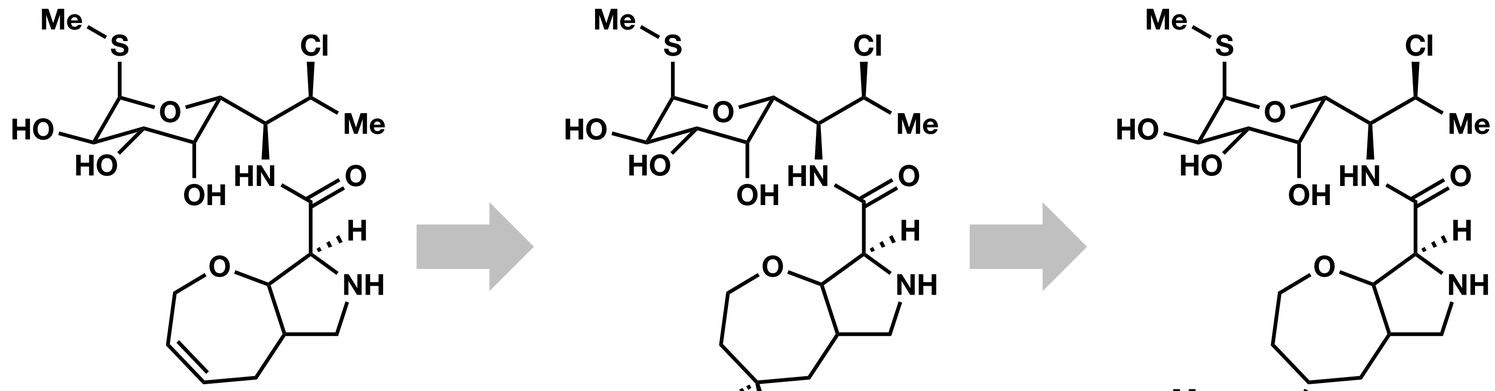

Iboxamycin (IBX)

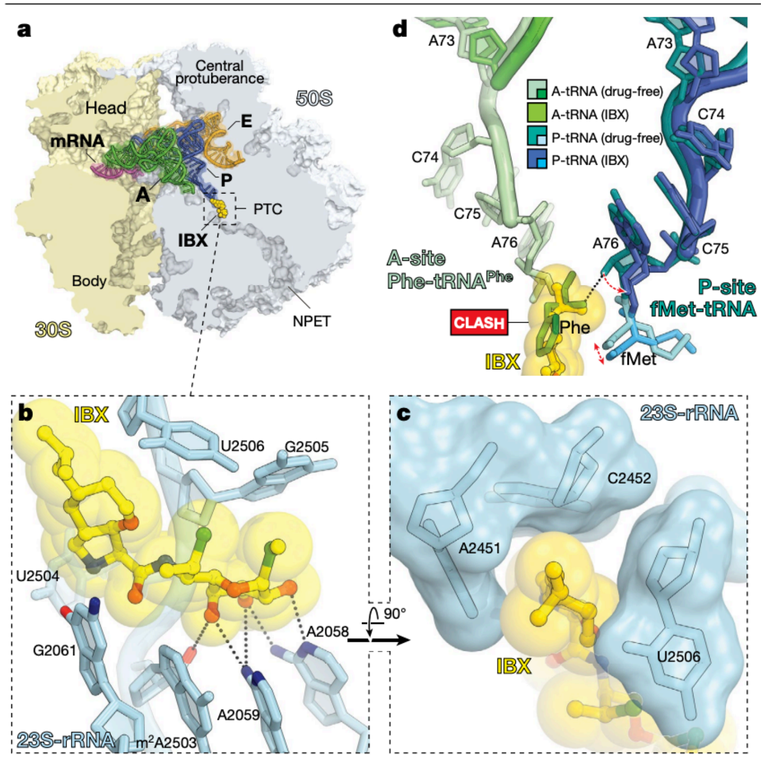

Structure optimization of an initial hit gave rise to IBX, which proved effective against many MLSB (Macrolide–Lincosamide–Streptogramin B)-resistant pathogens

Crystallographic data shows that IBX binds in the peptidyl transferase center (PTC) and nascent peptide exit tunnel (NPET), overlapping with the clindamycin binding pocket.

Most molecules (i.e. clindamycin) fail against Erm-Modified Ribosomes, but IBX is able to new hydrophobic interactions with the A-site cleft to stabilize binding interactions

However, it was noted that **flexibility in the molecule** limited some interactions

Nature, **599**, 507–512 (2021)

Lincosamides - Iboxamycin

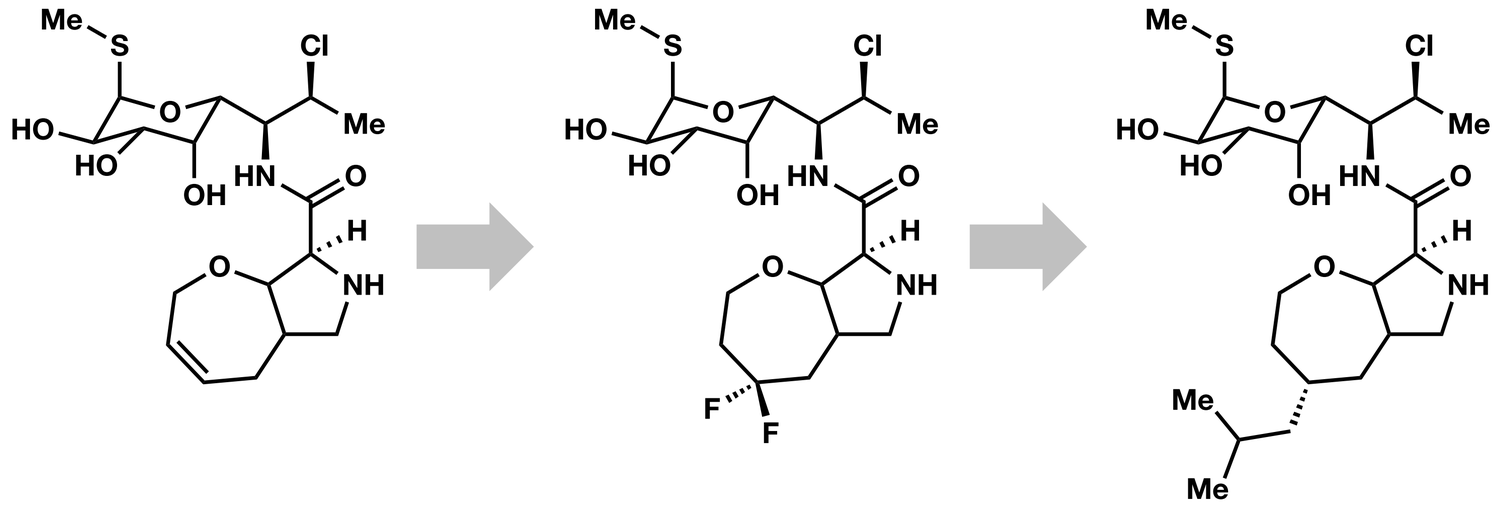

Iboxamycin (IBX)

a

	Species	Strain description	IBX	CLI
Gram-positive	*S. aureus*	ATCC 29213	0.06	0.125
	S. aureus	Clinical; MDR, *c-ermA*	1	>256
	S. aureus	Clinical; *msrA*	0.06	0.125
	S. aureus	Clinical; *cfr*	2	>128
	S. epidermidis	Clinical; *cfr*	8	>128
	S. haemolyticus	Clinical; LNZ-R, MEC-R	0.06	2
	S. pneumoniae	Clinical; *c-ermB*	0.25	256
	S. pneumoniae	ATCC 700673; MDR	0.5	>64
	S. pyogenes	ATCC 19615	0.03	0.06
	E. faecalis	ATCC 29212; *lsaA*	0.06	16
	E. faecalis	Clinical; *c-ermB*	1	>256
	E. faecium	Clinical; VRE, *vanA*	1	>64
	C. difficile	ATCC 700057	0.25	8
Gram-negative	*B. fragilis*	ATCC 25285	0.5	1
	E. coli	ATCC 25922	8	>128
	K. pneumoniae	ATCC 10031	0.25	8
	K. pneumoniae	Clinical; FQ-R	8	>128
	K. oxytoca	Clinical	8	>128
	A. baumannii	ATCC 19606	4	>128
	P. aeruginosa	ATCC 27853	128	>128
	H. influenzae	ATCC 9007	0.5	8
	N. gonorrhoeae	Clinical	0.125	2

b

Species	Strain description	IBX	CLI	CTR	LEVO	AZM	DOXY	LNZ	VAN
S. aureus	ATCC BAA-1707; MRSA	0.06	0.125	64	>128	1	0.25	2	1
S. aureus	Clinical; MRSA	0.06	0.25	>128	1	1	64	2	2
S. aureus	ATCC 700699; *c-ermA*	2	>128	>128	32	>128	16	2	8
S. aureus	Clinical; *cfr*	2	>128	128	8	>128	0.25	16	>64
S. pneumoniae	Clinical; MLS_B	0.25	>64	1	0.25	>64	2	4	2
S. pyogenes	MMX 946; *c-ermB*	0.25	>256	≤0.03	0.5	>64	0.125	1	0.5
E. faecalis	Clinical; VRE	1	>256	>256	128	>128	16	2	>128
E. faecalis	Clinical; VRE	2	>256	>256	64	>128	1	16	>128
E. faecium	Clinical; VRE, LNZ-R	≤0.06	>64	>256	128	8	16	64	>256
E. faecium	Clinical; VRE	1	>256	>256	128	>128	0.25	4	>128

c

Species	Strain description	IBX	CLI	CTR	LEVO	AZM	DOXY	LNZ	GEN
E. coli	Clinical	8	>128	0.125	32	64	0.5	64	2
E. coli	Clinical; *armA*	8	>256	≤0.06	≤0.06	4	2	128	>256
E. coli	Clinical; CRE, NDM-1	8	64	>128	64	8	32	128	4
E. coli	Clinical; ESBL	8	128	64	16	4	8	64	2
E. coli	Clinical; MDR, *arm*	8	>128	>128	32	4	32	128	64
K. pneumoniae	Clinical; CRE	8	>128	>128	32	32	16	>128	8
K. pneumoniae	Clinical; 3GC-R	16	>128	64	1	8	2	32	0.5
K. pneumoniae	Clinical; ESBL	16	>128	128	0.5	4	16	64	0.5
A. baumannii	Clinical; CRAB	16	128	64	32	4	32	64	4
A. baumannii	Clinical; CRAB, MDR	16	128	64	64	4	2	64	>128

Nature, **599**, 507–512 (2021)

Lincosamides - it gets better!

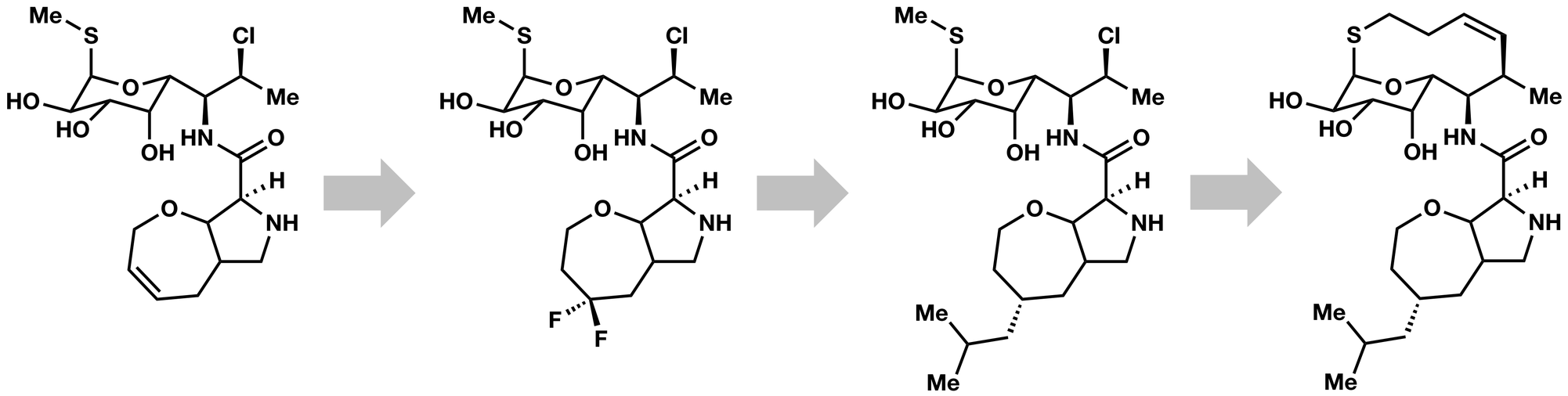

To rigidify IBX, a bridged, macrobicyclic structure was introduced

DFT was used to predict favorable conformations, and synthesis of CRM commenced after seeing that CRM had significantly less low energy conformers than IBX

Successful synthesis allowed for *in vivo* and *in vitro* studies

CRM showed stronger ribosomal engagement, enhanced potency, and retained activity against a wider range of resistant strains

Science ***383****, 721–726 (2024)*

Lincosamides - it gets EVEN better!

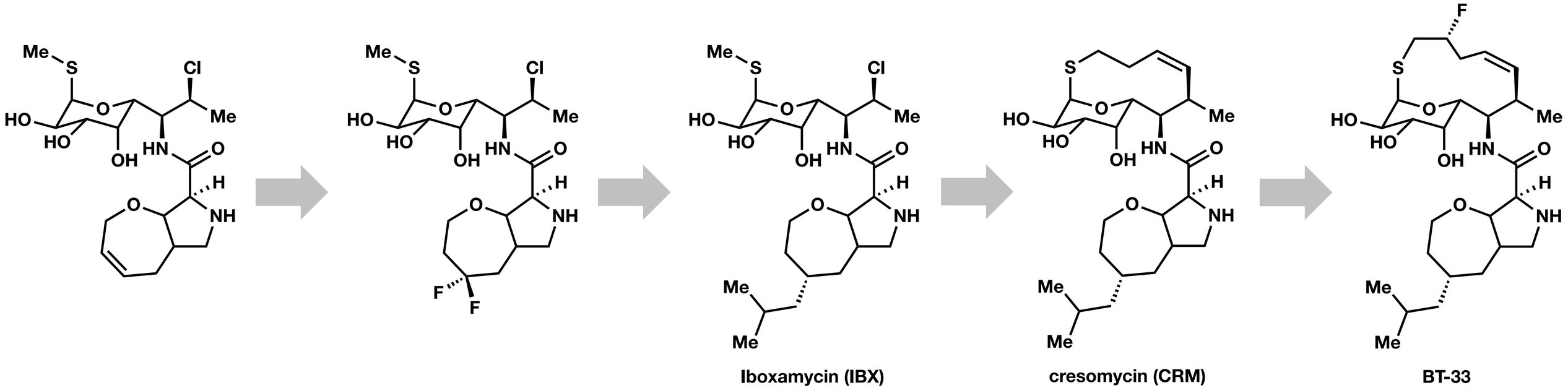

Additional fluoride provides additional van der Waals contact with nucleobase G2505 in the ribosome, enhancing binding affinity

BT-33 exhibited even lower MICs than CRM against a broader range of multi-drug resistant Gram-positive and Gram-negative bacteria

BT-33 also proved to be more metabolically stable, with a half-life in vivo (6.80 hours) compared to CRM (4.66 hours) and iboxamycin (2.05 hours)

Andrew G. Myers

Assistant, Associate, and then Full Professor (1994)

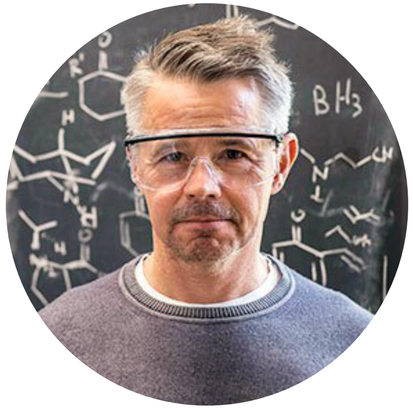

Department Chair 2007-2010

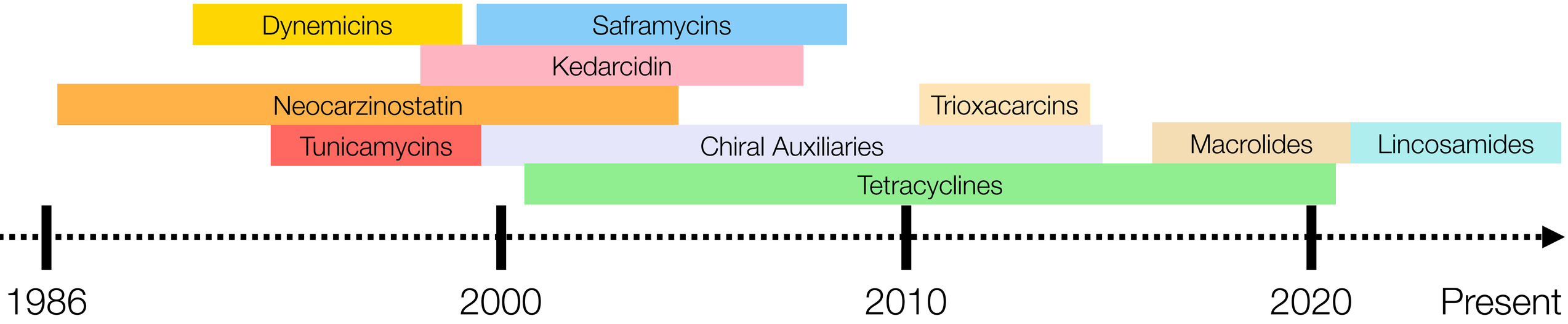

Andrew G. Myers

Assistant, Associate, and then Full Professor (1994)

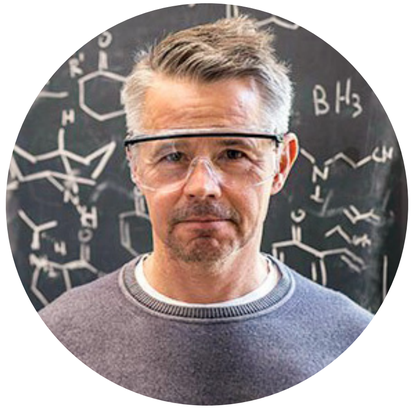

Department Chair 2007-2010

Dynemicins
Saframycins
Kedarcidin
Neocarzinostatin
Trioxacarcins
Tunicamycins
Chiral Auxiliaries
Macrolides
Lincosamides
Tetracyclines

Convergent Syntheses As Means to Interrogate Biological Questions

1986 2000 2010 2020 Present